This is to certify that the
dissertation entitled

T-TYPE CALCIUM CURRENTS IN SPINAL SENSORY INTEGRATION

presented by

Wen-hsin Ku

has been accepted towards fulfillment
of the requirements for the

Ph.D. degree in Physiology

Major Professor's Signature

12/22/09

Date

T-TYPE CALCIUM CURRENTS IN SPINAL SENSORY INTEGRATION

By

Wen-hsin Ku

A DISSERTATION

Submitted to
Michigan State University
in partial fulfillment of the requirements
for the degree of

DOCTOR OF PHILOSOPHY

Physiology

2010

ABSTRACT

T-TYPE CALCIUM CURRENTS IN SPINAL SENSORY INTEGRATION

By

Wen-hsin Ku

The spinal cord's dorsal horn receives sensory inputs encoded by primary sensory neurons that innervate the body and internal organs and is the origin of ascending pathways toward the brainstem and thalamus. Neurons in this region exhibit distinct intrinsic properties that are important for the integration of diverse sensory information. In this study, I focused on T-type Ca^{2+} currents (I_T) and their role on the intrinsic properties of these neurons. Whole-cell patch-clamp recordings were performed on dorsal horn neurons in a slice preparation obtained from the lumbosacral spinal cord of hamster pups (P9–P14). Cells were examined under both voltage- and current-clamp conditions, and I_T was isolated pharmacologically. Two T-type Ca^{2+} channel blockers Ni^{2+} and mibefradil were applied extracellularly in some experiments to verify the involvement of I_T in the intrinsic properties. Single cell reverse transcription polymerase chain reaction (RT-PCR) was performed after patch-clamp recordings in an attempt to uncover the molecular identity of I_T in individual dorsal horn neurons. The data show that I_T recorded in dorsal horn neurons had voltage-dependent activation and inactivation and similar sensitivity to the blockers, as did the T currents recorded in other neurons. Although I_T was expressed prevalently in the dorsal horn, its amplitude and kinetics varied widely from cell to cell. I_T had the highest current density in a group of phasic firing cells that are preferentially activated by rapid membrane depolarization resulting from direct current injection or fast moving skin stimuli. These cells also had the strongest expression

of a fast inactivating I_T component ($I_{T,f}$) revealed by an exponential stripping procedure. For both I_T and $I_{T,f}$, their current amplitude was correlated with the slope of depolarizing membrane ramps. This rate-dependent activation may underlie the ability of dorsal horn neurons to sense time-varying stimuli on the skin. I_T expression was associated with a rebound discharge after a hyperpolarization; further analysis indicates both $I_{T,f}$ and a slowly inactivating I_T component ($I_{T,s}$) contribute to this postinhibitory rebound behavior. Single-cell RT-PCR experiments indicate that $I_{T,f}$ is mediated by the $Ca_V3.1$ channel subtype. To summarize, my study confirms the presence of T-type Ca^{2+} currents in the spinal dorsal horn and suggests that this low-voltage-activated current is involved in differential capabilities of dorsal horn neurons to distinguish between static and moving skin stimuli by the mechanism of rate-dependent current activation.

To my parents

ACKNOWLEDGEMENTS

I would like to thank my committee, Drs. William Atchison, Steven Heidemann, David Kreulen, and Birgit Zipser, for their guidance from constructing the proposal to completing this dissertation. I am especially grateful to my mentor, Dr. Stephen Schneider, for his sensible advice, kindly support, and constant patience throughout these years. I would like to give a big thank you to Tracy Walker for her warm friendship and help both inside and outside the lab. I also want to extend thanks to Dr. Wenling Zhang and Timothy Houchin for providing a friendly and supportive working environment.

The single cell RT-PCR experiments cannot be done without the assistance from a number of individuals, and I would like to thank: Dr. Xiaoling Dai and Christine Harman for sharing valuable experiences and protocols, Dr. Laura McCabe for her counsel, Drs. Edward Perez-Reyes (University of Virginia) and Ravindra K. Hajela for providing materials for pilot experiments, and colleagues from Kreulen and Weber labs for technical support. Also, this study has been made possible through the National Institute of Neurological Disorders and Stroke grand NS25771.

Pursuing this degree has been quite a journey, and I am glad and truly thankful to have family and friends along the way, supporting me and encouraging me.

TABLE OF CONTENTS

LIST OF TABLES

LIST OF FIGURES

ABBREVIATIONS

4-AP, 4-aminopyridine

ACSF, artificial cerebrospinal fluid

ADP, afterdepolarization

AHP, afterhyperpolarization

D, delay cells

dV/dt, membrane depolarization slope

EPSP(s), excitatory postsynaptic potential(s)

GAPDH, glyceraldehyde 3-phosphate dehydrogenase

HVA, high-voltage-activated

I_{NaP}, persistent Na^+ current

IPSP(s), inhibitory postsynaptic potential(s)

I_T, T-type Ca^{2+} current

$I_{T,f}$, fast inactivating T-type Ca^{2+} current

$I_{T,s}$, slowly inactivating T-type Ca^{2+} current

L, Rexed's lamina

LTAP(s), low-threshold-current-mediated action potential(s)

LVA, low-voltage-activated

MIB, mibefradil

Non-P_{SB}, non-short burst phasic cells

P, phasic cells

P_{SB}, short burst phasic cells

PIR, postinhibitory rebound

RA, rapidly adapting

RF(s), receptive field(s)

RT, reverse transcriptase or reverse transcription

RT-PCR, reverse transcription polymerase chain reaction

SA, slowly adapting

T, tonic cells

T-channel(s), T-type Ca^{2+} channel(s)

T-current(s), T-type Ca^{2+} current(s)

TEA, tetraethylammonium chloride

TTX, tetrodotoxin

τ_f, decay time constant of fast inactivating T-type Ca^{2+} current

τ_s, decay time constant of slowly inactivating T-type Ca^{2+} current

CHAPTER ONE

INTRODUCTION

A. The role of the spinal dorsal horn in somatic sensory system

The dorsal horn of the spinal cord receives terminations from primary sensory neurons innervating the body and internal organs, and is the origin of pathways projecting to the brainstem and thalamus. As the first central relay of the somatic sensory system, the dorsal horn plays an important role in integrating and processing the information transmitted by peripheral sensory receptors. Histological studies (Rexed, 1952; Molander *et al.*, 1984) show that the dorsal horn is divided into six layers or laminae (I-VI), which have important functional implications. Lamina I neurons receive inputs carried by fine afferent fibers, both myelinated (Aδ) and unmyelinated (C), and mainly respond to thermal, noxious (painful), or both stimuli. Lamina II, also known as the *substantia gelatinosa*, primarily receives its input from slowly conducting, usually unmyelinated, fibers and contains nociceptive, thermoreceptive, and low-threshold mechanoreceptive neurons; this part of the dorsal horn is mostly regarded for its role in pain processing. Laminae I and II together are called the "superficial dorsal horn". Laminae III-VI (the so-called "deep dorsal horn") consist of low-threshold, nociceptive specific (or high-threshold), and wide dynamic range neurons that respond to a broad intensity range of stimulation applied on primary afferent fibers. This area receives direct input from large, myelinated (Aβ) fibers that carry signals encoded by muscle proprioceptors and a variety of cutaneous mechanoreceptors with distinct adaptation properties and differential sensitivity to skin indentation and hair movement. Thus, the deep dorsal horn is directly involved in integrating and processing mechanosensory information about the body (Willis and Coggeshall, 2004).

Sensory information relayed at the dorsal horn is subsequently conveyed to higher

levels of the neuraxis, *i.e.* the brainstem and thalamus, through three major ascending pathways. The spinothalamic pathway is common in all orders of vertebrates and most highly developed in primates, including humans (Willis & Coggeshall, 2004). The cells of origin of this pathway are located in laminae I and IV-VI of the spinal cord and project their axons to the contralateral thalamus through the anterolateral system. These dorsal horn neurons receive afferent fibers that innervate skin, muscle, and viscera, and are low-threshold, high-threshold, or wide dynamic range cells based on the responses to mechanical stimuli applied on their cutaneous receptive fields (Chung *et al.*, 1979). Some of the lamina I cells are thermoreceptive and project to the medial thalamus (Craig & Kniffki, 1985). The postsynaptic dorsal column pathway originates from neurons of the spinal laminae III-V and ascends to the dorsal column nuclei through the dorsal funiculus (Rustioni & Kaufman, 1977; Brown & Fyffe, 1981). These dorsal horn neurons often receive convergent inputs from skin, muscle, and joint afferents and respond to both innocuous and noxious mechanical stimuli (Brown *et al.*, 1983). The spinocervico-thalamic pathway originates from laminae III and IV of the spinal cord, relays in the lateral cervical nucleus by way of the dorsolateral funiculus, and then ascends contralaterally to the thalamus. Dorsal horn neurons that project through this pathway can be excited by stimulation on cutaneous afferent fibers of all sizes, as well as high-threshold muscle and joint afferent fibers, and are primarily nociceptive based on their responses to skin stimuli (Brown, 1973). This pathway provides a rapidly conducting system for transmission of information from the skin to the cerebral cortex, especially in cats (Catalano & Lamarche, 1957; Mark & Steiner, 1958). Despite a lot being known about primary afferent inputs and ascending pathways, how diverse sensory information

is integrated by the spinal cord remains unclear. By studying the intrinsic properties of dorsal horn neurons, their role in somatosensory integration may be better understood.

B. Intrinsic properties of spinal dorsal horn neurons and their ionic mechanisms

Based on their axonal projections, dorsal horn neurons are divided into two groups. Projection cells have axons that extend outside the spinal cord and ascend through the pathways mentioned above, while interneurons have propriospinal axons that ramify locally within the cell's dendritic tree in some cells and are further extensive longitudinally in others. Interneurons outnumber projection cells by a large margin and make up maximally 97% of the population (Willis & Coggeshall, 2004). As a major element of spinal local circuits, dorsal horn interneurons play an important role in spinal sensory processing and have diverse intrinsic properties (Russo & Hounsgaard, 1999). Among them, the difference in firing patterns is a much noticeable characteristic and has been described in several studies (Thomson *et al.*, 1989; Lopez-Garcia & King, 1994; Jiang *et al.*, 1995; Russo & Hounsgaard, 1996a, b; Hochman *et al.*, 1997; Grudt & Perl, 2002; Prescott & De Koninck, 2002; Ruscheweyh & Sandkühler, 2002; Schneider, 2003; Graham *et al.*, 2004). Two types of firing patterns have been commonly documented in dorsal horn neurons even when different animal preparations and recording configurations were used (Thomson *et al.*, 1989; Lopez-Garcia & King, 1994; Hochman *et al.*, 1997; Grudt & Perl, 2002; Prescott & De Koninck, 2002; Ruscheweyh & Sandkühler, 2002; Schneider, 2003; Graham *et al.*, 2004). Tonic cells fire continuously throughout the duration of current stimulation, whereas phasic cells respond with only a short period of discharge. The degree of spike frequency adaptation, a decrease in firing

frequency during sustained current injection, is markedly different for both cell categories; tonic cells typically have weak spike frequency adaptation (small changes in frequency with time) while the discharge frequency of phasic cells decreases much more rapidly. In some studies, a third group of neurons, called 'delay cells', are reported as responding to depolarizing current steps with an irregular or accelerating firing following an apparent delay to the first action potential in both superficial (Grudt & Perl, 2002; Prescott & De Koninck, 2002; Ruscheweyh & Sandkühler, 2002; Graham *et al.*, 2004) and deep dorsal horn (Hochman *et al.*, 1997; Schneider, 2003). This type is relatively fewer in number than tonic and phasic cells, especially in deep laminae (Hochman *et al.*, 1997; Ruscheweyh & Sandkühler, 2002; Schneider, 2003).

In the deep dorsal horn, phasic cells are found to be preferentially activated by fast membrane depolarization (> 13–34 mV/s) with the number and frequency of the action potentials positively correlating with the slope of stimulating current ramps, whereas the discharge frequency of tonic cells is unrelated to current trajectory (Schneider, 2003). In a hemisected spinal cord-skin patch preparation, phasic cells selectively respond to rapid brush flicks applied on their cutaneous receptive field and have strongest excitation in response to skin displacement that exceeds 8 μm/ms. Tonic cells, in contrast, respond to both moving and stationary cutaneous stimulation and are best activated by static skin indentation or contact (Schneider, 2005). Both studies (Schneider, 2003, 2005) suggest that these two cell types possess differential capabilities of signal processing. A similar concept is also reported in lamina I neurons: tonic cells appear to linearly transduce stimulus intensity into firing frequency and can act as "integrators" (see next paragraph for its ionic mechanisms), whereas phasic cells, with

rapid spike frequency adaptation, are able to follow high frequency stimulus and function as "coincidence detectors" (Prescott & De Koninck, 2002). In addition, based on their responses to skin stimuli, tonic cells appear to be activated by a wide range of mechanical stimulation, suggesting a mixture of low and high threshold inputs, while phasic cells likely receive sensory information from a rather narrow range of mechanoreceptors (Lopez-Garcia & King, 1994; Schneider, 2005). Taken together, these data indicate a role of different firing patterns in sensory information processing, and a better understanding of these properties, *e.g.* the underlying ionic mechanisms, can further advance the knowledge of sensory integration by dorsal horn neurons.

A few ionic mechanisms have been suggested to mediate different firing patterns in the spinal dorsal horn. A non-inactivating Na^+ current that activates at subthreshold potentials and has dendritic distribution (Safronov, 1999) is proposed to amplify and, by working synergistically with a slowly-activating persistent Ca^{2+} current, prolong synaptically-evoked depolarization in spinal lamina I neurons exhibiting tonic-firing. As a result, these tonic cells are capable of encoding stimulus intensity through temporal summation and act as integrators (Prescott & De Koninck, 2005). In lamina II of the spinal cord, a basic pattern of tonic firing is generated by a fast activating and inactivating voltage-gated Na^+ current and a delayed-rectifier K^+ current (Melnick *et al.*, 2004b) while a lower expression of the Na^+ current contributes to the spike frequency adaptation of phasic firing neurons (Melnick *et al.*, 2004a). In spinal lamina V neurons, an accelerating discharge following a delayed onset is mediated by the slow inactivation of a K^+ current that is highly sensitive to 4-aminopyridine (4-AP) (Morisset & Nagy, 1998); on the other hand, the activation of a transient K^+ current is suggested to underlie

the delayed firing pattern in superficial dorsal horn neurons by other studies (Yoshimura and Jessell, 1989; Ruscheweyh & Sandkühler, 2002; Ruscheweyh *et al.*, 2004). Both high- and low-threshold-activated Ca^{2+} current are documented in dorsal horn neurons (Huang, 1989; Ryu & Randic, 1990); among them, the T-type current is proposed to mediate a burst firing following membrane hyperpolarization in a subpopulation of turtle dorsal horn neurons (Russo & Huguenard, 1996a). In this study, the roles of this current in the spinal dorsal horn were investigated, and some previous reports about T-type current and critical to the present study are reviewed in the last part of the next section.

C. T-type calcium channels

Discovery

Coexistence of multiple Ca^{2+} conductances is first reported back in 1975 by Hagiwara and colleagues, who performed two-microelectrode voltage-clamp recording from starfish eggs. They noted that one of the two inward currents, channel I as they called it, was activated and inactivated at more negative membrane potentials and decayed faster, which was different from the properties of "typical", presumably high-voltage-activated (HVA), Ca^{2+} channels reported previously (Hagiwara *et al.*, 1975). Later in 1978, Moolenaar and Spector revealed a similar Ca^{2+} current in mouse neuroblastoma cell line N1E-115 using a Na^{+}-free external solution containing 15 mM TEA and an elevated Ca^{2+} concentration of 10 mM. This Ca^{2+} current was activated at −55 mV from a holding potential of −80 mV and reached the maximum magnitude at −20 mV with a time to peak of 8–10 ms. Its inactivation was also voltage-dependent and virtually competed within 100–150 ms. Application of Co^{2+} (5–10 mM) reversibly

abolished the current, which was otherwise TTX-resistant. Moolenaar and Spector's work is the first report of mammalian low-voltage-activated (LVA) channels, and the same group confirmed the presence of this transient Ca^{2+} current later and found a second Ca^{2+} current with a much longer inactivation time constant of 2000 ms in the same and another cell line NG108-15 (Fishman & Spector, 1981). By mid 1980s, the existence of LVA Ca^{2+} current across various tissues had been firmly established thanks to the efforts of many laboratories, including those led by Armstrong (Armstrong & Matteson, 1985), Bean (Bean, 1985), Carbone and Lux (Carbone & Lux, 1984, 1987), Feltz (Bossu *et al.*, 1985), Kostyuk (Fedulova *et al.*, 1985), and Tsien (Nilius *et al.*, 1985; Nowycky *et al.*, 1985). In 1985, the term "T-type" was proposed by Nowycky, Fox, and Tsien for this low-threshold current for its relatively "tiny" and "transient" unitary activity, while the designators L and N were assigned to a "long-lasting" HVA current and the third conductance that was "neither" T- nor L-type and found exclusively in "neurons", respectively. Since then, T-type Ca^{2+} channels have become the interest of an ever-expanding research field. These channels have hitherto been implicated in the mechanisms of cancer growth, cell development and proliferation, epilepsy, fertilization, hormone secretion, mechanosensation, nociception, sleep, and vascular tone control (Nilius *et al.*, 2006) Three T-channel α_1 subunits, α_{1G}, α_{1H}, and α_{1I} or $Ca_V3.1$, $Ca_V3.2$, and $Ca_V3.3$ in the current nomenclature (Ertel *et al.*, 2000), were cloned by the end of the 90s (Cribbs *et al.*, 1998; Perez-Reyes *et al.*, 1998; Lee *et al.*, 1999a), which enabled systematic studies of channel distribution, as well as examination of their patho-physiological roles using molecular tools (Nilius *et al.*, 2006).

Electrophysiology

T-type Ca^{2+} channels (T-channels) are widely expressed throughout the body and exhibit a number of signature features in electrophysiology (Perez-Reyes, 2003), which are described as follows. First, T-channels begin to open after small membrane depolarizations (usually between −75 and −60 mV), a characteristic giving them the name of "*low-voltage-activated*" channels. Second, the current mediated by these channels is *transient*, even during a prolonged stimulus. Third, native T-channels have *tiny* but equal single-channel conductance for Ba^{2+} and Ca^{2+}; at physiological Ca^{2+} concentration (2 mM), the value is expected to be ~ 1 pS (Talavera & Nilius, 2006). Fourth, they close slowly when the membrane potential is repolarized from a depolarized level, generating a slowly deactivating tail current. Fifth, the steady-state inactivation of T-channels occurs in a voltage range that partially overlaps that of the activation (the overlap usually between −70 mV and −40 mV), implicating the presence of a "window current" (Crunelli *et al.*, 2005). Last, T-channels are much less sensitive to HVA channel blockers, such as dihydropyridines, and can be identified and distinguished from HVA channels by their sensitivity to Ni^{2+} and low concentration of mibefradil[1] (Feltz, 2006), both of which were used in my studies.

The distribution and expression of T-type Ca^{2+} current (T-current) in the body has been carefully reviewed (Perez-Reyes, 2003; Yunker & McEnery, 2003), and heterogeneity is observed in native LVA current across different tissues even under the

[1]Mibefradil (Ro 40-5967), a tetralol derivative, was previously marketed as the antihypertensive and antianginal drug Posicor but was voluntarily withdrawn by Roche in early June 1998 due to its potentially fatal reactions with other drugs. Because of its inhibitory effect on the liver enzymes cytochrome P450 2D6 and 3A4, mibefradil can result in an increased plasma concentration of concomitantly administrated drugs to a dangerous level to the body (SoRelle, 1998).

same recording conditions (Yunker & McEnery, 2003). Differential expression of Ca_V3 subunits may partially contribute to these variations (Perez-Reyes, 2003; Yunker & McEnery, 2003) since distinct biophysical properties have been reported among three Ca_V3 subunits (reviewed by Talavera & Nilius, 2006). $Ca_V3.1$, $Ca_V3.2$, and $Ca_V3.3$ isoforms show larger, smaller, or equivalent current amplitude, respectively, in 2 mM Ca^{2+} than in isotonic Ba^{2+} concentration (McRory *et al.*, 2001) though the underlying mechanism is still uncertain (Talavera & Nilius, 2006). Recombinant $Ca_V3.1$ and $Ca_V3.2$ channels display similar activation and inactivation kinetics to native T-channels (Talavera & Nilius, 2006), while the $Ca_V3.3$ subtype has slower dynamics with an activation time constant of 30 ms (*vs.* 6–8 ms for $Ca_V3.1$ and 3.2) and an inactivation time constant of 137 ms (*vs.* 30–47 ms for the other two) (Klöckner *et al.*, 1999; Chemin *et al.*, 2002). Ni^{2+} is especially efficacious for the current mediated by the $Ca_V3.2$ subunit, with the IC_{50} of 6–12 μM in 10 mM Ba^{2+} *vs.* 167–250 μM and 87–216 μM for $Ca_V3.1$ and $Ca_V3.3$, respectively (Lee *et al.*, 1999b). Mibefradil doesn't have discriminative blockade on different Ca_V3 isoforms (IC_{50} = 1.1–1.5 μM in 10 mM Ba^{2+}), but its affinity for the channels increases when Ca^{2+} is used as the charge carrier (Martin *et al.*, 2000). Besides expression of different α_1 subunits, the subtype variants resulting from alternative slicing or single nucleotide polymorphism can also contribute to the heterogeneity in native T-current (Yunker & McEnery, 2003; Perez-Reyes, 2006; Perez-Reyes & Lory, 2006).

Molecular characterization

"*In silico* cloning", cloning based on computer searches of genetic database, led to the discovery of three T-type Ca^{2+} channel α_1 subunits: $Ca_V3.1/\alpha_{1G}$ (Perez-Reyes *et al.*,

1998), $Ca_V3.2/\alpha_{1H}$ (Cribbs *et al.*, 1998), and $Ca_V3.3/\alpha_{1I}$ (Lee *et al.*, 1999a). These pore-forming subunits are comprised of a large polypeptide (> 200 kDa), as observed in HVA Ca^{2+} and Na^+ channels, and have four domains of six transmembrane segments (S1–S6), a structure originally found in voltage-gated K^+ channels. The S4 segment from individual domains acts as the voltage sensor, P (pore)-loops between the S5 and S6 segments form the selectivity filter, and the S6 segments surround the pore forming its inner wall (Figure 1-1). The Ca_V3 channel proteins show 70%–95% sequence conservation among different species, but the homology within the channel family is only 40%, with the most highly conservative found in the membrane spanning regions (Perez-Reyes, 2006).

As a result of *in silico* cloning, no T-channel-specific auxiliary subunits are reported. Studies indicate that the β subunits of HVA Ca^{2+} channels are unlikely attached to the LVA channels, and whether other $\alpha_2\delta$ and γ subunits are associated with T-channels *in vivo* is still left unanswered. Even if T-channels possess auxiliary subunits, they may not act in similar ways as they do in HVA Ca^{2+} channels, *e.g.* regulating membrane trafficking, current amplitude, and voltage-dependent gating (Arikkath & Campbell, 2003; Perez-Reyes, 2006).

Three T-channel genes have been identified: *CACNA1G*, encoding $Ca_V3.1$; *CACNA1H*, encoding $Ca_V3.2$; and *CACNA1I*, encoding $Ca_V3.3$, and they are 70–130 kb long with 35–38 exons. Alternative splicing occurs in all three genes, and most splicing variants have tissue-specific expression and different kinetics and voltage dependence, which may affect their ability to influence cell excitability. Some single nucleotide polymorphisms in the coding region of *CACNA1H* are found to generate $Ca_V3.2$ channels with different

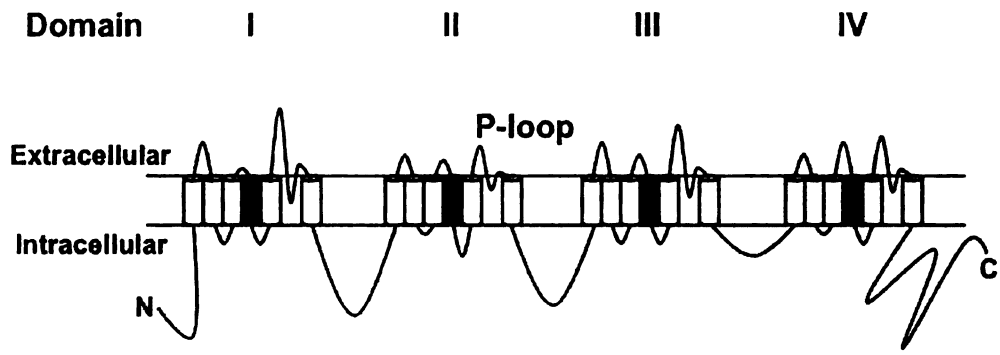

Figure 1-1. A structural model of T-type Ca^{2+} channels

The protein has four domains (I–IV), each one consisting of six transmembrane segments (from left to right: S1–S6; shown as the cylinders) and the corresponding links. The S4 segments (labeled in gray shade) act as the voltage sensor, P-loops between the S5 and S6 segments form the selectivity filter, and the S6 segments surround the pore and form its inner wall. N and C indicate the amino- and carboxyl-terminus of the protein, respectively.

gating properties and linked to absence epilepsy (Perez-Reyes & Lory, 2006).

T-type calcium current in spinal dorsal horn neurons

LVA (T-type) Ca^{2+} current has been reported to coexist with HVA Ca^{2+} current in the spinal dorsal horn neurons (Huang, 1989; Ryu & Randic, 1990), consistent with the findings in many other neuronal cells. The participation of Ca^{2+} conductances in the firing of these cells is first suggested by Murase and Randic (1983). They identified two distinct types of Ca^{2+}-dependent potentials that were evoked by modest and strong depolarizing current commands, respectively. The low-threshold Ca^{2+} electroresponsiveness was enhanced by hyperpolarized membrane potentials and showed fast inactivation (Murase & Randic, 1983), similar to what had been reported in inferior olivary neurons (Llinas & Yarom, 1981b, a). A transient low-threshold Ca^{2+} current was later recorded along with two high-threshold components in dorsal horn neurons using voltage-clamp technique (Huang, 1989; Ryu & Randic, 1990). The low-threshold current is presumably mediated by T-type Ca^{2+} channels because of the activation and inactivation kinetics and sensitivity to 200 – 400 μM Ni^{2+}, whereas the high-threshold counterparts are likely conducted by L- and N-type Ca^{2+} channels (Huang, 1989; Ryu & Randic, 1990). The molecular compositions of T-channels are also examined in the spinal dorsal horn using *in situ* hybridization (Talley *et al.*, 1999). $Ca_V3.1$ mRNA is present in all laminae at moderate levels. The expression of $Ca_V3.2$ transcripts is primarily restricted to laminae I and II while the distribution of $Ca_V3.3$ mRNA is more prominent in laminae III and IV.

The function of T-type Ca^{2+} current in the spinal dorsal horn is uncertain. The T-current has been suggested to underlie a burst firing in response to an electrically- or synaptically-evoked membrane hyperpolarization in a subpopulation of turtle dorsal horn

neurons, a phenomenon that may contribute to sensing the directionality of skin stimulation (Russo & Hounsgaard, 1996a). Nevertheless, T-current has gotten more attention recently because of its newly discovered role in peripheral and central pain processing (Todorovic & Jevtovic-Todorovic, 2006). In the spinal dorsal horn, the possible involvement of T-current in sensory transmission is indicated by both *in vivo* and *in vitro* studies. Behavioral experiments showed that the analgesic effect mediated by μ opioid receptors at the spinal level was potentiated by the T-channel blocker mibefradil, (Doğrul *et al.*, 2001). Also, T-current is found to be essential for the long-term potentiation of synaptic activity evoked by nociceptive afferent fibers in lamina I projection neurons, a possible cellular mechanism of central sensitization and hyperalgesia (Ikeda *et al.*, 2003). Matthew and Dickenson (2001) reported that the T-channel blocker ethosuximide depressed both mechanically and thermally evoked extracellular responses recorded from the spinal dorsal horn of anesthetized rats. In the dorsal root ganglia, a large T-current is expressed in medium diameter sensory neurons and carried by the $Ca_V3.2$ channel subtype. Although the functional identity of these cells as D-hair mechanoreceptors (Heppenstall and Lewin, 2006) or nociceptors (Jevtovic-Todorovic and Todorovic, 2006) is still controversial, an emerging role of T-current in sensory transmission is clear.

T-type Ca^{2+} current recorded in the lateral geniculate nucleus is preferentially activated by depolarizing voltage ramps with the slope exceeding 30 mV/sec (Crunelli *et al.*, 1989), and the low threshold Ca^{2+} spikes mediated by this current are also only evoked by the current ramps that produce a sufficient rate of membrane depolarization (Gutierrez *et al.*, 2001). This is a great interest of mine because phasic dorsal horn

neurons are selectively activated by fast current ramps and rapid skin movements (Schneider, 2003, 2005). Given that T-type Ca^{2+} current has been reported in the dorsal horn (Huang, 1989; Ryu & Randic, 1990), whether it is responsible for the rate sensitivity of phasic cells was one of the questions that I wanted to answer in this study (Specific Aim 1 and Chapter 2). Furthermore, since all three α_1 subunits of T-channels are expressed in the spinal dorsal horn (Talley *et al.*, 1999), the possible heterogeneity of T-current was also investigated (Specific Aim 2 and Chapter 3).

D. Single cell reverse transcription polymerase chain reaction in combination with patch clamp recording

The use of single cell reverse transcription polymerase chain reaction (RT-PCR) combined with patch clamp recording has been performed to study single neurons since early 1990s (Sucher & Deitcher, 1995). Generally, a whole-cell patch clamp recording is performed on cells in culture or slice preparations, and before termination of the recording, the cell content is collected by the electrode pipette. RNA is reverse transcribed into cDNA, which is then amplified by PCR with primers specific for the gene of interest. PCR product can be confirmed by electrophoresis and DNA sequencing or used for a second round of PCR. As the development of fluorescence-based real-time PCR techniques, the amplification can be detected while the reaction is still in progress, also allowing relative or absolute quantification of targeted cDNA molecules (Liss & Roeper, 2004). This experimental approach enables gene expression profiling of individual cells that are anatomically and functionally identified, as well as simultaneous detection of multiple genes from single cell samples (Phillips & Lipski, 2000). The

uncertainty as to whether mRNA detected by single cell RT-PCR are translated into functional proteins can be alleviated by performing whole-cell recording prior to cell harvesting, which provides functional assessment of membrane proteins, *e.g.* ion channels, and indirectly correlates mRNA analysis with protein expression in single cells (Phillips & Lipski, 2000). By combining single cell RT-PCR with whole-cell patch clamp recording, Ca_V3 channels are found to mediate the LVA Ca^{2+} currents in spermatocytes (Sakata *et al.*, 2001), and $Ca_V3.1$ is identified as the T-channel subtype underlying a low-threshold spike in hypothalamic paraventricular nucleus neurons (Lee *et al.*, 2008).

Spinal dorsal horn neurons are heterogeneous in anatomic locations, primary sensory inputs (see Section A in this chapter), as well as electrophysiological properties (see Section B in this chapter), which makes it appropriate, if not favorable, to study them at single cell level. Whole-cell patch clamp recording was used in this study to examine the roles of T-type Ca^{2+} current (I_T) in the intrinsic firing properties of dorsal horn neurons (Specific Aims 1 and 2), and single cell RT-PCR was performed following that to confirm expression of the channels and to determine their molecular identity (Specific Aim 3).

Specific Aims

In this study, I tried to answer three questions:

1. Does I_T contribute to the sensitivity of phasic-firing dorsal horn neurons to rapid membrane depolarization?
2. Is I_T in dorsal horn neurons composed of kinetically distinct current components? So, which current component is responsible for the rate sensitivity of phasic cells?
3. What is the molecular identity of I_T components in individual dorsal horn neurons?

To answer these questions, I first re-examined the basic properties of I_T in hamster dorsal horn neurons from a spinal cord slice preparation under voltage-clamp conditions. The rate-dependent activation of I_T, as previously reported in thalamic neurons (Crunelli *et al.*, 1989), was also investigated. These results are presented in Chapter 2, in which a general description of I_T expression in dorsal horn neurons is also included. The experiments directly addressing Specific Aims 1 and 2 were performed by measuring I_T in the cells whose intrinsic firing properties were characterized in current-clamp mode. T-channel blockers Ni^{2+} and mibefradil were added to the external media in some experiments to verify the involvement of I_T in different properties. The analyses regarding Specific Aim 1 are presented and elaborated in Chapter 2 while the data for attending to Specific Aim 2 are shown in Chapter 3. To address Specific Aim 3, single cell RT-PCR experiments were conducted using the cell content from neurons that were previously examined in patch clamp recordings, and the results are also shown in Chapter 3. Chapters 2 and 3 were both written in the format of journal articles.

CHAPTER TWO

T-TYPE CALCIUM CHANNELS CONTRIBUTE TO SIGNALING OF MEMBRANE DEPOLARIZATION RATE BY SPINAL DORSAL HORN NEURONS

Abstract

Spinal dorsal horn neurons differ in their responses to membrane depolarization rate and time-varying afferent sensory inputs. Using whole-cell patch-clamp recordings in slice preparations of hamster spinal cord, we investigated whether the transient, low-threshold calcium current (I_T) plays a role in generating rate-sensitive responses of dorsal horn neurons to changes in membrane potential. I_T was evoked by depolarizing voltage steps and ramps having slopes exceeding 46 mV/s. The peak amplitude of I_T activated by voltage ramps increased with increasing ramp slope over the range of 240 mV/s to 2400 mV/s. The time-to-peak of I_T decreased with increasing rate of membrane depolarization. Bath application of 200 μM Ni^{2+} depressed the ramp-activated I_T in a manner similar to I_T activated by step depolarizations. I_T was widely, though not uniformly, expressed by neurons in Rexed's lamina I–IV. Peak amplitude of I_T was correlated with the pattern of firing evoked under current clamp conditions: I_T in neurons responding to constant membrane depolarization with one or two action potentials was 2.8- and 7-fold larger than I_T in cells with tonic or delayed-firing patterns, respectively. Cells exhibiting a postinhibitory, rebound excitation had significantly larger I_T than those without. These results are evidence that I_T probably contributes to the ability of phasic-firing dorsal horn neurons to signal rapid membrane depolarizations and thereby discriminate between afferent sensory inputs that encode high- and low-frequency stimulus information.

Introduction

The dorsal horn of the spinal cord is a structure of major importance for processing sensory information from the body. It receives synaptic terminations of primary sensory neurons that innervate a variety of tissues, including skin, muscle, tendons, joints and viscera (Willis & Coggeshall, 2004). In this region, diverse sensory information is integrated by local neural circuits, which are made from synaptic connections between multiple, physiologically distinct types of interneurons (Lu & Perl, 2003, 2005; Santos *et al.*, 2007; Schneider, 2008), and then relayed to segmental reflex circuitry and ascending sensory pathways to the brain and brainstem.

Differences in electrophysiological properties of neurons can influence the transmission of sensory information within dorsal horn circuits. Three or four cell types have been identified in this region based on firing characteristics (Thomson *et al.*, 1989; Hochman *et al.*, 1997; Prescott and De Koninck, 2002; Ruscheweyh and Sandkühler, 2002; Schneider, 2003) and several studies have begun identifying the underlying ionic conductances. Repetitive discharge of tonically firing cells has been reported to be regulated by a combination of voltage-gated Na^+ and K^+ channels and persistent Ca^{2+} currents (Melnick *et al.*, 2004b; Prescott and De Koninck, 2005). Other evidence suggests that a transient, low-voltage-activated (T-type) Ca^{2+} conductance underlies a rapidly adapting, "phasic" discharge of other dorsal horn neurons (Russo and Hounsgaard, 1996a).

T-type Ca^{2+} channels are widely expressed in the central nervous system (Talley *et al.*, 1999; McKay *et al.*, 2006; Nilius *et al.*, 2006) where they promote burst firing, intrinsic oscillatory activity, and participate in synaptically-evoked Ca^{2+} influx

(Huguenard, 1996). Evidence of a Ca^{2+} current mediated by T-type channels has also been reported in dorsal horn neurons (Huang, 1989; Ryu and Randic, 1990). Our interest in the contribution of T-type channels to spinal somatosensory processing was prompted by two observations. First, fast depolarizing current ramps activate a transient membrane depolarization and discharge in many phasic-firing dorsal horn neurons, with the depolarization amplitude and firing frequency being graded with the ramp slope (Schneider, 2003). Second, phasic cells in the dorsal horn region where cutaneous mechanoreceptive afferents terminate respond selectively to mechanical stimuli that produce rapid deformations in the skin (Schneider, 2005), suggesting that this class of neurons may be part of specialized spinal circuits for encoding velocity information. A similar observation has been made by Prescott and De Koninck (2002), who found that phasic cells in dorsal horn lamina I are driven by high frequency stimulus trains and argued that they function to detect simultaneous occurrence of separate afferent inputs. In thalamic neurons, T-type currents are selectively activated by fast voltage ramps (Crunelli *et al.,* 1989) and generate large, transient Ca^{2+} depolarizations that contribute to oscillatory behavior (Gutierrez *et al.*, 2001). Given the importance of T-type channels to rhythmic firing behavior in thalamic neurons, we considered the possibility that these channels also shape responsiveness of dorsal horn neurons to dynamic membrane depolarizations induced by direct current injection or synaptic activation by primary sensory receptors.

In this study, we used whole-cell patch-clamp recordings in a rodent spinal cord slice preparation to isolate and re-examine T-type Ca^{2+} currents of dorsal horn neurons. We investigated activation of T-type currents by voltage ramps and compared current

amp

curr

firin

type

mer

fast

the

amplitude to neuronal intrinsic membrane and firing properties characterized under current clamp conditions. Our observations indicate that dorsal horn neurons with phasic firing patterns express high T-type Ca^{2+} current density and provide evidence that a T-type current is instrumental in tuning the selective responses of these cells to rapid membrane depolarizations. Selective sensitivity of phasic-firing dorsal horn neurons to fast depolarizations may underlie detection of transient afferent stimuli and encoding of the stimulus velocity.

Methods

All protocols involving the use of live animals were performed in accordance with the National Institutes of Health *Guide for the Care and Use of Laboratory Animals* and were approved by the Institutional Animal Care and Use Committee at Michigan State University.

Slice preparation

Spinal cord tissue was obtained from 9- to-14-day-old Syrian hamsters of both sexes under urethane anesthesia (1.5 mg/g, intraperitoneal), followed by exsanguination. After removing vertebrae and meninges, a block of lumbosacral spinal cord was glued to the stage of a vibrating microtome (Vibratome 3000, St. Louis, MO) and 300-μm-thick transverse slices were made as previously described (Schneider, 2003). Dissection and slicing steps were carried out at 4–8°C in a solution containing (mM) 179 sucrose, 2.5 KCl, 0.2 $CaCl_2$, 10 $MgCl_2$, 1.25 NaH_2PO_4, 26 $NaHCO_3$ and 25 glucose (pH 7.35–7.45, 290–310 mOsm/l) equilibrated with 95% O_2–5% CO_2. In some experiments, sucrose was replaced by equi-molar glycerol in the dissection solution (Ye *et al.*, 2006). There were no differences in resting potential or action potential amplitude and half-width recorded from neurons in slices prepared using sucrose- or glycerol-based dissection solutions (Table A-1 in Appendix). Slices were incubated in an oxygenated artificial cerebrospinal fluid (ACSF) containing (mM) 120 NaCl, 2.5 KCl, 2.5 $CaCl_2$, 1.5 $MgSO_4$, 1.25 NaH_2PO_4, 26 $NaHCO_3$, and 10 glucose (pH 7.35–7.45; 290–310 mOsm/l) at room temperature for at least one hour prior to electrophysiological recording.

Recor

For el

mount

5–6 m

electr

Drum

K-glu

GTP

we sv

107)

and 1

conce

recor

temp

band

illum

clam

(Figu

nulli

conf

comp

(MD

Recording procedures

For electrophysiological recording, slices were transferred to a chamber (volume, 1.5 ml) mounted on a fixed-stage microscope (Olympus BX51WI) and continuously perfused at 5–6 ml/min with ACSF bubbled with 95% O_2–5% CO_2. Patch-pipette recording electrodes with a resistance of 4–7 MΩ were fabricated from borosilicate glass (N-51A, Drummond Scientific, Broomall, PA). The internal pipette solution contained (mM) 130 K-gluconate, 5 NaCl, 1 $CaCl_2$, 1 $MgCl_2$, 11 EGTA, 10 HEPES, 2 Mg-ATP, and 0.1 Li-GTP (pH 7.3, 280–285 mOsm/l). For isolating T-type Ca^{2+} currents under voltage-clamp, we switched to a modified extracellular solution with the following constituents (mM): 107 NaCl, 3 $BaCl_2$, 2 CsCl, 1.3 $MgCl_2$, 26 $NaHCO_3$, 10 glucose, 20 TEA, 0.5 μM TTX, and 10 μM $CdCl_2$ (pH 7.35–7.45; 290–310 mOsm/l). In some experiments, Ba^{2+} concentration was lowered to 2 mM and Cd^{2+} was raised to 20 μM or 40 μM. All recordings took place within 4–5 h after tissue dissection and were performed at a bath temperature of 27°C to promote slice viability.

Recording sites were first identified at low power (10x) relative to the translucent band corresponding to the *substantia gelatinosa* (Rexed's lamina II), visible under trans-illumination (Figure A-1*A* in Appendix). Individual neurons were then targeted for patch-clamping using a 40x water immersion objective and infrared differential contrast optics (Figure A-1*B* in Appendix). Recordings were initiated in voltage-clamp mode after nulling pipette offset and capacitance transients. After establishing whole-cell recording configuration, cell capacitance (12–53 pF) and series resistance (15–62 MΩ) were compensated. Signals were amplified (0–5 kHz bandwidth) by an Axopatch 1D amplifier (MDS Analytical Technologies, Toronto, Canada) and saved to hard drive with a

D

T

w

ex

5(

cu

ce

po

cu

mo

pot

ana

me

Res

usi

duri

by p

min

Post

chan

mem

Digidata 1320A data acquisition system running pCLAMP software (MDS Analytical Technologies). Membrane current exceeding −0.05 nA at a holding potential of –60 mV was indicative of an unstable recording or poor cell condition, and these recordings were excluded from analysis. For analyses, voltage-activated currents were low-pass filtered at 500 Hz (Gaussian). P/N leak subtraction was used to correct for passive membrane current. Recordings targeted neurons spanning a range of sizes visible in slices. Whole-cell capacitance was used as an indicator of cell size and read directly from the potentiometer after nulling capacity transients. In most cases, currents are expressed as current density (pA/pF) by dividing by cell capacitance.

In some experiments, membrane potential recordings were made in current-clamp mode to classify neuronal intrinsic properties. Neurons were stimulated to produce action potentials by applying depolarizing current pulses (3 s) through the recording pipette for analyses of spike-frequency adaptation patterns. Neuronal input resistance (R_{in}) was measured by recording passive membrane responses to pulses of hyperpolarizing current. Responses of neurons to time-dependent membrane depolarizations were determined using ramp-hold waveforms (4.5 s) that produced linear changes in membrane potential during the ramp phase. The sensitivity to rate of membrane depolarization was estimated by presenting a series of waveforms having increasing ramp slopes and determining the minimum rate of membrane potential change that activated action potentials. Postinhibitory rebound excitation, a property associated with low-threshold T-type channels, was examined by applying hyperpolarizing current steps (500 ms) at the resting membrane potential, sometimes followed by a sub-threshold depolarizing current pulse.

Drugs and chemicals

TTX was purchased from MP Biomedicals (Irvine, CA). Mibefradil (Ro 40-5967, dihydrochloride hydrate) was purchased from Sigma-Aldrich (St. Louis, MO). All other reagents were purchased from Sigma-Aldrich or Mallinckrodt Baker (Phillipsburg, NJ).

Statistical analyses

Numerical data are presented as mean ± SEM, unless noted otherwise. Statistical analyses were performed using InStat 3 (Ver 3.06, GraphPad Software). Statistical significance of difference between two groups was assessed using the unpaired *t* test with Welch correction or Mann-Whitney test as appropriate. Comparison of means among three or more groups was conducted using one-way ANOVA with Tukey-Kramer multiple comparisons or Kruskal-Wallis one-way ANOVA with Dunn's multiple comparisons. The criterion for statistical significance was a value of $P < 0.05$.

Results

Whole-cell recordings were obtained from a total of 97 dorsal horn neurons in spinal slices prepared from 66 hamsters. Neurons had resting membrane potentials more negative than –50 mV under current-clamp conditions. Membrane potential was held at –60 mV during voltage-clamp recordings, unless otherwise noted for specific experiments.

T-type calcium currents in hamster dorsal horn neurons

We first re-examined T-type Ca^{2+} current (I_T) in dorsal horn neurons to enable direct correlations with spike discharge patterns. Voltage-clamp recordings were performed in the presence of media containing TEA, TTX and Ba^{2+} under ionic conditions appropriate for isolating Ca^{2+} currents. In the absence of Cd^{2+}, depolarizing the membrane potential from a holding potential of –90 mV to –30 mV activated an inward current with two components, an initial rapidly decaying phase followed by a late sustained phase (Figure 2-1*A*). Addition of 10 μM Cd^{2+} reduced the amplitude of the initial phase and almost completely abolished the late sustained current within 3 min of application. Increasing the Cd^{2+} concentration to 20 μM had no additional effect on the current (Figure 2-1), suggesting that there was little or no contribution from high-voltage-activated Ca^{2+} channels using the lower Cd^{2+} concentration. Therefore, subsequent experiments were performed in the presence of 10 μM Cd^{2+}. Under these conditions, we found that I_T was widely expressed by neurons recorded within Rexed's laminae (L) I–IV (98%, n = 41/42), but current density varied considerably from cell to cell [6 ± 4 pA/pF (SD)]. I_T was not

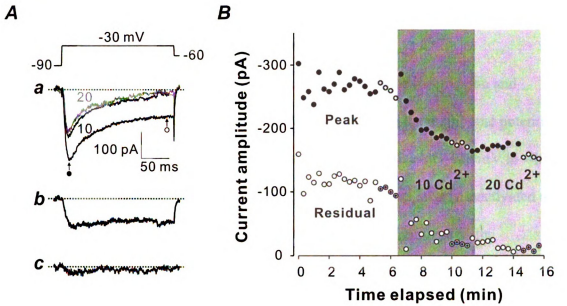

Figure 2-1. Isolation of low-voltage-activated Ca^{2+} currents

A: inward currents recorded from a representative dorsal horn neuron were activated every 20 s by a 200-ms voltage step at −30 mV from a holding potential of −90 mV for 500 ms (uppermost). *Aa*: each of the superimposed traces (black, before application of Cd^{2+}; gray, 10 μM Cd^{2+} and 20 μM Cd^{2+}) was averaged from four consecutive current responses (marked with crosses in *B*). *Ab*: inward current that was sensitive to 10 μM Cd^{2+} was obtained by subtraction. *Ac*: inward current that underwent additional blockade after increasing Cd^{2+} from 10 μM to 20 μM. Dotted lines indicate the baseline for current measurements. *B*: the amplitude of peak and residual current was plotted against the time elapsed. Cursor positions for measuring peak (●) and residual (○) current are shown in *Aa*. 10 μM and 20 μM Cd^{2+} were sequentially added into the external solution as indicated by shading.

differe

1 pA p

activat

to −30

mV he

holding

membr

plotted

(I I_{ma}

for halt

were st

of −90

low-vol

membra

potentia

fitted w

paramet

(Huguen

currents

to I_T ant

solution

different for neurons in the superficial (LI/II) and deep (LIII/IV) dorsal horn laminae (6 ± 1 pA/pF *vs.* 7 ± 1 pA/pF; $P = 0.46$; Table A-3 in Appendix).

We next examined the voltage-dependence of steady-state inactivation and activation of I_T. Inactivation kinetics were analyzed by stepping the membrane potential to –30 mV every 20 s in 10 mV increments from holding potentials of –120 mV to –40 mV held for 500 ms. An example is shown in Figure 2-2*A*. I_T was largely inactivated at holding potentials positive to –60 mV and this inactivation was removed as the membrane potential approached –100 mV. Averaged normalized currents (I / I_{max}) were plotted as a function of holding potential ($n = 4$) and fitted with the Boltzmann equation ($I / I_{max} = 1/\{1 + \exp[(V - V_{1/2}) / k]\}$) having a slope factor (k) of 12 mV and voltage for half-maximal current ($V_{1/2}$) of −74 mV (Figure 2-2*C*). Activation properties of I_T were studied by delivering 200-ms depolarizing voltage pulses from a holding potential of –90 mV to –10 mV in 10 mV increments. As shown in Figure 2-2*B*, I_T appeared in the low-voltage range with an activation threshold near –60 mV and reached a maximum at a membrane potential near –20 mV. Values for I / I_{max} were plotted against the membrane potential to generate an activation curve yielding $k = 8$ mV and $V_{1/2} = -47$ mV when fitted with the Boltzmann equation (Figure 2-2*C*). Overall, activation and inactivation parameters were consistent with I_T reported previously under similar conditions (Huguenard and Prince, 1992; Huang, 1989; Ryu and Randic, 1990).

Having established that I_T in hamster dorsal horn neurons resembled T-type Ca^{2+} currents described by previous studies, we then determined the sensitivity of the current to I_T antagonists. As illustrated in Figure 2-3*A*, 200 μM Ni^{2+} added to the bathing solution depressed I_T by 52% ± 6% ($n = 6$) after 4 to 9 min of perfusion. The effect was

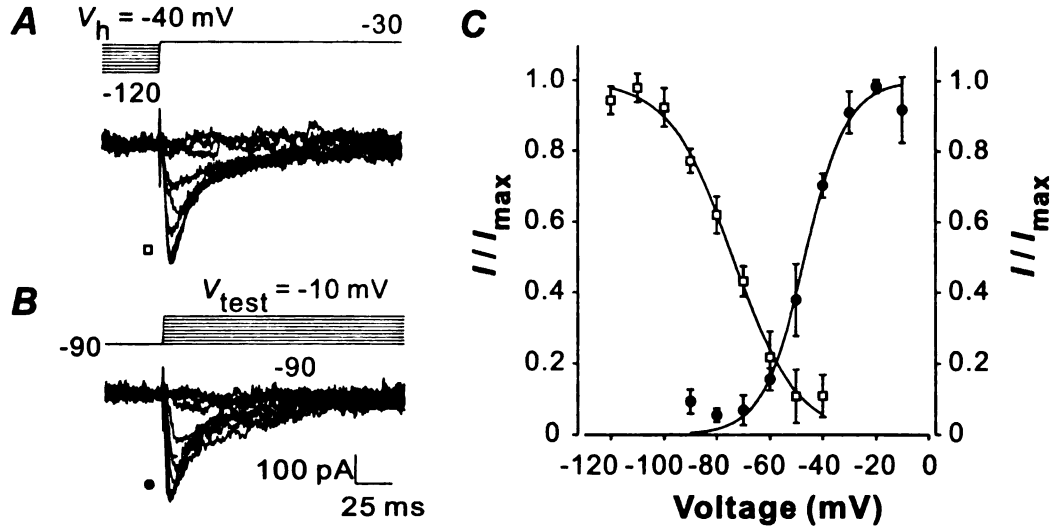

Figure 2-2. Voltage-dependent activation and inactivation of T-type Ca^{2+} currents in spinal dorsal horn neurons

A: I_T was activated in a representative dorsal horn neuron by a 200-ms voltage step to −30 mV following a series of 500-ms holding potentials (V_h) ranging from −120 mV to −40 mV at increments of 10 mV. *B*: the membrane potential of the same dorsal horn neuron was held at −90 mV for 500 ms before I_T was activated by a series of 200-ms testing potentials (V_{Test}) ranging from −90 mV to −10 mV at 10-mV increments. *C*: I_T from four dorsal horn neurons was examined using the voltage commands described in *A* and *B*. The current amplitude was normalized to the maximum level (I / I_{max}), averaged, and plotted with V_h for the inactivation curve (□) or V_{Test} for the activation curve (●). The curves were fitted with the Boltzmann equation. Errors bars represent SD. (n = 4).

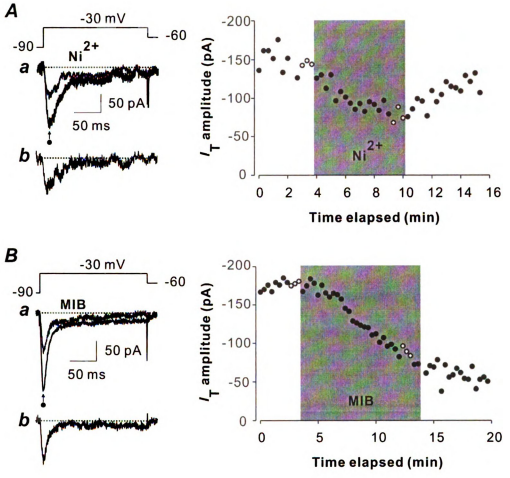

Figure 2-3. Effect of T-type Ca^{2+} channel blockers

Effect of T-type Ca^{2+} channel blockers Ni^{2+} (*A*) and mibefradil (*B*) on I_T in spinal dorsal horn neurons. I_T was activated every 20 s by stepping the membrane potential to −30 mV for 200 ms following a 500-ms holding potential of −90 mV. The peak current amplitude is plotted on the right as a function of time elapsed (filled circle symbols in *Aa* and *Ba* indicate cursor position for current measurements). Shading indicates when drug was present in the external solution. *Aa*, *Ba*: the black trace was averaged from three consecutive measurements marked with a white cross before the application of Ni^{2+} or mibefradil (MIB), and the gray trace was averaged from three white-cross-marked points near the end of the drug presentation. The inward currents that were sensitive to either of the blockers, obtained by subtraction, are shown in *Ab* and *Bb*.

rev

was

of 5

perf

initi

Rate

Afte

wan

depo

(Cru

I_T m

mem

mem

pulse

incre

appli

activa

from

Both

Voltag

reversible with the current recovering to 78% ± 10% of control after 4 to 16 min of washout. The I_T antagonist mibefradil (MIB) was tested on three cells at a concentration of 5 μM and resulted in a 47% ± 4% reduction in I_T amplitude after 6 to 10 min of perfusion (Figure 2-3*B*). The effect of MIB on I_T in spinal slice neurons persisted after initiating drug washout.

Rate-dependent activation of T-type calcium currents in spinal dorsal horn neurons

After determining steady state voltage-dependence of I_T in dorsal horn neurons, we wanted to know if the magnitude of I_T was also related to the slope of membrane depolarization (dV/dt), a characteristic that has been described for I_T in thalamic neurons (Crunelli *et al.*, 1989; Gutierrez *et al.*, 2001). This is important because of our view that I_T may contribute to the differential responses of dorsal horn neurons to rate of membrane depolarization and time-varying sensory stimuli (Schneider, 2003, 2005).

I_T activation dynamics were examined by using voltage ramps to depolarize membrane potential at different rates to −30 mV following a 500-ms hyperpolarizing pre-pulse to −90 mV. As can be seen by the example shown in Figure 2-4*A*, I_T amplitude increased along with dV/dt between ramp slopes of 400 mV/s and 2400 mV/s. Bath application of Ni^{2+} depressed ramp-activated currents in a manner similar to those activated by step depolarizations (Figure 2-4*A*, gray). Best-fit regression lines calculated from plots of I_T amplitude versus ramp slope for seven cells are shown in Figure 2-4*B*. Both the *x*-intercept and slope varied widely within our sample of cells recorded under voltage clamp. Threshold for I_T activation, as estimated from the *x*-intercept values,

A

-9

C

t_p (ms)

Fig
A:
dep
fro
and
ana
rec
dat
0.9
resp
tim
act

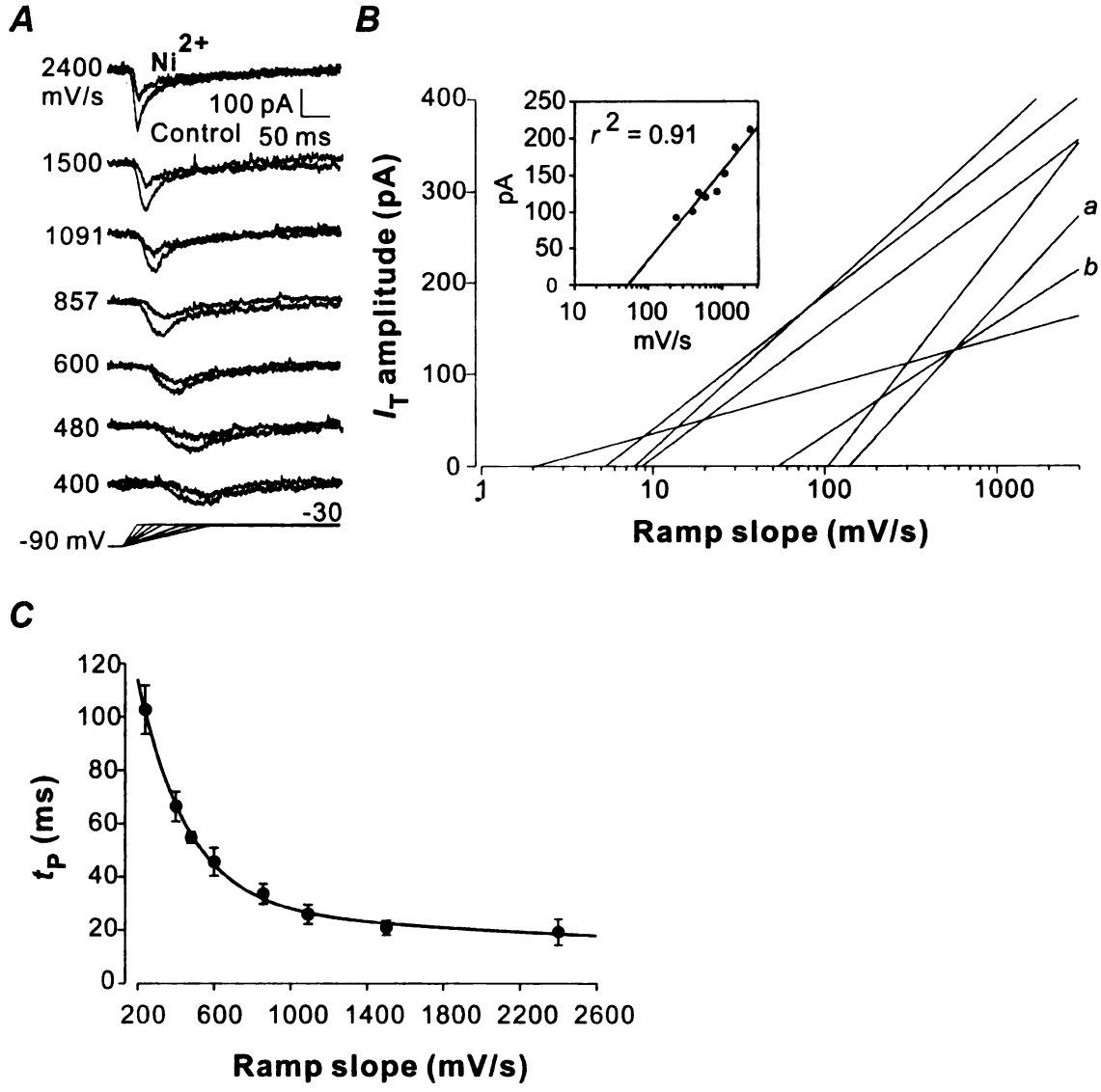

Figure 2-4. Activation of I_T in dorsal horn neurons with ramp depolarizations
A: I_T in a representative dorsal horn neuron was activated by using voltage ramps to depolarize the membrane potential at different rates (indicated to the left of each trace) from a 500-ms holding potential of −90 mV to −30 mV. I_T before (control, black traces) and during (Ni^{2+}, gray traces) presentation of 200 μM Ni^{2+} is shown. *B*: linear regression analysis between I_T amplitude and ramp slope is shown for seven dorsal horn neurons recorded in media containing 2 or 3 mM Ba^{2+}. Inset shows representative linear fit to data points for *b*. The coefficients of determination (r^2) from regression analyses (0.72 to 0.99) indicate that I_T amplitude and ramp slope are highly correlated. Individual responses to ramp depolarizations for regression line *a* are shown in *A*. *C*: the averaged I_T time-to-peak (t_P) from the seven cells in *B* plotted against the ramp slope at which I_T was activated. Error bars represent SEMM. (n = 7).

averaged 46 ± 21 mV/s (range 2 to 138 mV/s). The sensitivity of I_T to ramp dV/dt (defined as slope of the regression lines, pA·s/mV) varied almost five-fold, from 51 to 242 pA·s/mV, for the cells studied. Despite the cell-to-cell variability, regression analyses showed that 87 ± 4% of the current amplitude was determined by dV/dt (range 72% to 99%). Taken together, the data suggest that dorsal horn neurons are quite heterogeneous with respect to activation by voltage ramps.

Since I_T activation appeared to be dependent on the slope of the voltage ramp, we investigated the rate-dependence of I_T kinetics. As shown in Figure 2-4*C*, I_T time-to-peak (t_p) was dependent on dV/dt over the range of 240 mV/s to 2400 mV/s, suggesting that rate of activation increased with increasing speed of membrane depolarization. Four other neurons were examined using a similar protocol ramping the membrane voltage from a holding potential of –100 mV ~ –90 mV to –30 mV ~ –20 mV, but with the Ba^{2+} concentration lowered to 2 mM Ba^{2+} and Cd^{2+} increased to 40 μM. The maximum amplitude, threshold and rate sensitivity of I_T under these circumstances were not significantly different from data obtained using the standard conditions described above.

T-type calcium currents in spinal dorsal horn neurons with identified membrane and discharge properties

Although I_T appeared to be a ubiquitous property of dorsal horn neurons, the current density varied considerably from cell-to-cell under similar experimental conditions. This variability might be expected if I_T contributes to the differential responses of dorsal horn neurons to static and time-varying membrane depolarizations (Schneider, 2003, 2005). We therefore examined I_T in a population of dorsal horn

neur

clam

depc

ms a

mini

in fir

pipet

sumn

conti

small

curre

arrow

activa

(50%

frequ

(right

respo

super

The r

poten

spike

activa

neurons following initial characterization of intrinsic firing properties under current-clamp in standard ACSF solution (see METHODS). Measurements of I_T were made by depolarizing the membrane potential to –30 mV from a potential of –90 mV held for 500 ms and subtracting residual current activated from a holding potential of –40 mV to minimize contribution from any unblocked high-voltage-activated Ca^{2+} current.

Dorsal horn neurons recorded under current clamp exhibited distinct differences in firing behavior when activated by depolarizing current applied through the recording pipette, as described previously (Schneider, 2003). The results from the present study are summarized in Tabel 2-1 and Figure 2-5. Tonic cells (42%, n = 16) fired action potentials continuously throughout the period of depolarization (Figure 2-5*Ab*). A second, much smaller group of neurons (8%, n = 3) resembled tonic cells but responded to depolarizing current following a marked delay to the first action potential (Figure 2-5*Aa*, open arrowheads). A third group, phasic cells, generated a rapidly adapting discharge when activated by a constant level of depolarizing current and amounted to half of our sample (50%, n = 19). Since phasic cells as a group displayed a fairly wide range of spike frequency adaptation (Schneider, 2003), we further divided them into two subgroups (rightmost columns in Tabel 2-1, Figure 2-5*Ac* and *d*). Short burst phasic cells (P_{SB}), responded to depolarizing current injection with only one or two action potentials superimposed on a transient membrane depolarization (Figure 2-5*Ac*, filled arrowheads). The remaining phasic cells (non-P_{SB}) typically responded with 3 or more action potentials at rapidly diminishing frequency to depolarizing current, and the number of spikes increased with stimulus amplitude (Figure 2-5*Ad*). The transient depolarization activated in non-P_{SB} cells was smaller than in P_{SB} cells (compare upper trace in Figure

Table 2-1.
horn neur

Firing pat			
Number of			
I_T (pA			
Resting (mV			
R_{in} (M			
Ramp th (mV			
Postinhi rebo			

All values
value is gi
* Signific
† Signific
‡ Signific

Table 2-1. Comparison of I_T and intrinsic membrane properties of spinal dorsal horn neurons in this study

Firing pattern	Delay (D)	Tonic (T)	Phasic (P)	Short burst phasic (P_{SB})	Non-short burst phasic (non-P_{SB})
Number of cells	3	16	19	7	12
I_T (pA /pF)	2 ± 1	5± 1	9 ± 2†	14 ± 4*,†,‡	6 ± 1
Resting V_m (mV)	−58 ± 4	−56 ± 2 (14)	−65 ± 1*	−68 ± 1*,†,‡	−63 ± 1*
R_{in} (MΩ)	651 ± 77	654 ± 84	319 ± 38*,†	261 ± 66*,†	352 ± 46*,†
Ramp threshold (mV/s)	7 ± 1	9 ± 3 (12)	45 ± 5*,† (18)	43 ± 3*,†	46 ± 7*,† (11)
Postinhibitory rebound	0% (0/2)	64% (9/14)	94% (16/17)	100% (7/7)	90% (9/10)

All values are listed as mean ± SEM. The number of measurements used to calculate each value is given in parentheses if different from the number of cells for the group.

* Significantly different from T cells.

† Significantly different from D cells.

‡ Significantly different from non-P_{SB} cells.

Figur
A: res
curren
delay;
details
first re
indicat
depola
ramp-h
superir
and mi
mV's fo
the sam
indicate

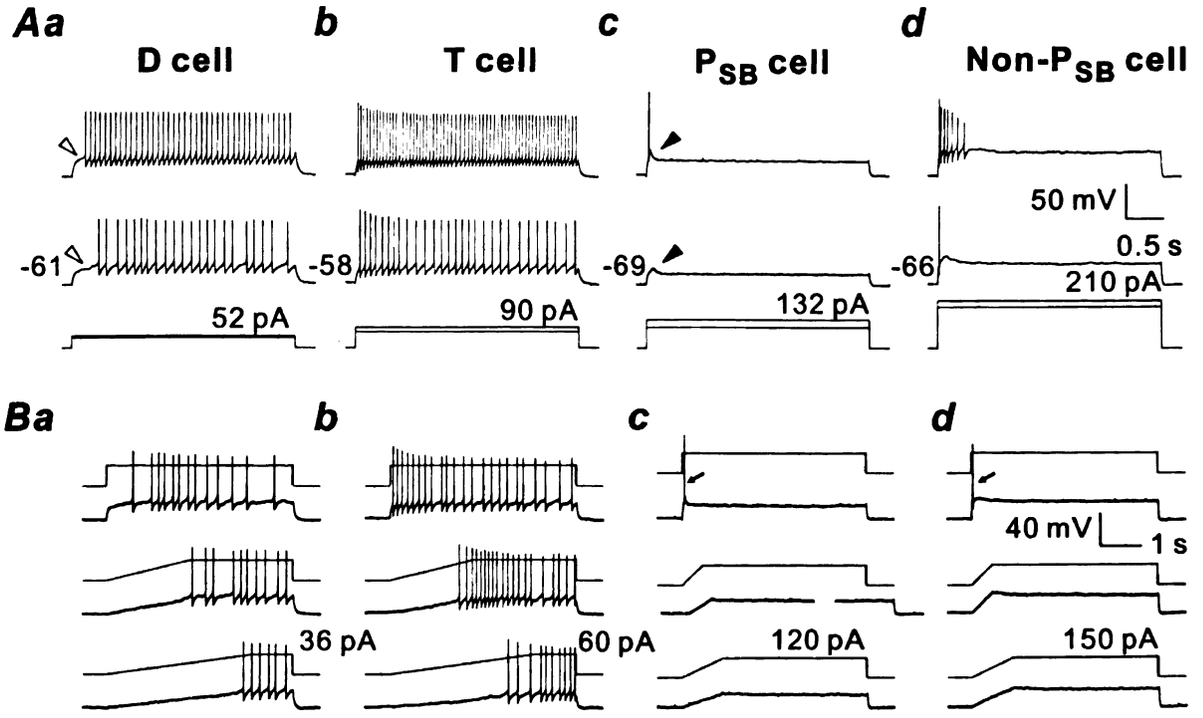

Figure 2-5. Firing patterns of hamster dorsal horn neurons

A: responses of a representative cell from each category (top two traces) to depolarizing current pulses applied through the recording pipette (lowermost trace). (Categories: D, delay; T, tonic; P_{SB}, short burst phasic; Non-P_{SB}, non-short burst phasic; see text for details.) Resting membrane potential (V_m) for each neuron is indicated to the left of the first response. Delay between pulse onset and first action potential for the D cell is indicated by the open arrowhead. Filled arrowheads in *c* indicate transient membrane depolarizations characteristic of P_{SB} neuron activation. *B*: responses of the same cells to ramp-hold current commands that depolarized V_m at different rates (waveforms are superimposed on individual traces). Slope of membrane depolarization (dV/dt) for lower and middle traces: 6 mV/s and 9 mV/s for D; 5 mV/s and 10 mV/s for T; 18 mV/s and 37 mV/s for P_{SB} 25 mV/s and 55 mV/s for non-P_{SB}. Upper trace: rectangular current step to the same level of depolarization (upper trace). Action potential responses in *c* and *d* are indicated by arrows.

2-5*Ac* wit

summariz

potential (

consistent

current co

discharge

neurons w

ramp-hold

by the mos

needed to

activation

activation

the respons

$\mu M Ni^{2+}$ (*r*

low-thresh

Twe

rebound me

current (Figu

cells than to

firing pattern

depolarizing

increased in a

(Figure 2-8*A*)

2-5*Ac* with middle trace in Figure 2-5*Ad*) or absent altogether (Figure 2-6). As summarized in Tabel 2-1, phasic cells had a more hyperpolarized resting membrane potential (–65 mV) and lower R_{in} (319 MΩ) than tonic cells (–56 mV; 654 MΩ), consistent with previous observations (Schneider, 2003). When depolarized by ramp-hold current commands, tonic cells discharged primarily during the steady-state depolarization; discharge frequency was unrelated to the ramp slope (Figure 2-5*Bb*). Delay cells, like neurons with tonic firing patterns, fired action potentials during the hold phase of the ramp-hold current command (Figure 2-5*Ba*). Typically, phasic cells were activated only by the most rapid membrane depolarizations (Figure 2-5*Bc* and *d*). Depolarization rates needed to activate phasic cells were five- to six-times higher than those required for activation of tonic- and delayed-firing neurons, and were close to the threshold for activation of I_T studied in our voltage clamp experiments. As can be seen in Figure 2-7, the responses of phasic cells to step or ramp-hold depolarizations were depressed by 200 μM Ni^{2+} ($n = 4$) and 5 μM MIB ($n = 3$), consistent with underlying participation from a low-threshold T-type Ca^{2+} current.

Twenty-five of 33 cells tested (76%) exhibited postinhibitory rebound (PIR), a rebound membrane depolarization and discharge following injection of hyperpolarizing current (Figure 2-8*A*). Although PIR appeared to be observed more frequently in phasic cells than tonic cells (Tabel 2-1), there was no statistically significant association with firing pattern ($P = 0.067$). PIR in hamster dorsal horn neurons was typically activated by depolarizing the membrane potential to –45 to –60 mV from around –80 mV, and increased in amplitude when activated from more hyperpolarized membrane potentials (Figure 2-8*A*). A time-dependent rectification (voltage "sag" in Figure 2-8*B*) was evident

Figure 2-
Transient
threshold
typically a
non-P_{SB} c

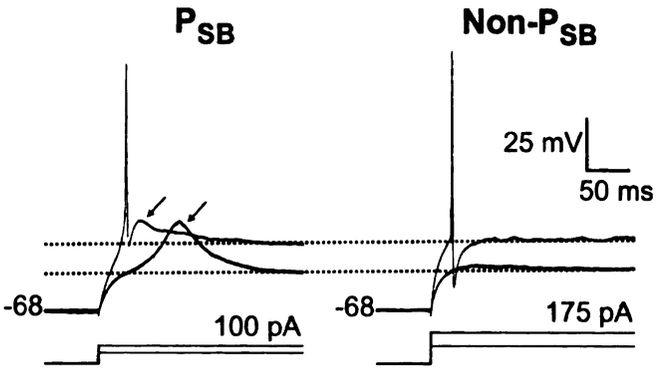

Figure 2-6. Transient depolarization in phasic cells

Transient depolarizing potentials (arrows, upper traces) were observed in supra- and sub-threshold responses of P_{SB} cells to depolarizing current pulses (lower traces) but were typically absent from non-P_{SB} cells at the same V_m (dotted lines). R_{in}: P_{SB} cell, 344 MΩ; non-P_{SB} cell, 194 MΩ.

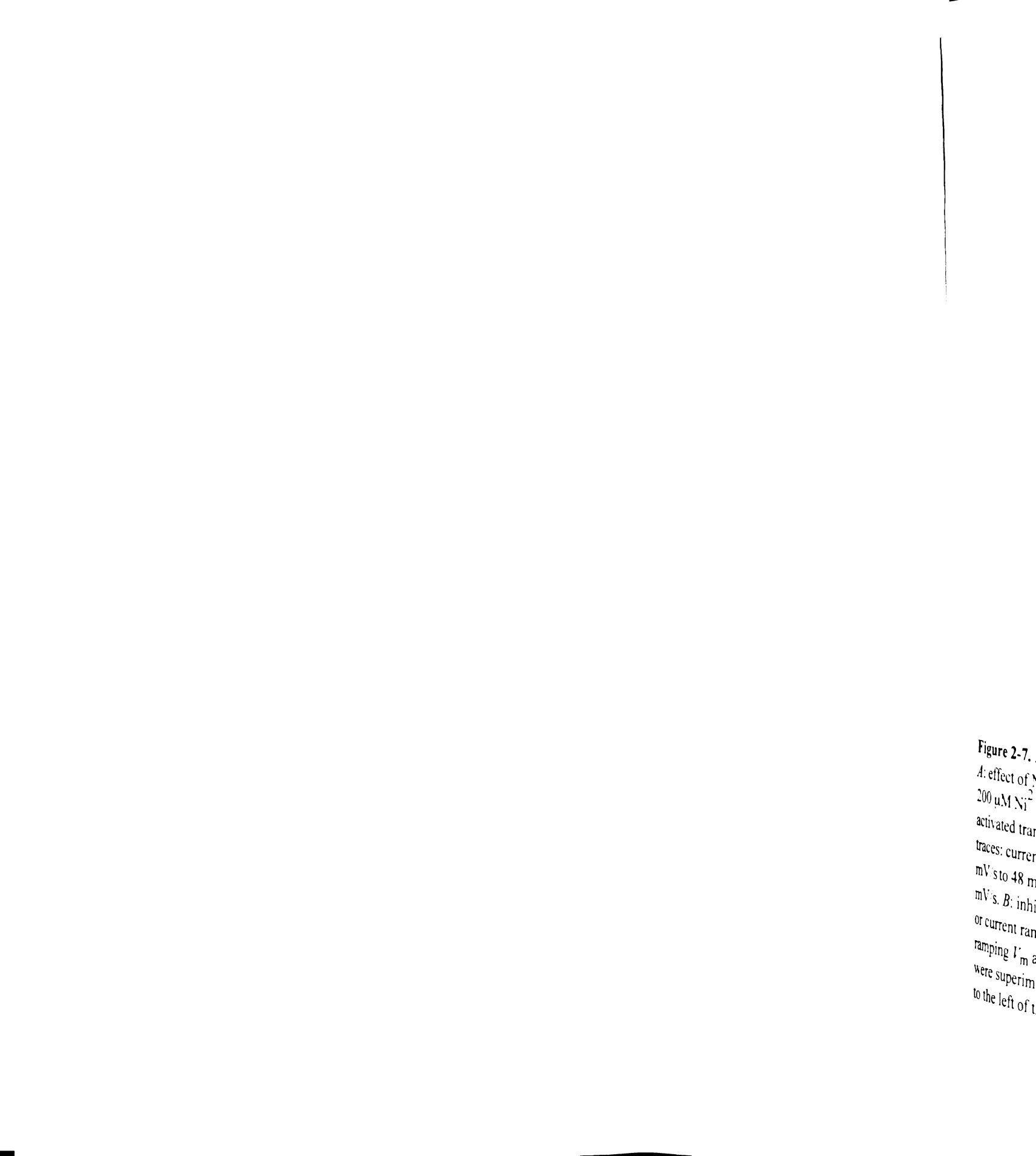

Figure 2-7.
A: effect of
200 μM Ni^{2}
activated trar
traces: currer
mV/s to 48 m
mV/s. *B*: inhi
or current ran
ramping V_m a
were superim
to the left of t

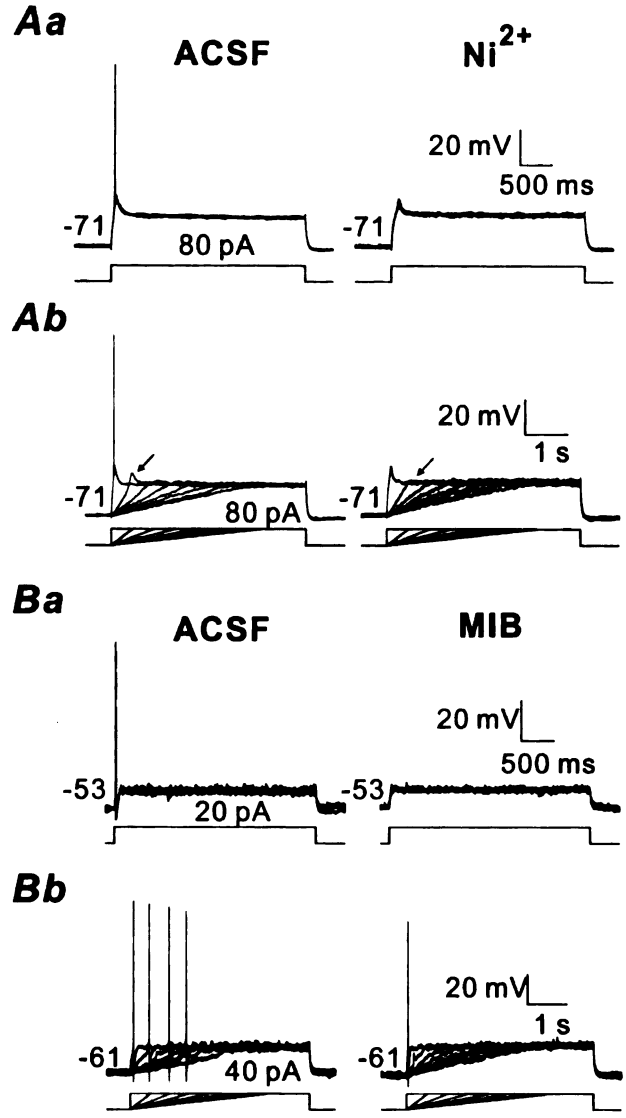

Figure 2-7. Effect of Ni^{2+} and mibefradil on phasic firing

A: effect of Ni^{2+} on ramp- and step-activated responses of a representative phasic cell. 200 μM Ni^{2+} blocked the spike discharge generated by a current step (*a*) and a ramp-activated transient depolarization (*b*, arrows). Upper traces: voltage responses. Lower traces: current commands. Current commands used in *Ab* depolarized V_m at rates of 6 mV/s to 48 mV/s and the transient depolarization was activated by a voltage ramp of 48 mV/s. *B*: inhibitory effect of 5 μM mibefradil on phasic firing evoked by a current step (*a*) or current ramps (*b*) in two other dorsal horn neurons. The cell in *Bb* was activated by ramping V_m at 12 mV/s or greater (range 4 mV/s to 31 mV/s). Five consecutive traces were superimposed and shown in *Aa* and *Ba*. Resting V_m for each condition is indicated to the left of the traces.

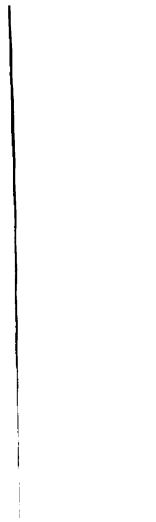

Figure 2.
A: a dorsa
(upper tra
cell exhib
92 mV (d
discharge
action pot
hyperpola
dependent
neuron wa
−57 mV a
0.5 μM TT
traces in *A*

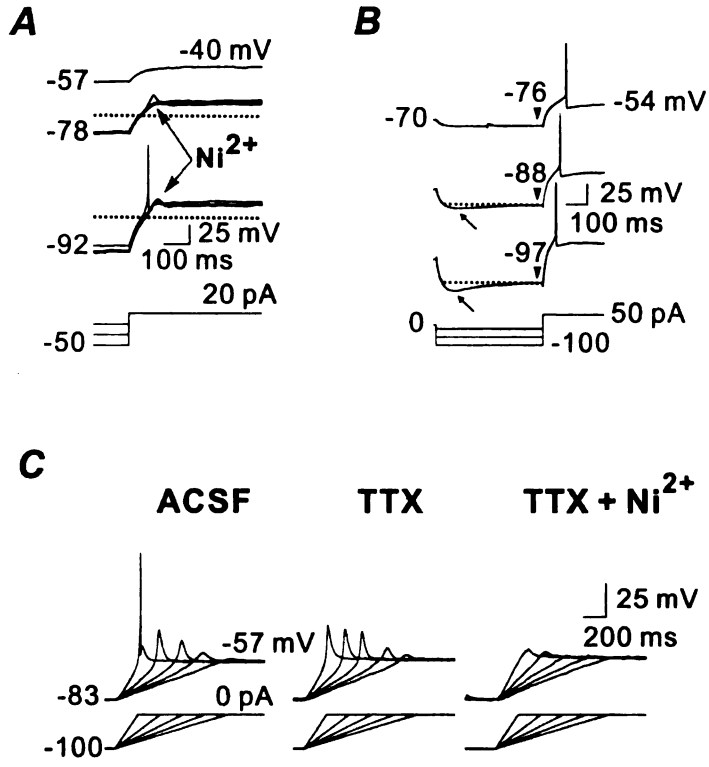

Figure 2-8. Postinhibitory rebound in hamster dorsal horn neurons
A: a dorsal horn neuron was given a depolarizing current pulse from the resting V_m (upper trace) or following hyperpolarizing current steps (middle and lower traces). The cell exhibited rebound depolarizations following prior hyperpolarization to −78 mV and −92 mV (dotted lines indicate resting V_m at −57 mV). Both rebound depolarization and discharge were blocked by 200 μM Ni^{2+} applied in ACSF (gray traces). *B*: a rebound action potential was generated in a dorsal horn neuron depolarized to −54 mV from hyperpolarized V_m (arrowheads; resting V_m, −70 mV). PIR was independent of a time-dependent rectification (voltage "sag", indicated by the arrows). *C*: another dorsal horn neuron was hyperpolarized to −83 mV for 500 ms and then returned to the resting level of −57 mV at rates ranging from 28 mV/s to 131 mV/s. The PIR responses were resistant to 0.5 μM TTX but blocked by 200 μM Ni^{2+}. Current commands are shown as lowermost traces in *A*–*C*. Firing pattern type: T cells for *A* and *B*; non-P_{SB} cell for *C*.

in steps t

suggestir

tested (1(

rise of m

8C), simi

7Ab, left

(Figure 2

A

characteri

[7 = 6 pA

representa

all cells in

significant

Mean I_T e

that in toni

in Appendi

0.0002) tha

in steps to membrane potential below –70 mV in 60% of neurons exhibiting PIR (15/25), suggesting the presence of a hyperpolarization-activated cation current (I_h). For all cells tested (100%, n = 23), the rebound depolarization increased in amplitude as the rate of rise of membrane voltage during the return to resting potential became steeper (Figure 2-8*C*), similar to the responses of phasic cells to ramp-hold depolarizing currents (Figure 2-7*Ab*, left). The rebound depolarization was resistant to TTX but blocked by Ni^{2+} (n = 2) (Figure 2-8*C*) and MIB (n = 2; not shown).

As we expected, I_T was observed in the majority of dorsal horn neurons characterized in current-clamp (95%, n = 36/38) with considerable variation in amplitude [7 ± 6 pA/pF (SD); range 1 pA/pF to 36 pA/pF]. Examples of I_T recorded from representative cells of each firing pattern class are shown in Figure 2-9, and the data from all cells in the sample is summarized in Tabel 2-1. Average I_T density in phasic cells was significantly greater than in delay cells, but comparable to I_T in tonic neurons (Tabel 2-1). Mean I_T expressed in P_{SB} cells was 2.3-fold greater than in non-P_{SB} cells and exceeded that in tonic and delay cells by comparable amounts (Tabel 2-1; also refer to Figure A-2 in Appendix). I_T was significantly larger in cells exhibiting PIR (9 ± 1 pA/pF, n = 25; P = 0.0002) than in those neurons without PIR (2 ± 1 pA/pF, n = 8).

Figure
Dorsal
depolar
and 10
in norm
median
P_{SB}, sh
(D): 13
pA pF (
baseline

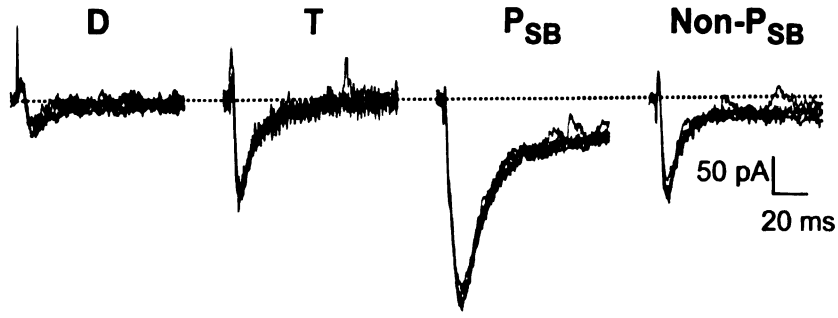

Figure 2-9. I_T in neurons with identified firing patterns

Dorsal horn neurons were voltage clamped at a V_h of –90 mV and I_T was evoked by depolarizing voltage steps to –30 mV. External bathing solution contained 3 mM Ba^{2+} and 10 μM Cd^{2+} and was added after firing pattern characterization under current clamp in normal ACSF (see METHODS). Five traces were superimposed and illustrate the median I_T amplitude for each firing pattern classification (categories: D, delay; T, tonic; P_{SB}, short burst phasic; Non-P_{SB}, non-short burst phasic). Median I_T amplitudes: 31 pA (D); 134 pA (T); 244 pA (P_{SB}); 116 pA (non-P_{SB}). I_T density in examples shown: 1 pA/pF (D); 6 pA/pF (T); 8 pA/pF (P_{SB}); 4 pA/pF (non-P_{SB}). Dotted line indicates the baseline for inward current measurements.

Discussion

Our result
earlier stu
Here, we p
to depolari
potentials.
demonstra
dependent
(Crunelli *e*
phasic-firir
movements
and respons
type Ca^{2+} c
an importan
time-varyin

We f
which is hig
Randic (199
may reflect a
ionic mechan
consistent wit
horn (Talley *e*
suggests that e

Discussion

Our results show that dorsal horn neurons possess T-type Ca^{2+} currents, consistent with earlier studies (Ryu and Randic, 1990; Huang, 1989; Russo and Hounsgaard, 1996a). Here, we presented new findings suggesting I_T expression is highest in cells that respond to depolarizing current injection with a rapidly adapting discharge of one or two action potentials, and lowest in neurons with tonic or delayed-firing properties. Furthermore, we demonstrated for the first time that activation of I_T in dorsal horn neurons is strongly dependent on the rate of membrane depolarization, similar to I_T reported in thalamic cells (Crunelli *et al.*, 1989). We believe this property contributes to selective excitation of phasic-firing dorsal horn neurons by rapid membrane depolarizations and stimulus movements (Schneider, 2003, 2005). This conclusion is based on our observation that I_T and responses of phasic cells to ramp membrane depolarizations are blocked by the T-type Ca^{2+} channel antagonists Ni^{2+} and mibefradil. Taken together, our results support an important role for I_T in helping dorsal horn neurons differentiate between static and time-varying afferent input (Schneider, 2005).

We found that nearly all neurons in the hamster dorsal horn (98%) exhibit I_T, which is higher than the proportion of rat LII–V neurons (72%) reported by Ryu and Randic (1990) to have low-voltage-activated Ca^{2+} currents under similar conditions and may reflect a species-dependent difference. Both studies suggest that I_T is a ubiquitous ionic mechanism regulating neuronal excitability in the spinal dorsal horn and are consistent with widespread expression of T-type Ca^{2+} channel transcripts in the dorsal horn (Talley *et al.*, 1999). Our data showing wide variance in I_T current density strongly suggests that expression of I_T by dorsal horn neurons is non-uniform. Modeling studies

have in

influen

differe

electric

measur

dendrit

section

slice su

protoc

activat

The I_T

ranges

(Niesp

(Moug

was sh

rat dor

voltag

potent

(1990)

curren

studies

subtyp

have indicated that subtle changes in T-type Ca^{2+} channel density can have a potent influence on neuronal electrical activity (Chorev *et al.*, 2006). Thus, we might expect that differences in T-channel density would also have substantial effects on neuronal electrical behavior and integrative properties of dorsal horn networks. However, our measurements may not take into account the contribution of T-type Ca^{2+} channels with a dendritic distribution (Destexhe *et al.*, 1998) that may have been removed during the sectioning process, as is typically the case for recordings made from neurons near the slice surface.

Despite differences in divalent cation concentrations and voltage clamping protocols, the I_T expressed in hamster dorsal horn neurons resembles low-voltage-activated, transient Ca^{2+} currents reported in other neurons recorded from brain slices. The I_T in this study has broadly similar steady-state activation and inactivation voltage ranges as T-type Ca^{2+} currents found in thalamus (Crunelli *et al.*, 1989), hypothalamus (Niespodziany *et al.*, 1999), suprachiasmatic nucleus (Kim *et al.*, 2005) and cerebellum (Mouginot *et al.*, 1997). Steady-state inactivation ($V_{1/2} = -74$ mV) in the present study was shifted by about 12 mV more positive in comparison with that reported previously in rat dorsal horn neurons (Ryu and Randic, 1990). This shift may reflect the stronger voltage (−30 mV versus −45 mV) used to activate I_T; a relatively more depolarizing potential for inactivating half of the current is therefore to be expected. Ryu and Randic (1990) also reported a more potent Ni^{2+} blockade (91%) of the low-threshold Ca^{2+} current (versus 52% in the present study). The Ni^{2+} concentration (200 μM) used in both studies was sufficient to produce half-blockade of the three known T-type channel subtypes (Lee *et al.*, 1999b). However, Ni^{2+} blockade is voltage-dependent, with less

block at th

found that

reported f

2002: Kim

half (47% o

One is tha

Ca^{2-} as th

cells recor

neurons.

T-type cal

Involveme

injection c

2008: Sun

dorsal hor

hamster d

T-type Ca

potentials

of PIR typ

which arou

be evoked

that require

that block

block at the –30 mV test potential used in the present studies (Lee *et al.*, 1999b). We also found that potency of the T-channel antagonist mibefradil was lower than what has been reported for other neurons (Viana *et al.*, 1997; McDonough and Bean, 1998; Lee *et al.*, 2002; Kim *et al.*, 2005). In the present study, mibefradil (5 μM) decreased I_T by about half (47%). There are two explanations for the lower mibefradil potency in our studies. One is that mibefradil may be less efficacious as a T-channel blocker when Ba^{2+} replaces Ca^{2+} as the charge carrier (Martin *et al.*, 2000). Another possibility is that drug access to cells recorded in slice preparations may be lower than in preparations using isolated neurons.

T-type calcium currents and postinhibitory rebound (PIR)

Involvement of low-voltage activated Ca^{2+} channels in rebound firing following an injection of hyperpolarizing current has been reported for many neurons (Israel *et al.*, 2008; Sun and Wu, 2008; Alviña *et al.*, 2009) and has also been described for turtle dorsal horn cells (Russo and Hounsgaard, 1996a). We found PIR in the majority (76%) of hamster dorsal horn neurons we recorded and associated this property with activation of a T-type Ca^{2+} current for the following reasons. First, PIR was activated at membrane potentials of –45 mV to –60 mV, falling in the range for I_T activation. Second, generation of PIR typically required prior membrane hyperpolarizations near –80 mV, a voltage at which around 60% of I_T is available for activation (Figure 2-2*C*). Third, PIR could only be evoked by fast membrane depolarizations (Figure 2-7*B*) with d*V*/d*t* consistent with that required to activate I_T. Finally, PIR was blocked by Ni^{2+} and MIB at concentrations that block T-type channel activation. It should be noted that hyperpolarization-activated

cation

I_h-lik

2002

a maj

perfo

that I_h

seems

prese

Low-

firing

Rhyth

Eeble

under

perspe

that a

Schne

depol

the T-

Ionic

I_T has

neuron

cation currents (I_h) may also contribute to rebound firing (van Welie *et al.*, 2006) and an I_h-like current has been reported in rat superficial dorsal horn neurons (Grudt and Perl, 2002). We also observed an I_h-like sag in voltage responses to hyperpolarizing current in a majority cells with PIR (Figure 2-8*B*). Since our current clamp recordings were performed without blocking Na^+, K^+ or Ca^{2+} currents, we cannot rule out the possibility that I_h also contributes to rebound firing documented in our experiments. However, I_h seems unlikely to be the only ionic mechanism of PIR since rebound firing could be present in the absence of voltage sag.

The functional significance of PIR in spinal dorsal horn neurons is uncertain. Low-threshold Ca^{2+} channel-mediated PIR has been suggested to influence rhythmic firing behavior of neurons in the thalamus and other brain regions (Huguenard, 1996). Rhythmic firing can be recorded from dorsal horn neurons *in vivo* (Sandkühler and Eeblen-Zajjur, 1994) but is not normally characteristic of hamster dorsal horn neurons under standard *in vitro* conditions (Schneider, unpublished observations). From the perspective of encoding afferent information related to stimulus velocity, it is possible that activation of local inhibitory pathways (Lu and Perl, 2003; Yasaka *et al.*, 2007; Schneider, 2008) could amplify the sensitivity of dorsal horn neurons to rapid membrane depolarizations by hyperpolarizing the membrane potential and removing inactivation of the T-current.

Ionic basis of phasic dorsal horn neuron responses to rapid membrane depolarizations

I_T has been implicated for a long time in the production of oscillatory behavior of CNS neurons (see Huguenard, 1996). Our present findings strongly suggest that I_T also

contribute

selectively

to the skin

exceeded ~

phasic-firi

sensitive a

with assoc

channel an

phasic neu

ramps and

The

bears a stro

Ca^{2+} curren

depolarizati

olfactory re

exceeding 3

(Crunelli *et*

reverse the r

are fewer ch

amplitude at

2001). It sho

dorsal horn n

for thalamic

contributes to the striking ability of phasic-firing dorsal horn neurons to respond selectively to fast membrane depolarizations and signal rapid mechanical stimuli applied to the skin (Schneider, 2003, 2005). First, activation of I_T began only when dV/dt exceeded ~ 46 mV/s and increased in amplitude with the speed of depolarization. Second, phasic-firing cells expressed the highest I_T density in the dorsal horn. Third, rate-sensitive activation of I_T under voltage clamp conditions and a transient depolarization with associated action potential discharge under current clamp are blocked by the T-channel antagonists Ni^{2+} and MIB. These results are in line with previous findings that phasic neurons in Rexed's LIII–V are selectively excited by fast depolarizing current ramps and rapidly-moving stimuli applied to the skin (Schneider, 2003, 2005).

The activation of I_T by voltage ramps that we describe for dorsal horn neurons bears a strong resemblance to T-type Ca^{2+} currents characterized in other cells. T-type Ca^{2+} currents that are activated from hyperpolarized resting potentials by rapid ramp depolarizations have also been described in glomerulosa cells (Várnai *et al.,* 1995) and olfactory receptor neurons (Kawai and Miyachi, 2001). Membrane depolarizations exceeding 30 mV/s are required for activating an I_T in cat lateral geniculate neurons (Crunelli *et al.*, 1989). In thalamic cells, voltage ramps of lower velocity appear to reverse the removal of T-channel inactivation by a prior hyperpolarization, so that there are fewer channels available for activation, resulting in a diminishing of the current amplitude at slower membrane depolarizations (Crunelli *et al.,* 1989; Guiterrez *et al.,* 2001). It should be noted that cell-to-cell variability in I_T activation threshold for hamster dorsal horn neurons (46 ± 21 mV/s) is greater than that reported by Crunelli *et al.* (1989) for thalamic cells (30 ± 2 mV/s). Furthermore, the sensitivity of dorsal horn neurons to

rate of me

4*B*). These

differing i

Th

certain do

ionic mech

membrane

than for ac

suggesting

2-1). Safro

accounting

resembles a

1998; Mag

reported an

activated by

current has

contribute t

present stud

The

depolarizati

dendrotoxin-

of phasic-fir

(Ferragamo a

rate of membrane depolarization showed considerable variability between cells (Figure 2-4*B*). These differences could reflect differential expression of T-channel subunits differing in activation kinetics (Chemin *et al.*, 2002; Talley *et al.*, 1999).

The present findings support a major involvement of I_T in shaping the ability of certain dorsal horn neurons to signal dynamic membrane depolarizations, although other ionic mechanisms may also contribute to this ability. Our results showed that the rate of membrane depolarization for activating P_{SB} and non-P_{SB} cells was significantly higher than for activating tonic and delay cells. However, I_T was elevated only in P_{SB} cells, suggesting that another mechanism may underly rate sensitivity in non-P_{SB} cells (Tabel 2-1). Safronov *et al.* (1997) described a slowly-inactivating, TTX-sensitive Na^+ current accounting for ~ 5 – 20% of total Na^+ current in rat dorsal horn neurons that broadly resembles a persistent Na^+ current (I_{NaP}) activated near ~ –65 mV (Parri and Crunelli, 1998; Magistretti and Alonso, 1999; Magistretti *et al.*, 2006). Recent studies have reported an I_{NaP} in spinal lamina I neurons and ventral horn motoneurons that are activated by voltage ramps (Prescott and De Koninck, 2005; Kuo *et al.*, 2006). This current has a slower threshold (~ 10 mV/s) for ramp activation than I_T but could contribute to neuronal excitation over the range of ramp depolarizations used in the present study.

The sensitivity of phasic-firing dorsal horn neurons to rate of membrane depolarization may also be influenced by activation of K^+ currents. A low-threshold, dendrotoxin-sensitive K^+ conductance has been reported to underlie selective responses of phasic-firing neurons in the ventral cochlear nucleus to rapid depolarizations (Ferragamo and Oertel, 2002). Other voltage-gated K^+ channels (M-type) that are

inhibited by the cholinergic agonist muscarine have been reportedly expressed by dorsal horn neurons (Rivera-Arconada and Lopez-Garcia, 2005). Recent modeling studies suggest that activation of M-type currents can increase spike-frequency adaptation and enhance neuronal responses to fast inputs (Prescott and Sejnowski, 2008). Because of its relatively slow kinetics, the M-current may only permit high frequency signals to drive membrane depolarizations leading to firing.

Functional significance

Our recordings establish the ubiquity of a low-threshold, transient Ca^{2+} current in spinal dorsal horn neurons. However, it is clear from the data that I_T is most strongly expressed within a subpopulation of phasic-firing cells. I_T may thus be essential for the signaling of information related to stimulus velocity within the dorsal horn intrinsic network (Schneider, 2003, 2005). Our previous studies showed that cells in dorsal horn LIII–V that are selectively excited by rapid membrane depolarizations are interneurons with short, longitudinally oriented axons and establish local circuit connections with neighboring cells (Schneider, 2003, 2008). However, I_T may be also expressed to a lesser extent in other functional types of dorsal horn neurons, as low-threshold Ca^{2+} currents have also been reported in output cells having ascending axonal projections to the thalamus (Huang, 1989; Ikeda *et al.,* 2003).

The molecular counterparts of I_T that participate in velocity-sensitive responses of dorsal horn neurons have not been identified. However, mRNA transcripts of the T-type Ca^{2+} channel subfamily, $Ca_V3.1$, $Ca_V3.2$ and $Ca_V3.3$, have been reported in rat spinal dorsal horn (Talley *et al.,* 1999). Cloned $Ca_V3.1$ and $Ca_V3.2$ channels generate large,

rapidly inactivating currents (Chemin *et al.*, 2002) that are well-suited to the short burst firing exhibited by phasic dorsal horn neurons sensitive to high rates of dV/dt and thus may contribute to the proposed velocity encoding function of these cells. Interestingly, the $Ca_V3.2$ channel isoform has been found to be expressed by D-hair receptors, a class of vertebrate cutaneous mechanoreceptor, and could underlie their high sensitivity to moving stimuli applied to the skin (Shin *et al.*, 2003). Our results suggest that T-type channels may be integral components of specialized central dorsal horn circuits for processing information related to stimulus velocity.

Finally, the present results should be taken in context with other studies that have reported persistent cation currents in spinal neurons. Our findings do not exclude the possibility that activation of I_{NaP} contributes to the responses of phasic-firing dorsal horn neurons to dynamic membrane depolarizations. However, I_{NaP} appears to function principally in spinal neurons by enhancing responses to sustained excitatory inputs (Kuo, *et al.*, 2006). I_{NaP} expression is greater in tonic-firing dorsal horn neurons than in phasic-firing cells and prolongs responses to transient inputs, leading to an idea that persistent inward currents facilitate encoding of stimulus intensity (Prescott and De Koninck, 2005). Our results suggest that differential expression of transient and persistent inward currents in dorsal horn cells may contribute to differential processing of stimulus intensity and velocity information by functionally-defined spinal circuits (Schneider, 2005). These currents could be subject to actions by neurotransmitters, thus modulating integration of sensory information within the networks (Mittmann and Alzheimer, 1998; Gorelova and Yang, 2000; Chemin *et al.*, 2006).

CHAPTER THREE

A FAST INACTIVATING T-TYPE CALCIUM CURRENT IS INVOLVED IN SENSING MEMBRANE DEPOLARIZATION RATE BY SPINAL DORSAL HORN NEURONS

Introduction

The spinal dorsal horn, first central relay of somatic sensory system, plays an important role in integrating diverse sensory inputs encoded by primary sensory neurons innervating skin, muscle, joints, and internal organs (Willis & Coggeshall, 2004). The neurons in this area exhibit various electrophysiological properties, which as well as the intrinsic ionic conductances, determine how the sensory information is processed (*e.g.* Prescott and De Koninck, 2005). It has been shown previously that expression of T-type Ca^{2+} currents is associated with the selective responses of some phasic-firing dorsal horn neurons to rapidly-changing membrane depolarization caused by direct current injection (Schneider, 2003; Chapter 2) or fast-moving cutaneous stimuli (Schneider, 2005), and the rate-dependent activation of this current may be the underlying mechanism (Chapter 2).

Three pore-forming α_1 subunits ($Ca_V3.1$, $Ca_V3.2$, and $Ca_V3.3$) of T-type Ca^{2+} channels have been cloned (Cribbs *et al.*, 1998; Perez-Reyes *et al.*, 1998; Lee *et al.*, 1999a), and when expressed in HEK 293 cells, the recombinant channels generate low-voltage-activated Ca^{2+} currents with distinctive kinetic properties, which may contribute differently to neuronal excitability (Chemin *et al.*, 2002). Similarly, native T currents in thalamic neurons also show distinct activation and inactivation kinetics, and different physiological functions are proposed for these currents (Huguenard & Prince, 1992; Zhuravleva *et al.*, 2001; Joksovic *et al.*, 2005). In the spinal dorsal horn, mRNAs of all three Ca_V3 subunits are detected by *in situ* hybridization (Talley *et al.*, 1999). However, whether T currents in dorsal horn neurons exhibited heterogeneous properties is not clear, and neither were the molecular constituents of the currents in individual cells.

Therefore, in this study, I examined T-type Ca^{2+} currents in dorsal horn neurons from a hamster spinal cord slice preparation using whole-cell patch-clamp recordings. The currents were analyzed using an exponential stripping procedure to isolate the constituent current components. Cells were also characterized under current-clamp mode to compare expression of the current components and intrinsic firing properties. To identify the Ca_V3 subunit that mediate each current component, single cell RT-PCR was performed after electrophysiological recordings. The data show that a fast inactivating T-type Ca^{2+} current was selectively activated by fast membrane depolarization and highly expressed in rapidly-adapting phasic-firing dorsal horn neurons. This fast T current may underlie the ability of these cells to detect dynamic mechanical stimulation and is probably mediated by $Ca_V3.1$ channel subtype.

Methods

All protocols involving the use of animals were performed in accordance with the National Institutes of Health *Guide for the Care and Use of Laboratory Animals* and were approved by the Institutional Animal Care and Use Committee at Michigan State University.

Slice preparation

Spinal cord slices were prepared from 9- to 14-day-old Syrian hamsters of both sexes anesthetized with urethane (1.5 mg/g, intraperitoneal) as described previously (Schneider, 2003). Briefly, following the removal of vertebrae and meninges from the spine, a block of lumbosacral spinal cord was dissected and glued on the stage of a vibrating microtome (Vibratome 3000, St. Louis, MO), and 300-μm-thick transverse slices were cut slowly (<1 mm/min) at the maximum available vibration frequency. Dissection and slicing steps were carried out in cold (4–8°C) dissection solution containing (in mM) 179 sucrose or glycerol, 2.5 KCl, 0.2 $CaCl_2$, 10 $MgCl_2$, 1.25 NaH_2PO_4, 26 $NaHCO_3$, and 25 D-glucose (pH 7.35–7.45, 290–310 mOsm/l) equilibrated with 95% O_2–5% CO_2. The use of glycerol to replace sucrose in dissection solution to enhance viability of neurons was reported previously (Ye *et al.*, 2006), and no difference in neuronal electrophysiological properties was observed from the slices prepared using either of the solutions (Tables A-1 and A-2 in Appendix). Slices were then incubated in an oxygenated artificial cerebrospinal fluid (ACSF) containing (in mM) 120 NaCl, 2.5 KCl, 2.5 $CaCl_2$, 1.5 $MgSO_4$, 1.25 NaH_2PO_4, 26 $NaHCO_3$, and 10 D-glucose (pH 7.35–7.45; 290–310 mOsm/l) at room temperature for at least one hour before electrophysiological recording.

Electrophysiological recording

Four to six transverse spinal cord slices were obtained from each animal, and one dorsal horn neuron was recorded from each slice. For electrophysiological recording, slices were transferred to a chamber (volume, 1.5 ml) mounted on a fixed-stage microscope (Olympus BX51WI, Central Valley, PA) and continuously perfused at 5–6 ml/min with ACSF gassed with 95% O_2–5% CO_2. Patch recording electrodes were fabricated from borosilicate glass pipettes (N-51A, Drummond Scientific, Broomall, PA) and filled with internal solution containing (in mM) 130 K-gluconate, 5 NaCl, 1 $CaCl_2$, 1 $MgCl_2$, 11 EGTA, 10 HEPES, 2 Mg-ATP, and 0.1 Li-GTP (pH 7.3, 280–285 mOsm/l; DC resistances, 4–7 MΩ). T-type Ca^{2+} currents were isolated under voltage clamp using an external solution containing (in mM) 107 NaCl, 3 $BaCl_2$, 2 CsCl, 1.3 $MgCl_2$, 26 $NaHCO_3$, 10 D-glucose, 20 TEA, 0.5 μM TTX, and 10 μM $CdCl_2$ (pH 7.35–7.45; 290–310 mOsm/l) adopted from Ryu & Randic (1990). All recordings were performed at 27°C maintained by an in-line temperature controller (Warner TC-324B, Hamden, CT) within 4–5 h after dissection.

Recording locations were first identified at low power (10x) by using the *substantia gelatinosa* (lamina II), a thin translucent band under transillumination, as a visual landmark (Figure A-1*A* in Appendix). Individual cells were then approached under a 40x water immersion objective and infrared differential contract optics (Figure A-1*B* in Appendix). All recordings were initiated in voltage-clamp mode after nulling pipette offset and capacitance transients. After whole-cell recording configuration was established, cell capacitance [26 ± 9 pF (SD), n = 52] and series resistance [30 ± 9 MΩ (SD), n = 52] were compensated. Signals were amplified (0–5 kHz bandwidth) by an

Axopatch 1D amplifier (MDS Analytical Technologies, Toronto, ON, Canada) and saved to hard drive with a Digidata 1320A data acquisition system running pCLAMP 8 software (MDS Analytical Technologies). Membrane current exceeding −0.05 nA at a holding potential of –60 mV was usually indicative of an unstable recording configuration or poor cell condition, and these recordings were excluded from analysis. Prior to the isolation of T-type Ca^{2+} currents, the recordings were temporarily switched to current-clamp mode to examine the intrinsic properties of dorsal horn neurons using the procedure described previously (Chapter 2). T-type currents were isolated and recorded after voltage-clamp recordings resumed. Passive membrane current was corrected by the implementation of P/N leak subtraction, in which the cell is applied with a command waveform (or pulse "P") that is scaled down by a factor of 1/"N" for "N" times. For analysis, whole-cell currents were low-pass filtered at 500 Hz (Gaussian). In most cases, currents were expressed as current density (pA/pF) by dividing by whole-cell capacitance, an indicator of cell size and read directly from the potentiometer after neutralizing capacity transients.

To analyze T-type Ca^{2+} current components and estimate their amplitude, an exponential stripping procedure developed by Zhuravleva and colleagues (1999) was adopted. T-type current was activated at –30 mV from a potential of –90 mV held for 500 ms, and an averaged current trace from 3–5 trials was used for the analysis. In ten cells, a sustained residual current resembling high-voltage-activated Ca^{2+} current was recorded from a holding potential of –40 mV and therefore subtracted from the current activated from –90 mV before the analysis. The current trace was then converted to a semi-logarithmic plot of the current amplitude in a logarithmic scale along with the linear

time course. The current decay phase was fitted with linear functions, and the slope of the linear regression was used to determine the decay time constants of individual current components. The amplitude of a current component with slower decay was estimated by extrapolating the linear function to the current peak, and the amplitude of a faster-decayed current component was approximated by subtracting the slow current amplitude from the peak T-type current, as shown in Figure 3-1.

Drugs and chemicals

TTX was purchased from MP Biomedicals (Irvine, CA). Mibefradil (Ro 40-5967, dihydrochloride hydrate) was purchased from Sigma-Aldrich (St. Louis, MO). All other chemicals were purchased from either Sigma-Aldrich (St. Louis, MO) or Mallinckrodt Baker (Phillipsburg, NJ).

Single cell reverse transcription polymerase chain reaction (RT-PCR)

To identify the Ca_V3 subunit mediating T-type Ca^{2+} currents in dorsal horn neurons, single cell RT-PCR was carried out on the cells recorded in electrophysiological experiments. Gloves were worn throughout these experiments. Patch pipettes were sterilized, and the internal solution was made with nuclease-free water (Fisher Scientific, Fair Lawn, NJ). Following the completion of whole-cell patch clamp recordings, the cell content of the neuron was aspirated into the patch pipette without loss of the seal (Figure A-1*C* in Appendix). The pipette tip was broken, and the contents (5–8 μl) were expelled into a PCR tube containing 5 μl of nuclease-free water (Fisher Scientific), 1 μl of dithiothreitol (DTT, 0.1 M, Invitrogen, Carlsbad, CA), 1 μl of RNase inhibitor (40 U/μl,

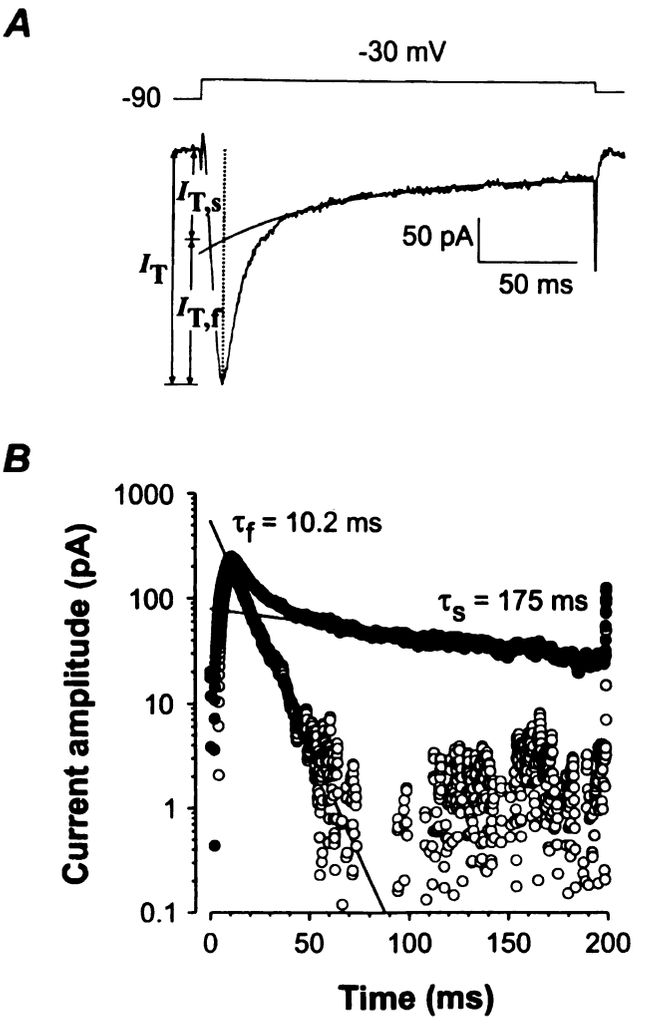

Figure 3-1. Analysis of T-type Ca^{2+} current components by using an exponential stripping procedure

A, a T-type Ca^{2+} current (I_T, lower trace) composed of a fast ($I_{T,f}$) and a slow current component ($I_{T,s}$) was activated from a representative dorsal horn neuron by the voltage command shown above the trace. A single-term exponential fitted to $I_{T,s}$ decay is superimposed on the current trace and extended to the beginning of the inward current. The vertical dotted line indicates the time of the current peak, at which the amplitude of $I_{T,s}$ is estimated by extrapolation of the fit. The amplitude of $I_{T,f}$ is obtained by subtracting the $I_{T,s}$ amplitude from the peak amplitude of I_T. *B*, the current trace in *A* was converted to a semi-logarithmic plot, and the current decay phase was fitted with two linear functions. The decay time constant of $I_{T,f}$ (τ_f) and $I_{T,s}$ (τ_s) was derived from the slope of the linear functions and indicated on the plot.

Promega, Madison, WI) and 1 μl of random hexanucleotides (0.5 μg/μl, Promega). The tube was placed immediately in dry ice and then stored at −80°C. Reverse transcription was carried out as previously reported (Han *et al.*, 2005) with minor modification. The cell content mixture was heated to 70°C for 10 min and quickly chilled on ice. After brief centrifugation, the solution was mixed with 4 μl of 5X First-Strand Buffer (250 mM Tris–HCl, 375 mM KCl, 15 mM $MgCl_2$, Invitrogen), 1 μl DTT (0.1 M, Invitrogen), 1 μl mixed deoxynucleotide triphosphates (dNTPs, 10 mM, Invitrogen), and 1 μl SuperScript™ II reverse transcriptase (RT, Invitrogen). Following 10-min incubation at room temperature, the solution was warmed to 42°C for 50 min for cDNA synthesis. The reaction was terminated by heating at 70°C for 15 min, and RNase H (2 U/μl, Invitrogen) was added to remove RNA from the RNA-DNA hybrid. The single cell cDNA was then stored at −20°C until used in PCR.

The presence of glyceraldehyde-3-phosphate dehydrogenase (GAPDH) cDNA was first examined using real-time PCR to confirm success in cell harvesting and reverse transcription. For GAPDH-positive single cell samples, a two-step PCR protocol was carried out to detect the cDNA of three known Ca_V3 subunits. The first amplification for all Ca_V3 cDNAs was performed on a TGradient thermocycler (Biometra, Goettingen, Germany), and the product was diluted 10 times and used in the subsequent real-time PCR using an inner forward primer specific to one of the Ca_V3 subunit cDNAs.

For the first-step of the Ca_V3 PCR, one 50-μl reaction mixture was prepared for each single cell sample and contained 25 μl of PCR Master Mix (Promega), 5 μl of single cell cDNA template, and the outer primers: Ca_V3 forward, 5'-CGCTCCAGCCGGAACA GC-3'; Ca_V3 reverse, 5'-GCAATGGTGATACAGTTGAGGA-3'. The reaction went

through 40 cycles of 95°C for 1 min, 53°C for 1 min, and 72°C for 1 min. Real-time PCR was performed with the Stratagene Mx3000P® QPCR system (Agilent Technologies, Santa Clara, CA) using SYBR® GreenER^{TM} qPCR SuperMix (Invitrogen). Triple 25-μl reactions with 2 μl of cDNA or diluted PCR product template were prepared for each cDNA examined. The amplification proceeded with the following profile: 50°C for 2 min and 95°C for 10 min, followed by 45 cycles (50 cycles for GAPDH) of 95°C for 30 s, 60°C for 1 min, and 72°C for 30 s. The sequences of the primers used are as follows: GAPDH forward, 5'-AGCAATGCATCCTGCACCACCA-3'; GAPDH reverse, 5'-ACAGCCTTGGCAGCACCAGT-3'; $Ca_V3.1$ forward, 5'-GCTTCCTGCCTGTTGCCG AG-3'; $Ca_V3.2$ forward, 5'-TGCTCGAACCCTATGCTCC CC-3'; $Ca_V3.3$ forward, 5'-GCAGAATGCCCAACATCGCCA-3'. The Ca_V3 reverse primer was paired up with the subunit-specific forward primers and used in the second-step semi-nested Ca_V3 PCR. All primers were designed by Primer3 (Rozen & Skaletsky, 2000) using reported cDNA sequences [DDBJ/EMBL/GenBank accession number: GAPDH, U10983; $Ca_V3.1$, AF027984 (rat); $Ca_V3.2$, AF290213 (rat); $Ca_V3.3$, AF086827 (rat)] and are intron spanning. The identities of the PCR-generated fragments were verified by electrophoresis and sequencing, and the melting temperature of the fragments was used for confirmation of specific amplification in real-time PCR. The sizes of the amplicons are (bp): GAPDH, 209; $Ca_V3.1$, 153; $Ca_V3.2$, 166; $Ca_V3.3$, 277. No amplification of GAPDH was detected in no-RT controls from reverse transcription. Negative controls without cDNA template and positive controls using total hamster spinal cord cDNA template were included in each PCR. Detection of a transcript was confirmed if the linear phase of the amplification plot crossed the fluorescence intensity threshold before reaching the 40th (or 45th for

GAPDH) amplification cycle (C_t < 40 or 45).

Statistics

Numerical data are presented as mean ± SEM unless noted otherwise. Statistical analysis was performed using InStat 3 (Ver 3.06, GraphPad Software, Inc., San Diego, CA). Nonparametric methods were adopted when one or more of the compared groups had less than five values or failed Kolmogorov-Smirnov normality test. Two groups were compared using the unpaired t test with Welch correction or Mann-Whitney (nonparametric) test as appropriate. Comparison of the means among three or more groups was conducted using one-way ANOVA with Tukey-Kramer multiple comparisons test or Kruskal-Wallis (nonparametric) one-way ANOVA with Dunn's multiple comparisons test. The criterion for statistical significance was a value of $P < 0.05$.

Results

Whole-cell recordings were made from a total of 52 dorsal horn neurons in spinal cord slices prepared from 35 hamsters. Membrane potential was held at –60 mV during voltage-clamp recordings unless otherwise noted for specific experiments. Neurons had resting membrane potentials of –50 mV or more hyperpolarized under current-clamp conditions.

Fast and slow T-type calcium currents in spinal dorsal horn neurons

T-type Ca^{2+} currents (I_T) are widely expressed in dorsal horn neurons (Ryu and Randic, 1990; Chapter 2) though the current density varies considerably from cell to cell (Chapter 2). I also observed substantial variations in I_T kinetics and surmised that more than one type of T-channel mediates I_T in dorsal horn neurons. In addition, the inactivation of I_T was better described with a double or triple exponential in most of the cases (77%, n = 33), also suggesting that multiple types of T-channels co-exist in the same cells. By using the exponential stripping procedure (see METHODS, Figure 3-1), two I_T components were revealed in 29 (67%) out of 43 cells, while a third component was isolated from four other neurons, accounting for 9% of the sample. Ten (23%) of the analyzed cells had I_T inactivating in a single exponential term and presumably mediated by only one type of T-channel. The analysis yielded a total of eighty decay time constants (τ), and the distribution is shown in Figure 3-2*A*. This frequency histogram suggests that two types of I_T components are expressed in dorsal horn neurons. A fast-inactivating current component ($I_{T,f}$) had an averaged decay time constant (τ_f) of 12.0 ± 1.1 ms (n = 48, Figure 3-2*B*), and the slow current component ($I_{T,s}$) inactivated with a longer decay

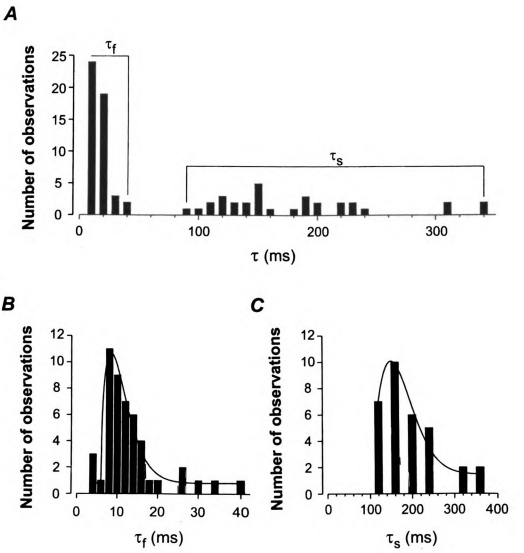

Figure 3-2. Distribution of the decay time constants of I_T current components in spinal dorsal horn neurons

A, eighty decay time constants (τ) of I_T current components analyzed from 43 dorsal horn neurons divide into two groups: τ_f (range, 2.7–38.2 ms) and τ_s (range, 81–339 ms). *B*, the smooth line indicates the best fit of τ_f distribution to the Weibull probability density function ($r^2 = 0.94$). *C*, τ_s is also best fitted with the Weibull distribution ($r^2 = 0.88$). Bar intervals: 10 ms for *A*; 2 ms for *B*; 40 ms for *C*.

time constant (τ_s) of 177 ± 12 ms (n = 32; *vs.*. τ_f, $P < 0.0001$; Figure 3-2*C*). The activation of individual components was assessed by measuring the 10% to 90% rise time ($t_{10\text{-}90}$) of the inward current in the cells expressing only one current component, and the $t_{10\text{-}90}$ for $I_{T,f}$ and $I_{T,s}$ was 5.2 ± 0.8 ms (n = 7) and 14.3 ± 3.0 ms (n = 3), respectively. The amplitude of $I_{T,f}$ was 4.6 ± 0.7 pA/pF (n = 48), and $I_{T,s}$ had an average amplitude of 3.5 ± 0.4 pA/pF (n =32). Interestingly, two $I_{T,f}$ components with two different τ_f were sometimes observed in the same cells (n = 8) with or without the companion of a slowly-inactivating current component. Therefore, a number of components, rather than a number of cells, was given with the presentation of $I_{T,f}$ statistics.

After establishing a way to analyze $I_{T,f}$ and $I_{T,s}$ in dorsal horn neurons, I next examined the voltage-dependence of steady-state inactivation and activation of these current components. Inactivation kinetics were analyzed by stepping the membrane potential to −30 mV every 20 s in 10 mV increments from holding potentials of −120 mV to −70 mV held for 500 ms. Activation properties were studied by delivering 200-ms depolarizing voltage pulses (testing steps) in 10 mV increments from −50 mV to −10 mV following a holding potential of −90 mV. When activated from a holding potential more positive than −70 mV or at a testing step more negative than −50 mV, I_T was too small to be analyzed by the exponential stripping procedure and therefore absent from the results presented. Average normalized currents (I / I_{max}) were plotted as a function of holding potentials for inactivation or testing steps for activation (n = 3 for $I_{T,f}$; n = 2 for $I_{T,s}$) and fitted with the Boltzmann equation ($I / I_{max} = 1 / \{1 + \exp [(V - V_{1/2}) / k]\}$) (Figure 3-3). The half-inactivation potentials for $I_{T,f}$ and $I_{T,s}$ were −82 mV and −66 mV, respectively,

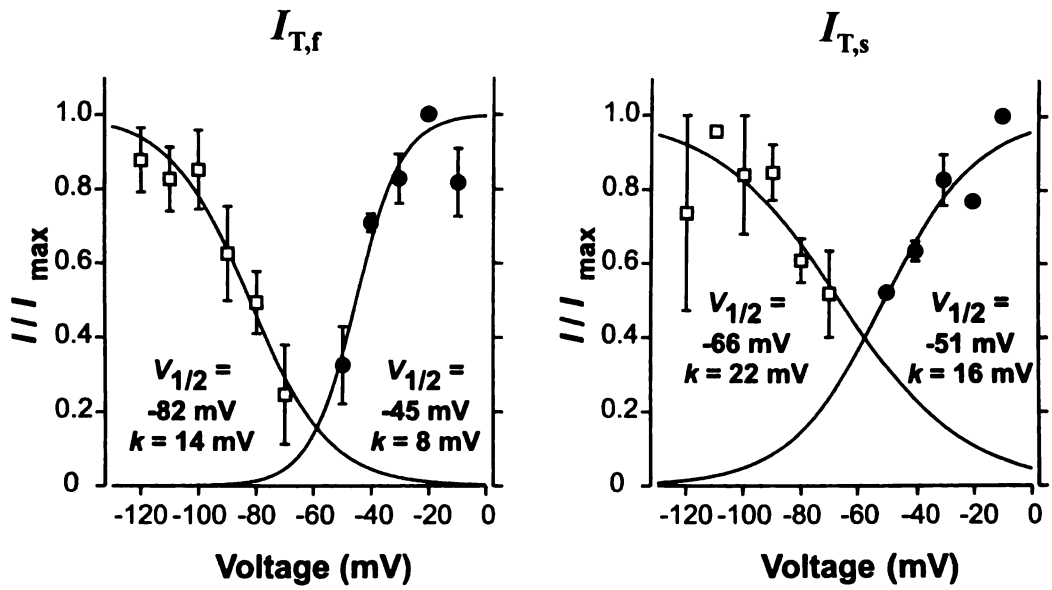

Figure 3-3. Voltage-dependent activation and inactivation of $I_{T,f}$ and $I_{T,s}$ in spinal dorsal horn neurons

Activation (●) and inactivation curves (□) were fitted with the Boltzmann equation ($I / I_{max} = 1 / 1 + \exp [(V - V_{1/2}) / k]$). $V_{1/2}$ and k are shown next to each curve. Error bars represent SEM ($n = 3$ for $I_{T,f}$ and $n = 2$ for $I_{T,s}$).

while the voltage required to activate half-maximal current was –45 mV for $I_{T,f}$ and –51 mV for $I_{T,s}$. These results are similar to what has been reported in a study using the same analysis strategy (Zhuravleva *et al.*, 2001).

Besides variations in current kinetics, $I_{T,f}$ and $I_{T,s}$ also showed differential sensitivity to Ni^{2+} blockade (Figure 3-4). Activated at –30 mV from a holding potential of –90 mV, the amplitude of $I_{T,f}$ was reduced by 51% ± 5% (n = 5) after 2–4 min exposure to 200 μM Ni^{2+}, while only 15% ± 11% (n = 5) of $I_{T,s}$ was blocked. Another I_T antagonist mibefradil generated comparable inhibitory effect on both current components (Figure 3-4). Treating dorsal horn neurons with 5 μM mibefradil for 5–8 min decreased $I_{T,f}$ by 52% ± 3% (n = 2) and $I_{T,s}$ by 37% ± 5% (n = 2).

Rate-dependent activation of fast T-type calcium currents in spinal dorsal horn neurons

It has been shown that the amplitude of I_T in dorsal horn neurons is dependent on the rate of membrane depolarization (dV/dt), a characteristic contributing to the ability of phasic-firing neurons to signal rapid membrane depolarization (Chapter 2). However, whether $I_{T,f}$ and $I_{T,s}$ behaved in the same way was unclear. I_T of three dorsal horn neurons possessing one $I_{T,f}$ component and one $I_{T,s}$ component were activated by ramping the membrane potential from a 500-ms hyperpolarizing pre-pulse of –90 mV to –30 mV at different rates ranging from 400 mV/s to 2400 mV/s. After they were isolated using the exponential stripping procedure, $I_{T,f}$ showed rate-dependent activation, while the amplitude of $I_{T,s}$ appeared independent of dV/dt (Figure 3-5). Linear regression analysis

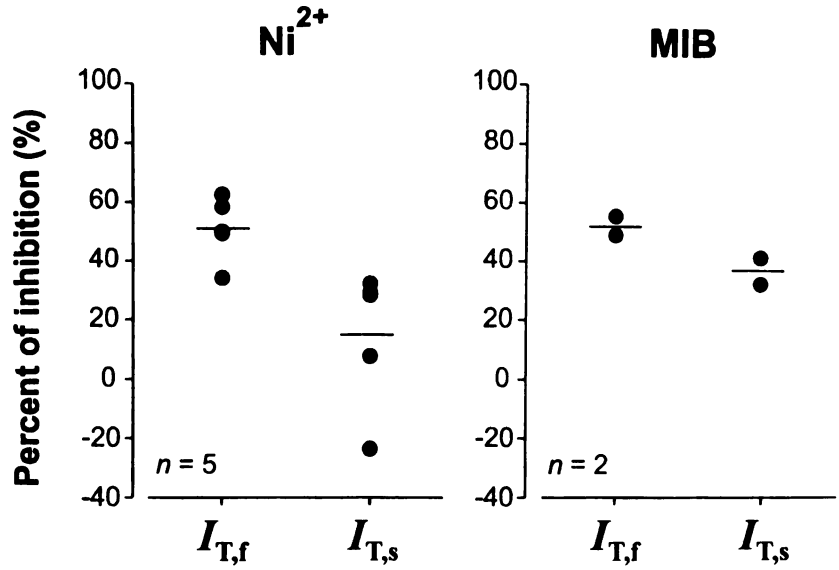

Figure 3-4. Inhibition of $I_{T,f}$ and $I_{T,s}$ in spinal dorsal horn neurons by T-type Ca^{2+} channel blockers

Each point was obtained from one dorsal horn neuron treated with either 200 μM Ni^{2+} or 5 μM mibefradil (MIB). The short horizontal bar indicates the average value of inhibition.

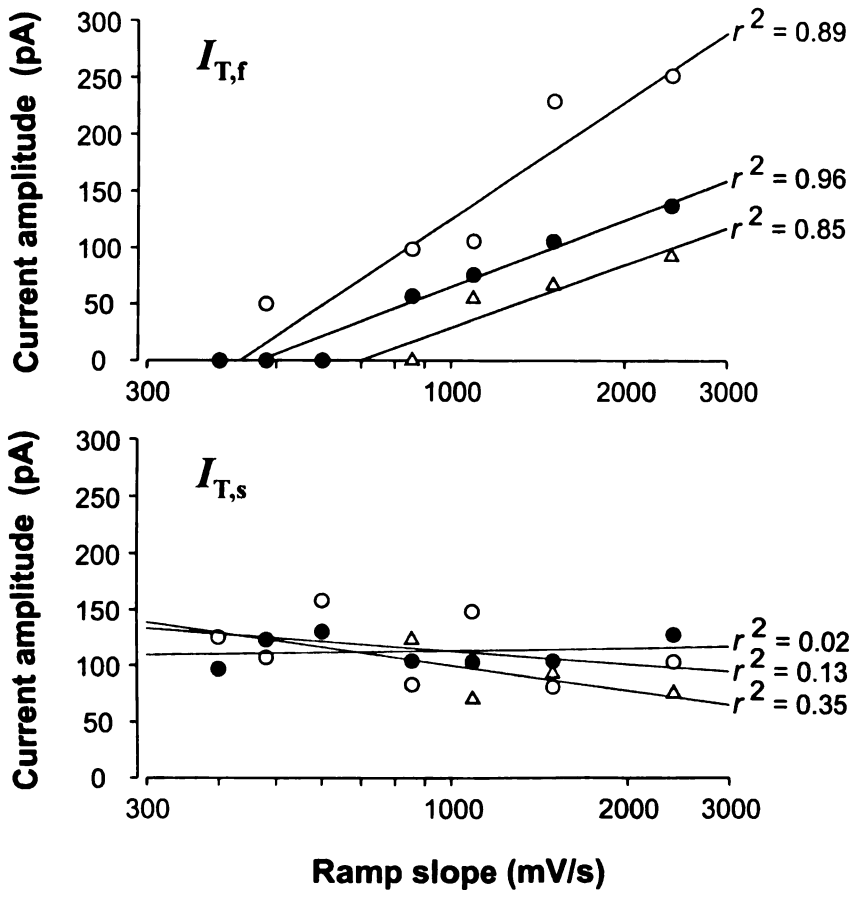

Figure 3-5. Rate sensitivity of $I_{T,f}$ in spinal dorsal horn neurons
The relationship between the amplitude of I_T current components and the ramp slope is described by a linear function for three dorsal horn neurons. The coefficient of determination (r^2) from linear regression analysis indicates that the $I_{T,f}$ amplitude and the slope are highly correlated, but the amplitude of $I_{T,s}$ does not parallel the change of the ramp slope.

indicated that 90% ± 3% (n = 3) of the $I_{T,f}$ amplitude was determined by dV/dt, and the activation threshold in these three cells, estimated from the x-intercepts, was 533 ± 83 mV/s (n = 3), higher than the value observed for the total T current (46 ± 21 mV/s) reported previously (Chapter 2).

Expression of fast and slow T-type calcium currents in spinal dorsal horn neurons with identified membrane and discharge properties

Having shown that $I_{T,f}$ could be the major current component responsible for the rate-sensitivity of I_T, I next examined the expression of $I_{T,f}$ and $I_{T,s}$ in dorsal horn neurons with different firing patterns. Non-uniform expression of I_T has been reported previously, with the highest current density in dorsal horn neurons responding to constant membrane depolarization with one or two action potentials (Chapter 2). It would be interesting to know if $I_{T,f}$ was also expressed more abundantly in these cells, which are preferentially activated by rapid membrane depolarization (Chapter 2).

Forty dorsal horn neurons used in the I_T component analysis above were categorized based on their firing behavior when activated by depolarizing current steps applied through the recording pipette. Three distinct discharge patterns were exhibited among these neurons as described previously (Schneider, 2003, 2005; Chapter 2). Tonic (T) cells (35%, n = 14) fired action potentials continuously throughout the period of depolarization (Figure 3-6*Ab*), while the prolonged discharge of delay (D) cells (8%, n = 3) followed a noticeable delay to the first action potential (Figure 3-6*Aa*). Phasic (P) cells (58%, n = 23) responded to depolarizing current steps with a rapidly adapting firing and were further divided into two subgroups based on the degree of spike frequency adaption.

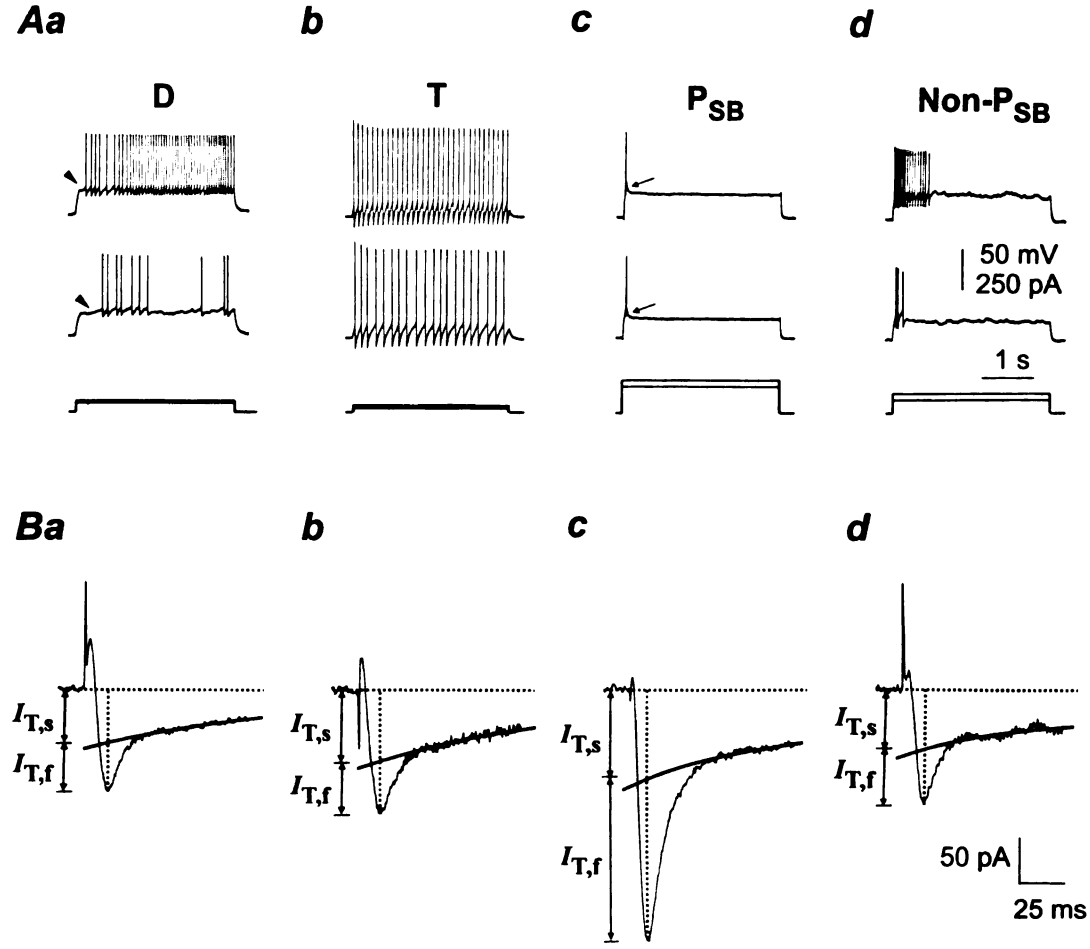

Figure 3-6. Firing patterns and I_T of spinal dorsal horn neurons

A, membrane responses of a representative cell from each group (top two traces) to depolarizing current pulses (lowermost trace) are shown. (Firing pattern groups: D, delay cells; T, tonic cells; P_{SB}, short burst phasic cells; Non-P_{SB}, non-short burst phasic cells) The arrowheads in *a* indicate the delay between pulse onset and first action potential in the delay cell. The transient membrane depolarization characteristic of P_{SB} cells is indicated by the arrows in *c*. *B*, I_T recorded from the same dorsal horn neurons in *A* was analyzed by an exponential stripping procedure, revealing one $I_{T,f}$ component and one $I_{T,s}$ component. The fit of $I_{T,s}$ decay with a single exponential overlays the current trace. The horizontal dotted line indicates the baseline for inward current measurement, and the vertical dotted line locates the peak of the current. Current density of $I_{T,f}$: 2.5 pA/pF for D; 2.7 pA/pF for T; 13.3 pA/pF for P_{SB}; 3.7 pA/pF for non-P_{SB}. $I_{T,s}$ density: 2.5 pA/pF for D; 3.3 pA/pF for T; 5.4 pA/pF for P_{SB}; 2.9 pA/pF for non-P_{SB}.

Short burst phasic (P_{SB}) cells (n = 7) were characteristic of one or two action potentials superimposed on a transient membrane depolarization when activated by depolarizing current injection (Figure 3-6*Ac*). The remaining non-P_{SB} phasic cells (n = 16) typically responded with 3 or more action potentials at rapidly diminishing frequency to depolarizing current pulses, and the number of spikes increased with stimulus amplitude (Figure 3-6*Ad*). I_T of these cells was activated at –30 mV from a holding potential of –90 mV, and the current components were analyzed by the exponential stripping procedure. The results of this analysis are summarized in Table 3-1, and examples of I_T current components recorded from representative cells of each firing pattern group are shown in Fig 3-6*B*. As expected, P_{SB} cells had two- to six-times higher $I_{T,f}$ current density than D, T, and non-P_{SB} cells did, while $I_{T,s}$ amplitude was fairly comparable among different firing pattern groups.

I also compared $I_{T,f}$ and $I_{T,s}$ expression in dorsal horn neurons with and without exhibition of postinhibitory rebound (PIR), a rebound membrane depolarization and discharge following hyperpolarizing current injection that has been associated with activation of T-type Ca^{2+} currents (Russo & Hounsgaard, 1996a; Chapter 2). Both $I_{T,f}$ and $I_{T,s}$ were significantly larger in cells showing PIR than in those neurons without PIR (Figure 3-7).

Table 3-1. Comparison of $I_{T,f}$ and $I_{T,s}$ in spinal dorsal horn neurons with different firing patterns

Firing pattern	D	T	P	P_{SB}	Non-P_{SB}
n	3	14	23	7	16
τ_f (ms)	9.0 ± 1.5 (3)	15.3 ± 2.6 (16)	10.0 ± 0.8 (26)	9.3 ± 1.2 (9)	10.3 ± 1.0 (17)
$I_{T,f}$ density (pA/pF)	1.6 ± 0.5 (3)	4.2 ± 0.9 (16)	5.1 ± 1.1 (26)[1]	9.0 ± 2.7 (9)[1,2,3]	3.0 ± 0.3 (17)
τ_s (ms)	171 ± 23 (2)	174 ± 18 (8)	180 ± 18 (20)	167 ± 26 (7)	187 ± 25 (13)
$I_{T,s}$ density (pA/pF)	1.9 ± 0.7 (2)	3.8 ± 0.9 (8)	3.5 ± 0.6 (20)	3.3 ± 0.8 (7)	3.6 ± 0.8 (13)

Data presented as mean ± SEM (cell number or component number for τ_f and $I_{T,f}$ density). [1] Significantly different from D cells. [2] Significantly different from T cells. [3] Significantly different from non-P_{SB} cells.

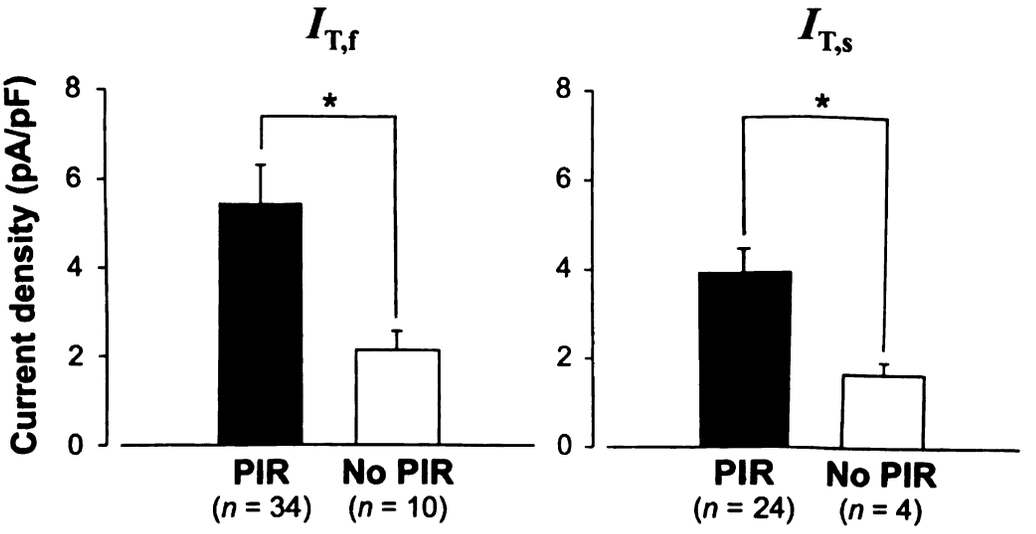

Figure 3-7. Comparison of $I_{T,f}$ and $I_{T,s}$ in spinal dorsal horn neurons with and without PIR

Bars show the mean current density of each group. Error bars represent SEM. * indicates the difference between two means is statistically significant.

Expression of Ca_V3 subunits in spinal dorsal horn neurons exhibiting fast and slow T-type calcium currents

In an attempt to identify the subunit type of T-type Ca^{2+} channels that mediate $I_{T,f}$ and $I_{T,s}$ in dorsal horn neurons, I performed single cell RT-PCR using the cells recorded in whole-cell configuration (see METHODS). Twenty-nine neurons were successfully harvested based on the detection of GAPDH cDNA. Ca_V3 subunit cDNAs were detected in 12 out of 27 cells expressing I_T in voltage-clamp recordings, and the results are summarized in Table 3-2. I_T from three cells was composed of only one $I_{T,f}$ component, and $Ca_V3.1$ cDNA was detected in all these neurons. In nine other cells, both $I_{T,f}$ and $I_{T,s}$ were expressed, but only one species of Ca_V3 cDNAs was amplified. An example of a $Ca_V3.1$ amplification plot resulting from a second-step real-time PCR is shown in Figure 3-8 along with I_T recorded from the same cell. No Ca_V3 subunit cDNA was detected in two cells in which I_T was absent in voltage-clamp recordings.

Table 3-2. Summary of the expression of T-type calcium channels in twelve spinal dorsal horn neurons

Cell	$I_{T,f}$	$I_{T,s}$	$Ca_V3.1$	$Ca_V3.2$	$Ca_V3.3$
080707-1	+	–	+	–	–
080708-1	+	–	+	–	–
080709-2	+	–	+	–	–
080523-1	+	+	+	–	–
080530-1	+	+	+	–	–
080619-1	+	+	+	–	–
080620-2	+	+	+	–	–
080718-1	+	+	+	–	–
080716-1	+	+	–	+	–
080605-3	+	+	–	–	+
080709-1	+	+	–	–	+
090212-4	+	+	–	–	+

I_T was recorded in whole-cell patch clamp experiments, and the current components $I_{T,f}$ and $I_{T,s}$ were assessed by using an exponential stripping procedure. The presence of Ca_V3 subunit mRNAs was examined using single cell RT-PCR. "+" indicates detection of a current component or subunit, while "–" shows no identification of the element.

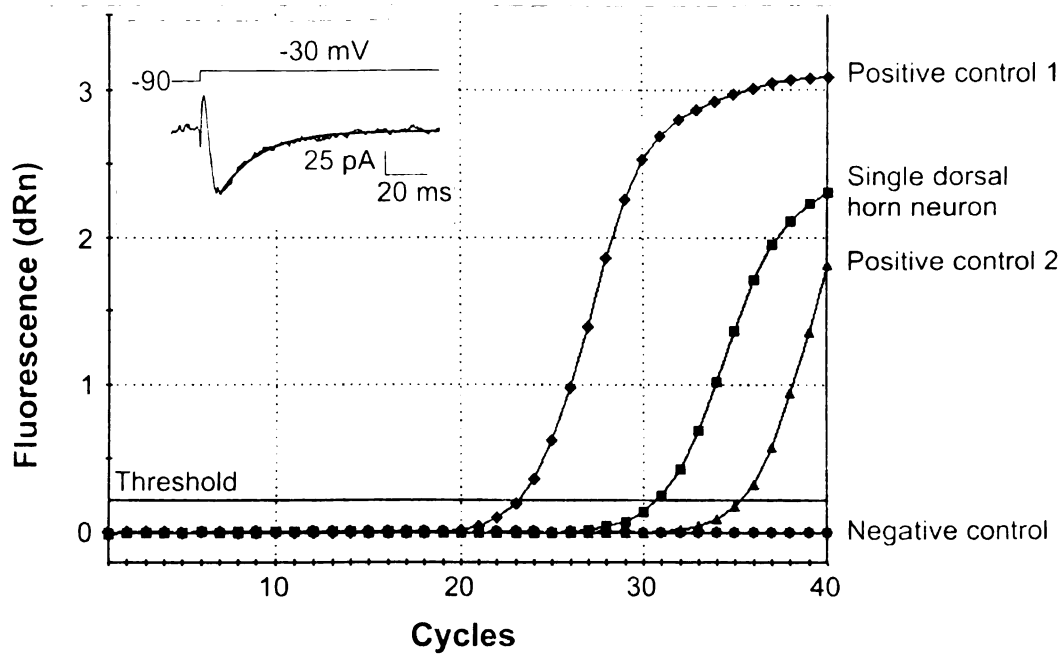

Figure 3-8. Detection of $Ca_V3.1$ subunit mRNA from a spinal dorsal horn neuron expressing I_T with one $I_{T,f}$ component

Amplification plots of $Ca_V3.1$ subunit fragments were generated from a real-time PCR experiment. Each measurement was averaged from three replicate reactions. The fluorescence signal normalized to the internal passive reference dye (ROX) is shown, and plots were base-lined by the MxPro software. Hamster spinal cord cDNA with (positive control 1) and without a previous Ca_V3 PCR amplification (positive control 2) was used as template in positive control. cDNA template was replaced with water in negative control. The threshold fluorescence value (indicated by the horizontal gray line) was determined by the MxPro software using an amplification-based algorithm, resulting in a threshold cycle (C_t) of 23, 31, and 35 for positive control 1, the single dorsal horn neuron, and positive control 2, respectively. Inset: the decay of I_T (lower trace) recorded from the same dorsal horn neuron can be fitted with a single exponential with τ equal to 20 ms.The voltage command used to activate the current is shown above the trace.

Discussion

In this study, I showed that spinal dorsal horn neurons possessed two types of T-type Ca^{2+} currents, differing in the time course of current decay. The fast inactivating current $I_{T,f}$ was expressed strongly in phasic-firing cells responding to depolarizing current injection with a brief discharge of one or two action potentials, while the expression of the slowly decaying current $I_{T,s}$ was rather uniform among dorsal horn neurons with different firing patterns. The amplitude of $I_{T,f}$, but not $I_{T,s}$, was dependent on the rate of membrane depolarization. This rate-sensitive property is shown by I_T in dorsal horn neurons (Chapter 2) and is associated with selective activation of phasic-firing cells by rapid membrane depolarization caused by direct current injection (Schneider, 2003) or peripheral sensory input (Schneider, 2005). Taken together, the results presented in this study suggest that expressing a fast-inactivating T-type Ca^{2+} current contribute to the ability of dorsal horn neurons to differentiate between afferent sensory inputs encoding static and dynamic cutaneous stimuli, and single cell RT-PCR experiments suggest that this current is mediated by $Ca_V3.1$ channels.

Fast and slow T-type calcium currents

Two kinetically and pharmacologically distinct T-type Ca^{2+} currents have been reported in thalamic neurons by different groups (Huguenard & Prince, 1992; Tarasenko *et al.*, 1997; Zhuravleva *et al.*, 1999, 2001; Joksovic *et al.*, 2005). In this study, I showed that a 'fast' and a 'slow' T-type Ca^{2+} current coexisted in spinal dorsal horn neurons. These two current types also had discrete activation and inactivation properties, as well as different sensitivity to Ni^{2+} blockade. $I_{T,f}$ showed 'classic' fast activation and

inactivation resembling to T currents recorded in other preparations, and the voltage-dependence of current kinetics was also similar to what has been reported for native low-voltage-activated Ca^{2+} currents (reviewed by Perez-Reyes, 2003). In contrast, $I_{T,s}$ rose and decayed more slowly (~3 and ~15 times longer for activation and inactivation, respectively, compared to $I_{T,f}$), and the steady-state activation and inactivation curves (Figure 3-3, right) indicates a larger 'window current' arising from these slow channels, similar to a slowly-inactivating T current reported in thalamic local circuit neurons (Zhuravleva *et al.*, 2001). In thalamic cells, window T current underlies membrane potential bistability, an important element of rhythmogenesis (Crunelli *et al.*, 2005). Spinal dorsal horn neurons are also capable of producing oscillatory activity under both *in vivo* and *in vitro* conditions (Sandkühler & Eblen-Zajjur, 1994; Ruscheweyh & Sandkühler, 2003; Asghar *et al.*, 2005); however, the contribution of T current to rhythmic behavior in these cells remains unknown. Alternatively, since most dorsal horn neurons had fairly comparable $I_{T,s}$ regardless of their ability to distinguish between different sensory inputs, this current could play an essential role in basic neuronal functionality, *e.g.* dendritic expansion and formation of new synaptic contacts (Zhuravleva *et al.*, 2001; Lory *et al.*, 2006).

Neuronal T currents show different sensitivity to Ni^{2+} blockade (Yunker, 2003), possibly due to heterogeneous Ca_V3 subunits constituting native T channels (Lee *et al.*, 1999b). In this study, I also found Ni^{2+} was more potent in blocking $I_{T,f}$ than $I_{T,s}$, consistent with what was reported in reticular thalamic neurons (Joksovic *et al.*, 2005). However, when treated with 100 μM Ni^{2+}, the slowly inactivating T current in thalamic local circuit cells was much more susceptible to blockade (56% *vs.* 15% inhibition by 200

μM Ni^{2+} in this study) (Zhuravleva *et al.*, 2001). Besides an easier access of Ni^{2+} to isolated cells used in Zhuravleva and colleagues' study, this discrepancy in Ni^{2+} sensitivity between different neuronal cells may also result from tissue-specific post-translational modifications and regulatory influences from auxiliary subunits. In fact, a slow T current mediated by cloned $Ca_V3.3$ channels also shows varied Ni^{2+} sensitivity when expressed in different cells (Lee *et al.*, 1999b). On the other hand, mibefradil had similar effects on $I_{T,f}$ and $I_{T,s}$ in this study, whereas it has been reported that this drug is equally efficacious on all three Ca_V3 subtypes, especially when Ba^{2+} is used as the charge carrier (Martin *et al.*, 2000).

Another difference between $I_{T,f}$ and $I_{T,s}$ found in this study is the relationship between the current amplitude and the rate of membrane depolarization that activated the current. The $I_{T,f}$ amplitude was correlated with the slope of depolarizing membrane potential ramps, while the magnitude of $I_{T,s}$ appeared to be rate-independent. I attributed this rate-sensitive property of $I_{T,f}$ to the same characteristic reported in I_T previously (Chapter 2), with one caveat. The activation threshold of I_T by voltage ramps is 46 mV/s (Chapter 2), but the threshold for $I_{T,f}$, estimated in the same way, was 533 mV/s. The discrepancy between these two results implies that $I_{T,s}$ might be also responsive to time-varying membrane depolarization with a slower range of rate. Given that $I_{T,s}$ had a longer decay time constant and voltage-dependent inactivation, this idea seems reasonable; however, further studies are required to validate it.

Molecular identity of fast and slow T-type calcium channels

When expressed in HEK 239 cells, $Ca_V3.1$ and $Ca_V3.2$ recombinant channels generate T-type Ca^{2+} currents with classic fast kinetics, while a slowly activating and inactivating low-voltage-activated current is generated by T channels with cloned $Ca_V3.3$ subunit (McRory *et al.*, 2001; Chemin *et al.*, 2002). In this study, the results of single cell RT-PCR experiments suggest that $I_{T,f}$ was mediated by $Ca_V3.1$ channels, and this is also supported by some findings obtained from voltage-clamp recordings. First, the time constant of $I_{T,f}$ decay is consistent with what has been reported for cloned $Ca_V3.1$ channels (McRory *et al.*, 2001; Chemin *et al.*, 2002). In addition, the sensitivity of $I_{T,f}$ to Ni^{2+} blockade is close to the current produced by the $Ca_V3.1$ channel isoform (IC_{50} = ~200 μM) (Lee *et al.*, 1999b). However, the 10% to 90% rise time of $I_{T,f}$ activation was longer in this study and is similar to the $Ca_V3.2$ subtype (Chemin *et al.*, 2002). The potential needed for half-activation and half-inactivation in $I_{T,f}$ is also comparable to that of cloned $Ca_V3.2$ channels reported by a previous study (McRory *et al.*, 2001). This contradiction can be explained by the discrepancies between native and cloned T-type channels that result from post-translational modifications and expression of splicing variants or auxiliary subunits, as suggested by previous studies (Zhuravleva *et al.*, 2001; Joksovic *et al.*, 2005). Alternatively, $I_{T,f}$ may rise from more than one type of T channels. Indeed, eight cells in this study had two $I_{T,f}$ components, and $Ca_V3.1$ and $Ca_V3.2$ mRNAs were both detected in cells possessing $I_{T,f}$. Therefore, this rapidly inactivating current could be mediated by the T-type Ca^{2+} channels with $Ca_V3.1$ or $Ca_V3.2$ subunit. Unlike $I_{T,f}$, $I_{T,s}$ so far has only one possible molecular counterpart being reported. Given that $Ca_V3.3$ mRNA was detected in dorsal horn neurons exhibiting $I_{T,s}$, it is probable that

this current was mediated by $Ca_V3.3$ channels, though it cannot be ruled out that a novel channel type also generates a slowly inactivating low-voltage-activated Ca^{2+} current.

Concluding remarks

The present study shows for the first time that two kinetically distinct T-type calcium currents are expressed in spinal dorsal horn neurons, and the fast current $I_{T,f}$ contributes to the ability of some phasic cells to sense rapidly-moving mechanical stimuli applied on the skin. The role of $I_{T,s}$ in dorsal horn neurons, however, is unclear at this point, though this slowly inactivating current may underlie the rebound depolarization or firing after the membrane potential of these cells returned from a hyperpolarized level. This rebound behavior suggests a mechanism for short-term plasticity based on previous neuronal activity (Uebachs *et al.*, 2006), and in the spinal dorsal horn, it has been proposed that the cells with T-current-mediated rebound bursting are capable of sensing the directionality of skin stimulation (Russo & Hounsgaard, 1996a). In conclusion, this study provides the evidence of a rapidly and a slowly inactivating T-type Ca^{2+} current co-existing in dorsal horn neurons. These currents may play different roles in the somatosensory functions carried out by these cells.

CHAPTER FOUR

SUMMARY AND DISCUSSION

A. Summary of experiments

My study on the role of T-type Ca^{2+} currents (I_T) in the sensory function of the spinal cord started with a re-examination of I_T in hamster dorsal horn neurons since this current has been reported in the same area in rats (Huang, 1989; Ryu & Randic, 1990). I_T from hamster cells, isolated using an external solution modified from a previous report (Ryu & Randic, 1990), had voltage-dependent activation and inactivation (Figure 2-2) and was blocked by Ni^{2+} and mibefradil (Figure 2-3) to the extent similar to other neuronal cells (reviewed by Perez-Reyes, 2003). Although I_T was present in the majority of dorsal horn neurons (> 95%), the current amplitude and kinetics varied from cell to cell. This finding led to the discovery of differential I_T expression among cells exhibiting distinct discharge properties and two I_T current components using an exponential stripping procedure (Zhuravleva *et al.*, 1999). I_T and its fast inactivating current component, $I_{T,f}$, could only be activated by depolarizing voltage ramps with slopes steeper than 46 mV/s and 533 mV/s, respectively, and the current amplitude was related to the rate of membrane depolarization (Figure 2-4*A,B* and Figure 3-5). In addition, the highest current density of I_T, as well as $I_{T,f}$, was found in phasic-firing dorsal horn neurons that fired one or two action potentials responding to depolarizing current injection (Tables 2-1 and 3-1). Phasic cells are preferentially responsive to rapid membrane depolarization that results from direct current injection (Schneider 2003; Figure 2-5*Bc,d*) or fast moving mechanical stimuli applied on the skin (Schneider, 2005). Moreover, the responses of phasic cells to depolarized membrane potential or ramps were inhibited by Ni^{2+} and mibefradil (Figure 2-7) at the concentration that also blocked I_T and $I_{T,f}$ (Figure 3-3). Therefore, the strong current expression in some phasic cells suggests that I_T, or more specifically $I_{T,f}$,

contributes to the ability of dorsal horn neurons to sense dynamic skin stimuli. Single-cell RT-PCR performed on the cells after whole-cell recordings indicates that $I_{T,f}$ is mediated by $Ca_V3.1$ channels. I also found a correlation between high I_T density and cells exhibiting rebound depolarization or discharge following a hyperpolarized membrane potential. This postinhibitory rebound (PIR) was sensitive to Ni^{2+}, and the activation was rate-dependent (Figure 2-8), suggesting the involvement of I_T. Further analysis indicates both $I_{T,f}$ and a slowly inactivating I_T current component $I_{T,s}$ contribute to this phenomenon. To summarize, my study confirmed the presence of T-type Ca^{2+} currents in the dorsal horn neurons of the spinal cord and their participation in a burst of discharge after membrane hyperpolarization previously reported in turtle dorsal horn neurons (Russo & Hounsgaard, 1996a). I proposed, based on the data, that this low-voltage-activated Ca^{2+} current underlies the differential capability of dorsal horn neurons to distinguish between static and dynamic skin stimuli by the mechanism of rate-dependent current activation, and this function is probably carried out primarily by a T-type current mediated by the $Ca_V3.1$ channel isoform.

B. Technical issues in single cell RT-PCR experiments

It has been a decade since three Ca_V3 subunits were cloned (Cribbs *et al.*, 1998; Perez-Reyes *et al.*, 1998; Lee *et al.*, 1999a); however, the *in situ* expression of T-type Ca^{2+} channel proteins has only been reported in a few studies (Latour *et al.*, 2003; Yunker *et al.*, 2003; Treviño *et al.*, 2004; Shao *et al.*, 2005; McKay *et al.*, 2006; Molineux *et al.*, 2006; Zhang *et al.*, 2006; De Proost *et al.*, 2007; Inagaki *et al.*, 2008), probably owing to '*in silico*' cloning of these channels (see Chapter 1). Immunolabeling of the Ca_V3

channel isoforms using antibodies developed by either research laboratories or commercial companies generated unexpected nuclear labeling that cannot be explained by the current knowledge of the T-type Ca^{2+} channel as a plasma membrane-associated protein (McKay *et al.*, 2006; Schneider, unpublished observations). Furthermore, a recent study demonstrates that an antibody that was anticipated to recognize specifically recombinant and endogenous $Ca_V3.3$ proteins cross-reacts with another neuronal membrane protein (Chen *et al.*, 2007), underlining the difficulty of correctly detecting these rather scarce channels by immunohistochemistry. Since selective blockers for T channels are currently unavailable (Huc *et al.*, 2009), in this study, I performed single cell RT-PCR to examine dorsal horn neurons that expressed I_T in voltage-clamp recordings and determine which Ca_V3 subunit mediated I_T in these cells.

Using a two-step PCR protocol (see METHODS in Chapter 3), I was able to detect all three subunit transcripts in the spinal dorsal horn, consistent with a previous report using *in situ* hybridization (Talley *et al.*, 1999). However, the finding from this analysis is inconclusive because only one subunit mRNA was identified in nine dorsal horn neurons that evidently expressed two kinetically distinct T currents. This could be explained by the degradation of targeted transcripts in the single cell samples owing to the unstable nature of mRNA molecules. However, some precautions had been taken during prior electrophysiological recordings. First, I limited the recordings to a maximum of 40 minutes since mRNAs are more likely to degrade when they are exposed to an exogenous solution during a prolonged recording process at room temperature. No difference in fact was observed in the recording time between the cells with detection of Ca_V3 mRNAs (mean ± SD, 34 ± 4 min, n = 12) and those without identification of these transcripts but

expressing I_T (35 ± 4 min, n = 15; P = 0.53, unpaired t test), suggesting that setting this recording time limit is effective. Because mRNAs could also be lost during the process of cell harvesting, in some experiments I used recording electrodes made from silanized glass pipettes to prevent mRNAs from adhering to the inner surface of the pipettes (Lin *et al.*, 2007). Although the detection rate of Ca_V3 mRNAs was higher when silanized pipettes were used (58% *vs.* 33%; Table A-4 in Appendix), contingency analysis indicates that coating the pipette surface is not the cause of better success in detecting the transcripts (P = 0.26, Fisher's exact test).

The inconclusive results could also be attributed to some uncertainty inherent in the design of this RT-PCR assay. Hamster spinal cord cDNA was used to optimize the protocol, but the copy number of each Ca_V3 subunit cDNA was unknown in these mixtures. As a result, it is difficult to estimate and therefore improve the efficiency of individual PCR. Theoretically, even a single copy of cDNA existing in the sample can be amplified and detected using PCR when given an adequate number of cycles; however, in reality it does not necessarily happen in this way owing to the Monte Carlo effect[2] (Karrer *et al.*, 1995). Therefore, the sparseness of Ca_V3 subunit transcripts in some single cell samples could cause the failure of detection. It is also uncertain whether any interaction, such as competition, occurs in the amplification of three Ca_V3 subunit cDNAs from single cell samples during the first step of PCR even though the 'outer'

[2] Monte Carlo effect: a limitation inherent in PCR amplification from any complex template of low abundance due to differences in amplification efficiency among individual template molecules. As a result, any PCR template diluted past a certain threshold of copy numbers will have large variations in amplification, and its true amount will be less likely reflected in the PCR product (Karrer *et al.*, 1995).

primers ('Ca_V3 forward' and 'Ca_V3 reverse') had the ability to recognize all three molecules in the cDNA sample obtained from the spinal cord tissue. Some competition for amplification among the three subunits seems possible cause because only one transcript was detected from each dorsal horn neuron, while the first step of PCR was the determinant of which subunit cDNA that got amplified (Ku & Schneider, unpublished observations).

C. T-type calcium currents in spinal sensory integration

I_T in lowering the threshold for firing

In this study, I hypothesized that I_T underlay the selective responses of phasic-firing dorsal horn neurons to fast membrane depolarizations caused by direct current injection (Schneider 2003, 2005) or rapidly moving skin stimuli (Schneider 2005). This idea was prompted by the observation that the amplitude of I_T in thalamic sensory neurons is dependent on the slope of depolarized membrane ramps (Crunelli *et al.*, 1989). This rate-sensitive activation is also found in I_T of dorsal horn neurons (Figure 2-4) and is attributed to more T-type Ca^{2+} channels going back to the inactivation state and becoming unavailable when the membrane potential is depolarized at slower speed (Crunelli *et al.*, 1989; Gutierrez *et al.*, 2001). In addition, I_T blockers Ni^{2+} and mibefradil are able to cease phasic firing and fast-ramp-evoked transient depolarization (Figure 2-7) at the concentration that also substantially inhibits I_T in dorsal horn neurons (Figure 2-3), further supporting my hypothesis. Meanwhile, these data also suggest that I_T may facilitate the initiation of firing at least in some dorsal horn neurons. It has been proposed that I_T can assist Na^+-mediated spike generation in neurons by lowing the threshold for

firing (Huguenard, 1996). I also noted from current-clamp recordings that a number of dorsal horn neurons were able to fire action potentials when the membrane potential was stepped, by direct current injection, to –40 mV or a more hyperpolarized level, at which no action potential current was recorded in the same cells under voltage-clamp mode. This phenomenon will be referred to as 'low-threshold-current-mediated action potentials' (LTAPs) in this document, and I speculated that I_T also contributed to LTAPs because of the subthreshold current activation. I think what happened was that the fast kinetics of I_T generated a depolarizing transient that briefly "leaped" the membrane potential to pass the threshold for voltage-gated Na^+ current activation in the beginning of an injected current pulse. This caused the cell to fire and left a rather hyperpolarized membrane potential observed at the end of the current pulse. This speculation was supported by a higher I_T density in dorsal horn neurons that were able to produce LTAPs than those without this capability (8 ± 2 pA/pF *vs.* 3 ± 1 pA/pF; Table A-5 in Appendix). When applied on phasic cells (presumably I_T-rich dorsal horn neurons), Ni^{2+} (200 μM) increased the threshold for firing (Ku & Schneider, unpublished observations). In addition, the observation of LTAPs was strongly associated with a postinhibitory rebound behavior in dorsal horn neurons ($P = 0.0033$, Fisher's exact test; Table A-6 in Appendix), also suggesting the involvement of I_T as a common mechanism. A similar idea has been reported in amphibian olfactory receptor cells, in which I_T is attributed to enhanced odor sensitivity by lowering the threshold for spike generation (Kawai & Miyachi, 2001).

In this study, not all phasic-firing dorsal horn neurons had the ability to produce LTAPs, consistent with the observation that phasic cells are a rather diverse group (Chapter 2). These LTAP-generating phasic cells may have lower threshold for

mechanical skin stimuli than those without LTAPs. The differential capability of producing LTAPs, and essentially the non-uniform expression of I_T, among phasic cells could be the reason why different conclusions were drawn from previous studies (Lopez-Garcia & King, 1994; Schneider, 2005) regarding the functional role of phasic firing dorsal horn neurons in sensory transmission (nociceptive specific *vs.* low threshold mechanical). I_T may, in turn, serve as a molecular marker for the dorsal horn neurons that are involved in processing sensory inputs from a certain type of primary sensory neurons, *e.g.* low threshold mechanoreceptors. It has been reported that large I_T mediated by the $Ca_V3.2$ channel subtype is uniquely expressed by D-hair receptors[3] and thus a useful marker for identification of these sensory cells (Heppenstall & Lewin, 2006). In D-hair receptors, I_T is proposed to contribute to the high sensitivity of these mechanoreceptors to slowly moving stimuli by "amplifying" the receptor potential and eventually leading to generation of action potentials (Shin *et al.*, 2003; Dubreuil *et al.*, 2004). Since it is possible that the receptor potentials evoked by slow skin stimuli are initiated by some mechanosensitive channels other than T-type Ca^{2+} channels (Heppenstall & Lewin, 2006), the function of I_T proposed in D-hair receptors does not necessarily contradict what was suggested by this present study for spinal dorsal horn neurons. However, it is also noteworthy that some small dorsal root ganglion cells also have large I_T that prominently arises from $Ca_V3.2$ channels and are C-thermonociceptors or C-

[3] D-hair receptors: mechanoreceptors that have an extremely low threshold, large branching receptive field in the skin, and conduction velocities of Aδ fibers. Their name comes from the observation in cats that these receptors can be selectively activated by moving small sinus or down hairs in the skin (Heppenstall & Lewin, 2006).

mechanonociceptors (Coste *et al.*, 2007), indicating a potential role of I_T in pain transmission (see Jevtovic-Todorovic & Todorovic, 2006 for a review).

I_T potentiation

Although this and previous studies have suggested that I_T play some role(s) in spinal sensory processing, a basic, but not so easy, question that has been left unanswered is whether T-type Ca^{2+} channels are able to function in a physiological condition. Using the data presented in this study as an example, the resting membrane potential of dorsal horn neurons is usually between −55 mV and −70 mV (Table 2-1), at which, by estimation no more than 10% of T-channels are available (de-inactivated) for activation (the inactivation curve in Figure 2-2*C*). To remove the inactivation, substantial and prolonged membrane hyperpolarization is required[4], making it uncertain whether dorsal horn neurons exhibit physiologically significant I_T *in vivo*. A possible answer to this question has recently been approached in sensory thalamocortical neurons, in which an ATP-dependent phosphorylation increases I_T amplitude and accelerates its inactivation (Leresche *et al.*, 2004). This potentiating process occurs only when T-channels are inactivated and therefore is able to facilitate I_T generation at resting membrane potential (where the majority of T-channels are inactivated) by reducing the number of channels required to recover from inactivation to produce a substantial I_T (Leresche *et al.*, 2004). I_T potentiation operates under the conditions in which few T-channels are available for activation and only weak depolarization is required (Bessaïh *et al.*, 2008), making it more

[4] For native T-type Ca^{2+} channels, to fully recover from inactivation requires a hyperpolarization to −90 mV for 100 ~ 3300 ms, depending on the type of different neuronal cells (Perez-Reyes, 2003).

likely a functional mechanism *in vivo*. Furthermore, I_T potentiation also enhances the occurrence and temporal precision of synaptically evoked burst firing in sensory thalamocortical neurons (Bessaïh *et al.*, 2008). This outcome is especially favorable to phasic cells, if I_T potentiation turns out also to modulate firing in dorsal horn neurons, since the discharge property of phasic cells is suited for coincidence detection, for which timely responses are essential (Prescott & De Koninck, 2002).

I_T de-inactivation

Although the potentiation mechanism provides a possibility for I_T to function under physiologically relevant conditions, a preceding hyperpolarization is still an imperative to de-inactivate the channels and make them available for activation. *In vivo*, hyperpolarized membrane potential can result from inhibitory postsynaptic potentials (IPSPs) or afterhyperpolarization (AHP). Low-threshold Ca^{2+} current has been proposed to contribute to fast afterdepolarization (ADP) in spinal lamina II neurons, which possibly follows, but may not be triggered by the prior AHP (Yoshimura & Jessell, 1989). The slower activation of the current, in contrast to spike-generating Na^{+} current, probably causes the presence of the Ca^{2+}-mediated transient depolarization as an afterpotential, which is still "conditioned" by resting membrane potential before spike generation (Yoshimura & Jessell, 1989). Although it appears unlikely that T-channels in dorsal horn neurons are "primed" by AHP, it is still possible that I_T-mediated ADP influences the response of these neurons to synaptically evoked events that occur concomitantly (Yoshimura & Jessell, 1989).

I_T, activated by subthreshold postsynaptic potentials, may contribute to synaptic integration even before the action potential is generated (Reyes, 2001). In that case,

IPSPs are likely to be the source of membrane hyperpolarization removing inactivation of T-channels. IPSPs in dorsal horn neurons can be evoked by volleys in cutaneous afferent fibers (Sahara *et al.*, 1990; Schneider, 1992) as well as mechanical stimuli on the skin (Schneider, 2005). They are seemingly polysynaptic since there is no evidence for inhibitory afferent inputs (Willis & Coggeshall, 2004), and may come from inhibitory interneurons in the adjacent or more distant dorsal horn area (Schneider, 1992). Functional inhibitory connections have been reported between dorsal horn neurons (Lu & Perl, 2003; Schneider, 2008), further supporting this idea. Stimulating cutaneous afferent fibers evokes both IPSP-EPSP and EPSP-IPSP sequences in dorsal horn neurons (Sahara *et al.*, 1990; Schneider, 1992). Given the biophysics of T-channels, the former would more likely activate I_T than the latter does. This is reminiscent of the function of I_T proposed previously for dorsal horn neurons, which is to sense the directionality of skin stimuli (Russo & Hounsgaard, 1996a). This seems possible because inhibitory receptive fields (RFs) in dorsal horn neurons, when identified using innocuous cutaneous stimuli, *e.g.* brush strokes and hair movements, are located adjacent or eccentric to excitatory ones (Hongo *et al.*, 1968; Brown *et al.*, 1987; Schneider, 1992, 2005). This spatial organization of RFs suggests a mechanism for detecting the moving direction of a tactile stimulus on the skin (Hongo *et al.*, 1968). Due to the prerequisite of membrane hyperpolarization for priming the channels, I_T in dorsal horn neurons could only be activated when a stimulus moves from an inhibitory skin RF to an excitatory one, but not in the opposite direction (Figure 4-1*A*). I_T therefore would be a plausible candidate for the underlying ionic mechanism of direction sensitivity. It has been reported in cat thalamic ventral posterolateral nucleus, a major relay of somatosensory inputs, that some

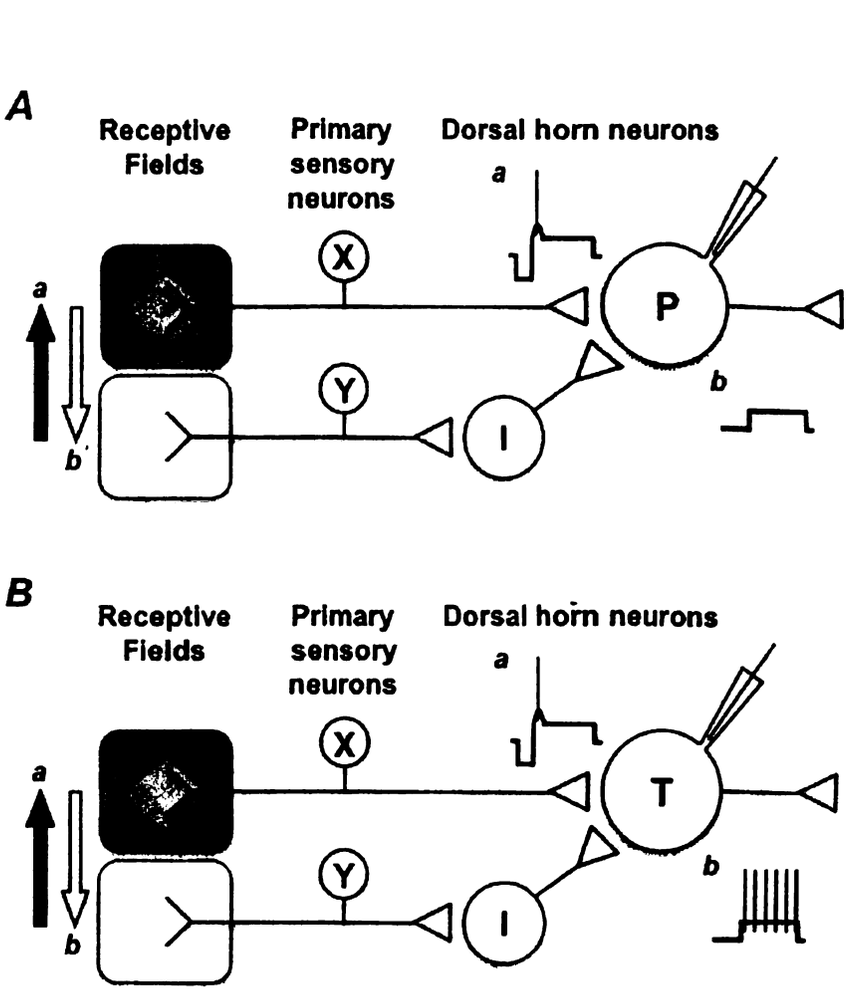

Figure 4-1. A hypothetical mechanism for dorsal horn neurons to distinguish the direction of a moving skin stimulus.

This mechanism can apply to either phasic (P, shown in *A*) or tonic (T, shown in *B*) cells, with an assumption that these cells express substantial I_T. To simplify, only two primary sensory neurons (X, Y) are shown here to project to dorsal horn neurons. Neuron X with a direct connection with the cell recorded and therefore forms an excitatory receptive field (in gray shade) for the dorsal horn neuron. On the other hand, Neuron Y projects to an inhibitory dorsal horn interneuron (I), which synapses with the P or T cell. As a result, IPSPs will be produced in the cell recorded when Neuron Y is activated; therefore, its receptive field (in white) is inhibitory for the P or T cell. The direction of moving skin stimuli are indicated by arrows next to the receptive fields, and the membrane responses evoked are shown next to the dorsal horn neuron, indicated by a corresponding alphabetical designator (*a*, *b*). See text for details.

cells can only be excited by the stimulus of light pressure moving proximally in the long axis of an opposite forelimb (Gordon & Manson, 1967). I_T potentially can contribute to this phenomenon since its expression has been reported in this region (Leresche *et al.*, 2004; McKay *et al.*, 2006). In the dorsal horn of the spinal cord, phasic firing neurons are especially responsive to moving skin stimuli (Schneider, 2005) and express large I_T (Chapter 2), so these cells could be direction sensitive. However, tonic cells may also have this ability because they are activated by brush strokes applied on the skin (Schneider, 2005), and some of them have substantial I_T (Figure A-2) as well. Instead of differentiating the orientation of skin stimuli by firing or not as phasic cells would do (Figure 4-1*A*), tonic cells could generate either tonic firing for a stimulus starting in their excitatory RF or a short burst of action potentials for a brush stroke moving from an inhibitory RF to an excitatory one, similar to PIR (Figure 4-1*B*). Of course, more experiments using an *in vivo* preparation or an *in vitro* one with intact RFs in a limb (Lopez-Garcia & King, 1994) or a skin patch (Schneider, 1992, 2005) attached to the spinal cord are needed to test this hypothesis.

I_T activation

After T-type Ca^{2+} channels are de-inactivated, they are available for activation. However, in a cell, how many channels will actually be activated by an excitatory event, either an EPSP or a compound of EPSPs, is determined by how fast the membrane potential is depolarized by the event. As a result, the amplitude of I_T (Crunelli *et al.*, 1989; Chapters 2 and 3) and the I_T-mediated transient depolarization or spike (Gutierrez *et al.*, 2001) is related to the rate of membrane depolarization. Fast and slow EPSPs can be generated by activating postsynaptic ionotropic and metabotropic receptors,

respectively (Gutierrez *et al.*, 2001). In the spinal dorsal horn, both types of receptors for glutamate, the major neurotransmitter producing EPSPs, are evident for synaptic transmission (Willis & Coggeshall, 2004). However, it is currently unknown if EPSPs mediated by different types of receptors would affect I_T activation in the neurons of this region. In addition, the rate of membrane depolarization is not the only determinant of the current activation. It has been reported that I_T-mediated low-threshold spike can be evoked even by very slow voltage ramps when leak K^+ conductance is blocked (Gutierrez *et al.*, 2001). This may provide another explanation for the rate insensitivity of tonic firing dorsal horn neurons found in this and previous studies (Schneider, 2003, 2005). Tonic cells have a two-times higher input resistance than phasic cells, suggesting less leak K^+ current, and a more depolarized resting membrane potential supports this conclusion (Table 2-1). Therefore, instead of expressing less I_T, it is the scarcity of leak K^+ current in these cells that is unable to "mask" I_T at the resting membrane potential and makes tonic cells less sensitive to the rate of membrane depolarization. This idea can be tested by examining their rate sensitivity in the presence of I_T blockers, *e.g.* Ni^{2+}. The firing threshold of tonic cells should increase if a constant window I_T is the cause. Alternatively, without substantial window I_T, slow membrane depolarization can still activate I_T if T-channels in dorsal horn neurons are subject to the potentiation mechanism reported in sensory thalamocortical cells (see ***I_T potentiation*** above; Leresche *et al.*, 2004; Bessaïh *et al.*, 2008). In that case, I_T in tonic cells could be better potentiated because of more depolarized resting membrane potential, and therefore would have lower ramp threshold for activation.

Nevertheless, the data presented in this study suggest that I_T, possibly its fast inactivating component, contributes to the rate sensitivity of phasic firing dorsal horn neurons, which have been proposed to receive more sensory inputs from rapidly adapting (RA) mechanoreceptors than from slowly adapting (SA) ones (Schneider, 2005) (Figure 4-2*A*). This idea is further supported by the finding that RA receptors, when activated by ramp stimuli, respond to increasing velocities of skin indentation with shortening interspike intervals (Knibestöl, 1973), which could, by temporal summation of EPSPs, lead to a faster depolarization in the postsynaptic membrane. The resulting I_T activation could further depolarize the membrane potential and lead to discharge of the phasic cell (Figure 4-2*B*). Therefore, by expressing I_T, phasic firing dorsal horn neurons may act as a 'high-pass filter', which only allows the transmission of sensory stimuli with a certain level of velocities, and the 'cutoff' level (threshold) could be determined by the current density as well as the channel subtype expressed.

I_T in synaptic function

It has been demonstrated in this study that most dorsal horn neurons possess a slowly inactivating I_T component (Chapter 3), which has been reported to be the "dendritic" type in thalamic neurons (Zhuravleva *et al.*, 2001; Joksovic *et al.*, 2005; but also see Huguenard & Prince, 1992). Currently there is no agreement regarding the subcellular distribution of the three known Ca_V3 subtypes, and the localization is unlikely the same in different neural tissues (McKay *et al.*, 2006). However, axodendritic contacts formed between primary afferent fibers and dorsal horn neurons as well as between interneurons in the region (Schneider *et al.*, 1995; Schneider, 2008) suggest the dendritic distribution of (at least some) T-channels and their role in synaptic transmission

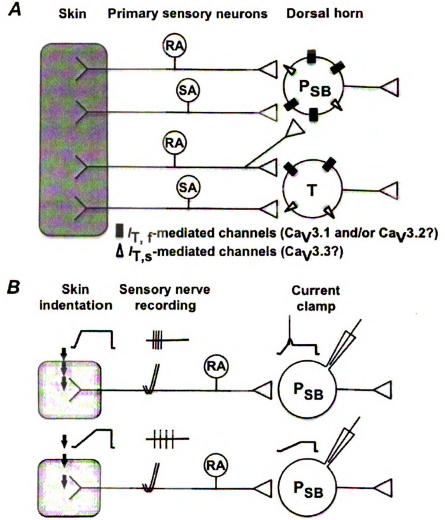

Figure 4-2. T-type Ca^{2+} channels in spinal sensory integration

A, a summary diagram showing that tonic firing dorsal horn neurons (T) and short burst phasic cells (P_{SB}) receive differential sensory inputs from rapidly (RA) and slowly adapting (SA) mechanoreceptors (Schneider, 2005) and also exhibit different levels of $I_{T,f}$, probably mediated by the $Ca_V3.1$ and/or $Ca_V3.2$ channel subtypes (Chapter 3). Higher density of $I_{T,f}$ in P_{SB} cells may contribute to their sensitivity to rapidly moving skin stimuli, and a possible mechanism shown in *B*. *B*, the RA receptor responds to a fast skin indentation with short interspike intervals, which result in a rapid membrane depolarization (a temporal summation of EPSPs) in the postsynaptic P_{SB} cell (upper). The rapid depolarization activates T-type channels, and a I_T-mediated transient further depolarizes the membrane and eventually leads to an action potential. When the skin is indented at a reduced velocity, T-type channels are inactivated by a slowly rising depolarization, and therefore neither I_T-mediated transient nor action potentials are generated (lower).

and integration within the dorsal horn network. In cortical and hippocampal pyramidal neurons, I_T has been reported to amplify synaptic input by enhancing the amplitude of EPSPs (Magee & Johnston, 1995; Magee *et al.*, 1995; Gillessen & Alzheimer, 1997; Urban *et al*,1998; de la Peña & Geijo-Barrientos, 2000). This process may counteract the passive attenuation of EPSPs from synapses in distal dendrites and increase the chance of integration when these EPSPs travel toward the soma (de la Peña & Geijo-Barrientos, 2000). Owing to the transient nature of the channel activation, the enhancement by I_T could be more effective for spatial than for temporal summation (de la Peña & Geijo-Barrientos, 2000). I_T therefore could assist phasic dorsal horn neurons in the intensity coding of flutter-vibration sensation, a plausible function for these cells requiring activation of a group RA receptors (Johnson, 1974) and spatial summation. By contrast, EPSPs in tonic dorsal horn neurons are amplified and prolonged by persistent Na^+ and Ca^{2+} currents and consequently tend to be summed temporally (Prescott & De Koninck, 2005). I_T may also play a role in synaptic plasticity. It has been reported in spinal lamina I neurons that I_T activation is required for the induction of long-term potentiation at C-fiber synapses (Ikeda *et al.*, 2003; Ikeda *et al.*, 2006). This may be an underlying mechanism of hyperalgesia caused by natural noxious stimulation including inflammation, trauma, and nerve injury (Sandkühler, 2009).

D. Remarks on the sensory functions of the spinal dorsal horn

It has been a consensus that dorsal horn neurons not only transmit but also integrate various sensory inputs from primary afferents, although the exact mechanisms have yet to be elucidated. Given the diversity of intrinsic properties found in dorsal horn neurons, it

would be no surprise if these neurons turn out to contribute to sensory processing in a number of different ways. Several sensory functions have been suggested for dorsal horn neurons in this and previous studies. The most intuitive and frequently studied function is to encode stimulus features. For example, Prescott and De Koninck (2002, 2005) proposed that tonic neurons, which fire repetitively during stimulation and exhibit prolonged EPSPs, are suited to encode stimulus intensity, while phasic firing neurons may act like coincidence detectors, relaying sensory inputs with temporal precision. In this study, I suggest that phasic cells may also signal the velocity of moving tactile stimuli, while some dorsal horn neurons could be capable of encoding in their discharge the direction of a stimulus moving across the skin (see Section C). In addition to extracting a specific feature from a stimulus, dorsal horn neurons may sometimes amplify the inputs by wind-up. This is an activity-dependent and progressive increase in the responses to repetitive stimuli, and denotes a potentially noxious event (Coste *et al.*, 2008). By contrast, dorsal horn neurons can also function by blocking the transmission of some sensory information. For example, phasic cells, as mentioned previously, may act like a high pass filter by which the inputs from slow skin indentation or movement are screened out. Other dorsal horn neurons may "ignore" the stimuli of one type (modality) when those of another type (modality) happen simultaneously. Lu and Perl (2003) reported an inhibitory connection between spinal lamina II neurons receiving direct excitatory input from different afferent C-fibers and proposed that this neural module may represent nociceptive input being suppressed by innocuous impulses. These dorsal horn neurons analyze and decipher the significance of peripheral inputs before

transmitting the flow of sensory information to higher centers and are therefore often subject to the modulation of descending control from the brain (Heinricher *et al.*, 2009).

E. Future studies

T-type Ca^{2+} channel research is a newly emerging but rapidly developing field, with more than a hundred related articles published each year for the last decade (Nilius *et al.*, 2006). Many of the studies were conducted in neurons (Nilius *et al.*, 2006), and the role of I_T in mechanosensation is also recently revealed (Heppenstall & Lewin, 2006). However, there have been few studies of I_T in the spinal dorsal horn, and a general description of I_T-expressing dorsal horn neurons was lacking before this study. Using a standardized voltage protocol, I examined I_T in superficial and deep dorsal horn neurons whose intrinsic properties were also assessed. The finding that I_T was ubiquitously expressed in dorsal horn neurons has provoked a great interest in the function(s) of the current in spinal sensory integration. I have made several conjectures about the functions throughout this chapter, which can serve as hypotheses for the future studies of this topic. Some of the proposed functions imply certain subcellular distribution of T-channels. This can be examined by using immunohistochemistry techniques (McKay *et al.*, 2006) or/and performing cell-attached patch on different cellular locations, *e.g.* dendrites and the soma (Joksovic *et al.*, 2005). The former procedure can also unveil the subtype(s) of the T-channel in dorsal horn neurons while the latter method will provide a better estimation on the channel density. To determine the time point at which I_T participates in the firing of dorsal horn neurons, the utilization of the action potential clamping technique (see Box 2 in Bean, 2007 for an overview) would be appropriate. The idea of I_T facilitating action

potential generation can also be tested using this approach. These preceding experiments can be conducted in spinal cord slice preparations. The physiological role of I_T in dorsal horn neurons, however, needs to be confirmed in *in vivo* preparations or *in vitro* ones in which natural stimulation can be applied, *e.g.* a hemisected spinal cord-skin patch preparation (Schneider 1992, 2005). It is also noteworthy that some genetic approaches, such as gene knock-out by gene targeting or gene knock-down by antisense techniques, have recently been developed and utilized to delete or block the function of a specific T-channel subtype (reviewed by Shin *et al.*, 2008). In the spinal dorsal horn, these genetic tools can be used in combination with electrophysiological recording to study the function of I_T mediated by individual Ca_V3 subunits. The results of these researches will not only advance our knowledge of sensory processing in normal physiological conditions but also benefit future clinical practice as T-type Ca^{2+} channels have become an emerging therapeutic target for at least absent seizures and pain management (Shin *et al.*, 2008).

APPENDIX

SUPPLEMENTAL DATA

Table A-1. Comparison of action potentials from neurons in slices prepared using sucrose- *vs.* glycerol-based dissection solution

Dissection solutions	Sucrose-based	Glycerol-based	p^1
Number of cells	20	20	
Resting V_m (mV)	−61 ± 8	−64 ± 5	0.29
Action potential amplitude (mV)	71 ± 12	75 ± 10	0.20
Action potential half-width (ms)	1.2 ± 0.3	1.1 ± 0.3	0.13

Data presented as mean ± SD. [1] Based on unpaired t test.
Action potentials were generated by direct injection of depolarizing current pulses through the recording pipette. The measurements were made and averaged from three 'first' action potentials obtained from each cell.

Table A-2. Comparison of inward currents recorded from neurons in slices prepared using sucrose- *vs.* glycerol-based dissection solution

Dissection solutions	Sucrose-based	Glycerol-based	p^1
Number of cells	20	20	
Half-width (ms)	41 ± 36	33 ± 25	0.92
Peak current amplitude (pA)	176 ± 169	191 ± 89	0.19
Time to peak (ms)	16 ± 17	10 ± 4	0.49

Data presented as mean ± SD. [1] Based on Mann-Whitney test.
Inward currents were recorded in an external solution suitable for isolating T-type Ca^{2+} currents (see METHODS in Chapter 2 or 3) and activated by a 200-ms voltage step to −30 mV from a 500-ms holding potential of −90 mV. Three current traces from each cell were low-pass filtered at 500 Hz (Gaussian) and averaged before the measurements were made.

Table A-3. Comparison of I_T from neurons in superficial *vs.* deep spinal dorsal horn

Laminae	I/II	III/IV	P^1
Number of cells	15	28	
I_T amplitude (pA)	135 ± 20	140 ± 20	0.74
I_T density (pA/pF)	6 ± 1	7 ± 1	0.46

Data presented as mean ± SEM. [1] Based on Mann-Whitney test.
The location of cells was determined under light microscopy (100x), based on the residence of the cell soma relative to spinal lamina II (see Figure A-1*A*). I_T was recorded using an I_T-isolating external solution (see METHODS in Chapter 2 or 3) and activated by a 200-ms voltage step to −30 mV from a 500-ms holding potential of −90 mV. Three to five current traces from each cell were low-pass filtered at 500 Hz (Gaussian) and averaged before the measurements were made. The current density was obtained by dividing the peak amplitude by whole-cell capacitance, an indicator of cell size and read directly from the potentiometer during patch clamping.

Table A-4. A contingency table showing the relationship between the use of silanized pipettes and the detection of Ca_V3 mRNA in single cell RT-PCR experiments

	Silanized pipettes	Non-silanized pipettes	Total
Detection of Ca_V3 mRNA	7	5	12
No detection	5	10	15
Total	12	15	27
Detection rate	58%	33%	

Fisher's exact test indicates no association between these two variables ($P = 0.26$). All 27 dorsal horn neurons presented here expressed some level of T-type Ca^{2+} currents in voltage-clamp recordings.

Table A-5. Comparison of I_T and intrinsic membrane properties in spinal dorsal horn neurons with and without the capability of generating 'low-threshold-current-mediated action potentials' (LTAPs)

Generation of LTAPs	Yes	No	
Number of cells	20	12	P
Threshold (mV)	−46 ± 1	−34 ± 1	< 0.0001 [1]
Resting V_m (mV)	−66 ± 1	−56 ± 2	0.0007 [2]
R_{in} (ΩM)	297 ± 33	680 ± 105	0.0041 [2]
I_T density (pA/pF)	8 ± 2	3 ± 1	0.0017 [3]

Data presented as mean ± SEM. [1] Based on unpaired t test. [2] Based on unpaired t test with Welch correction. [3] Based on Mann-Whitney test.
The threshold (of firing) was determined by measuring the membrane response of cells to a 3-s depolarizing current pulse of the lowest intensity at which they fired. The measurement was made during the last half second of the current pulse when action potentials were not present. Cells were designated to have the capability of generating LTAPs if the threshold was at −40 mV or a more hyperpolarized level. The measurement of other variables was described in Chapter 2.

Table A-6. A contingency table showing the relationship between the exhibition of postinhibitory rebound (PIR) and the ability to generate low-threshold-current-mediated action potentials (LTAPs) in twenty-eight spinal dorsal horn neurons

	PIR	No PIR	Total
LTAPs	17	1	18
No LTAPs	4	6	10
Total	21	7	28

Fisher's exact test indicates a significant association between these two variables (P = 0.0033). The designation of possessing PIR and LTAPs was described in Chapter 2 and Table A-5, respectively.

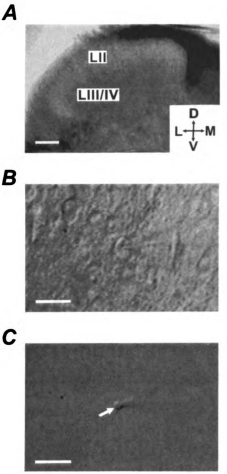

Figure A-1. Images of the dorsal horn and its neuron recorded in this study
A shows the magnified image (100x) of a transverse slice prepared from the lumbosacral section of a hamster spinal cord. In this study, whole-cell patch-clamp recordings were performed in the cells primarily located at laminae I to IV of the dorsal horn. Lamina II (LII) is the translucent band on the dorsal part of the horn, while laminae III and IV (LIII/LIV) looks darker and cannot be distinguished from each other under light microscopy. Orienting labels: D, dorsal; V, ventral; L, lateral; M, medial. *B* shows the magnified image (400x) of a dorsal horn neuron after the whole-cell configuration was formed. The same cell was harvested after termination of recording for single cell RT-PCR analysis. The cell was aspirated into the recording pipette and lifted away from the slice surface as shown in *C*. The arrow indicates part of the cell that was not sucked into the pipette. In order to harvest the whole cell, the pipette tip was broken and preserved along with the cell in a mixture containing the reagents for reverse transcription. Scale bars: 0.2 mm for *A*; 20 μm for *B* and *C*.

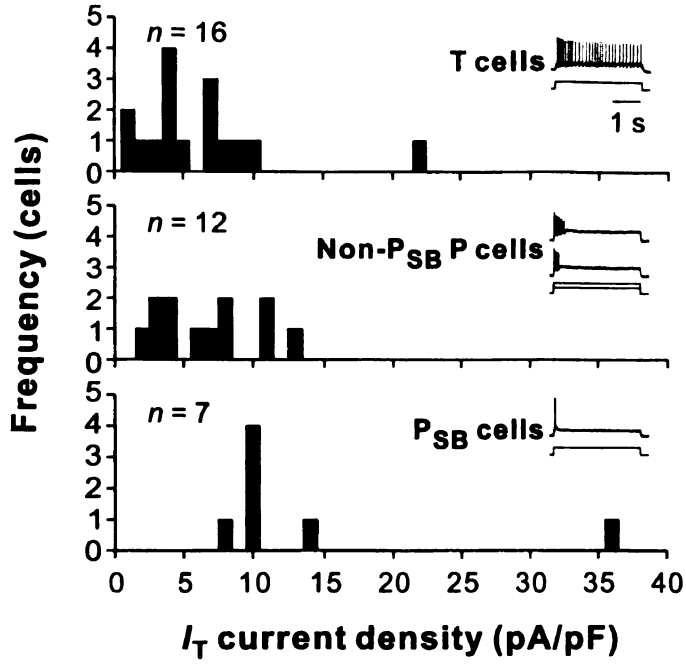

Figure A-2. Expression of I_T in phasic- and tonic-firing neurons
Histograms comparing I_T density for phasic- and tonic-firing dorsal horn neurons. Short burst phasic cells (P_{SB}) had significantly greater I_T than tonic (T) cells or other phasic (Non-P_{SB} P) cells did. Current density was calculated by dividing I_T amplitude by whole-cell capacitance. Insets show example voltage responses (upper traces) to depolarizing current pulses (lower traces).

REFERENCES

References

Alviña K, Ellis-Davies G & Khodakhah K. (2009). T-type calcium channels mediate rebound firing in intact deep cerebellar neurons. *Neuroscience* **158,** 635-641.

Arikkath J & Campbell KP. (2003). Auxiliary subunits: essential components of the voltage-gated calcium channel complex. *Curr Opin Neurobiol* **13,** 298-307.

Armstrong C & Matteson D. (1985). Two distinct populations of calcium channels in a clonal line of pituitary cells. *Science* **227,** 65-67.

Asghar AUR, Cilia La Corte PF, LeBeau FEN, Dawoud MA, Reilly SC, Buhl EH, Whittington MA & King AE. (2005). Oscillatory activity within rat substantia gelatinosa in vitro: a role for chemical and electrical neurotransmission. *J Physiol* **562,** 183-198.

Bean B. (1985). Two kinds of calcium channels in canine atrial cells. Differences in kinetics, selectivity, and pharmacology. *J Gen Physiol* **86,** 1-30.

Bean BP. (2007). The action potential in mammalian central neurons. *Nat Rev Neurosci* **8,** 451-465.

Bessaïh T, Leresche N & Lambert RC. (2008). T current potentiation increases the occurrence and temporal fidelity of synaptically evoked burst firing in sensory thalamic neurons. *Proc Natl Acad Sci U S A* **105,** 11376-11381.

Bossu JL, Feltz A & Thomann JM. (1985). Depolarization elicits two distinct calcium currents in vertebrate sensory neurones. *Pflugers Arch* **403,** 360-368.

Brown AG. (1973). Ascending and long spinal pathways: dorsal columns, spinocervical tract and spinothalamic tract. In *Handbook of Sensory Physiology Volume II: Somatosensory System*, ed. Iggo A, pp. 315-338. Springer-Verlag, Berlin, Heidelberg, New York.

Brown AG, Brown PB, Fyffe RE & Pubols LM. (1983). Receptive field organization and response properties of spinal neurones with axons ascending the dorsal columns in the cat. *J Physiol* **337,** 575-588.

Brown AG & Fyffe RE. (1981). Form and function of dorsal horn neurones with axons ascending the dorsal columns in cat. *J Physiol* **321,** 31-47.

Brown AG, Koerber HR & Noble R. (1987). An intracellular study of spinocervical tract cell responses to natural stimuli and single hair afferent fibres in cats. *J Physiol* **382,** 331-354.

Carbone E & Lux HD. (1984). A low voltage-activated, fully inactivating calcium channel in vertebrate sensory neurones. *Nature* **310,** 501-502.

Carbone E & Lux HD. (1987). Kinetics and selectivity of a low-voltage-activated calcium current in chick and rat sensory neurones. *J Physiol* **386,** 547-570.

Catalano JV & Lamarche G. (1957). Central pathway for cutaneous impulses in the cat. *Am J Physiol* **189,** 141-144.

Chemin J, Monteil A, Perez-Reyes E, Bourinet E, Nargeot J & Lory P. (2002). Specific contribution of human T-type calcium channel isotypes (α_{1G}, α_{1H} and α_{1I}) to neuronal excitability. *J Physiol* **540,** 3-14.

Chemin J, Traboulsie A & Lory P. (2006). Molecular pathways underlying the modulation of T-type calcium channels by neurotransmitters and hormones. *Cell Calcium* **40,** 121-134.

Chen Y, Sharp AH, Hata K, Yunker AMR, Polo-Parada L, Landmesser LT & McEnery MW. (2007). Site-directed antibodies to low-voltage-activated calcium channel $Ca_V3.3$ (ALPHA1I) subunit also target neural cell adhesion molecule-180. *Neuroscience* **145,** 981-996.

Chorev E, Manor Y & Yarom Y. (2006). Density is destiny – on the relation between quantity of T-type Ca^{2+} channels and neuronal electrical behavior. *CNS Neurol Disord Drug Targets* **5,** 655-662.

Chung JM, Kenshalo DR, Jr., Gerhart KD & Willis WD. (1979). Excitation of primate spinothalamic neurons by cutaneous C-fiber volleys. *J Neurophysiol* **42,** 1354-1369.

Coste B, Crest M & Delmas P. (2007). Pharmacological dissection and distribution of NaN/Nav1.9, T-type Ca^{2+} currents, and mechanically activated cation currents in different populations of DRG neurons. *J Gen Physiol* **129,** 57-77.

Coste J, Voisin D, Luccarini P & Dallel R. (2008). A role for wind-up in trigeminal sensory processing: intensity coding of nociceptive stimuli in the rat. *Cephalalgia* **28,** 631-639.

Craig AD & Kniffki KD. (1985). Spinothalamic lumbosacral lamina I cells responsive to skin and muscle stimulation in the cat. *J Physiol* **365,** 197-221.

Cribbs LL, Lee JH, Yang J, Satin J, Zhang Y, Daud A, Barclay J, Williamson MP, Fox M, Rees M & Perez-Reyes E. (1998). Cloning and characterization of α1H from human heart, a member of the T-type Ca^{2+} channel gene family. *Circ Res* **83,** 103-109.

Crunelli V, Lightowler S & Pollard CE. (1989). A T-type Ca^{2+} current underlies low-threshold Ca^{2+} potentials in cells of the cat and rat lateral geniculate nucleus. *J Physiol* **413,** 543-561.

Crunelli V, Toth TI, Cope DW, Blethyn K & Hughes SW. (2005). The 'window' T-type calcium current in brain dynamics of different behavioural states. *J Physiol* **562,** 121-129.

de la Peña E & Geijo-Barrientos E. (2000). Participation of low-threshold calcium spikes in excitatory synaptic transmission in guinea pig medial frontal cortex. *European Journal of Neuroscience* **12,** 1679-1686.

De Proost I, Brouns I, Pintelon I, Timmermans JP & Adriaensen D. (2007). Pulmonary expression of voltage-gated calcium channels: special reference to sensory airway receptors. *Histochem Cell Biol* **128,** 301-316.

Destexhe A, Neubig M, Ulrich D & Huguenard J. (1998). Dendritic low-threshold calcium currents in thalamic relay cells. *J Neurosci* **18,** 3574-3588.

Doğrul A, Yeşilyurt Ö, Işimer A & Güzeldemir ME. (2001). L-type and T-type calcium channel blockade potentiate the analgesic effects of morphine and selective μ opioid agonist, but not to selective δ and κ agonist at the level of the spinal cord in mice. *Pain* **93,** 61-68.

Dubreuil A-S, Boukhaddaoui H, Desmadryl G, Martinez-Salgado C, Moshourab R, Lewin GR, Carroll P, Valmier J & Scamps F. (2004). Role of T-type calcium

current in identified D-hair mechanoreceptor neurons studied in vitro. *J Neurosci* **24,** 8480-8484.

Ertel EA, Campbell KP, Harpold MM, Hofmann F, Mori Y, Perez-Reyes E, Schwartz A, Snutch TP, Tanabe T, Birnbaumer L, Tsien RW & Catterall WA. (2000). Nomenclature of voltage-gated calcium channels. *Neuron* **25,** 533-535.

Fedulova SA, Kostyuk PG & Veselovsky NS. (1985). Two types of calcium channels in the somatic membrane of new-born rat dorsal root ganglion neurones. *J Physiol* **359,** 431-446.

Feltz A. (2006). Low-threshold-activated Ca channels: from molecules to functions: over 25 years of progress. *Crit Rev Neurobiol* **18,** 169-178.

Ferragamo MJ & Oertel D. (2002). Octopus cells of the mammalian ventral cochlear nucleus sense the rate of depolarization. *J Neurophysiol* **87,** 2262-2270.

Fishman MC & Spector I. (1981). Potassium current suppression by quinidine reveals additional calcium currents in neuroblastoma cells. *Proc Natl Acad Sci U S A* **78,** 5245-5249.

Gillessen T & Alzheimer C. (1997). Amplification of EPSPs by low Ni^{2+}- and amiloride-sensitive Ca^{2+} channels in apical dendrites of rat CA1 pyramidal neurons. *J Neurophysiol* **77,** 1639-1643.

Gordon G & Manson JR. (1967). Cutaneous receptive fields of single nerve cells in the thalamus of the cat. *Nature* **215,** 597-599.

Gorelova NA & Yang CR. (2000). Dopamine D1/D5 receptor activation modulates a persistent sodium current in rat prefrontal cortical neurons in vitro. *J Neurophysiol* **84,** 75-87.

Graham BA, Brichta AM & Callister RJ. (2004). An in vivo mouse spinal cord preparation for patch-clamp analysis of nociceptive processing. *J Neurosci Methods* **136,** 221-228.

Grudt TJ & Perl ER. (2002). Correlations between neuronal morphology and electrophysiological features in the rodent superficial dorsal horn. *J Physiol* **540,** 189-207.

Gutierrez C, Cox CL, Rinzel J & Sherman SM. (2001). Dynamics of low-threshold spike activation in relay neurons of the cat lateral geniculate nucleus. *J Neurosci* **21,** 1022-1032.

Hagiwara S, Ozawa S & Sand O. (1975). Voltage clamp analysis of two inward current mechanisms in the egg cell membrane of a starfish. *J Gen Physiol* **65,** 617-644.

Han SH, Murchison D & Griffith WH. (2005). Low voltage-activated calcium and fast tetrodotoxin-resistant sodium currents define subtypes of cholinergic and noncholinergic neurons in rat basal forebrain. *Brain Res Mol Brain Res* **134,** 226-238.

Heinricher MM, Tavares I, Leith JL & Lumb BM. (2009). Descending control of nociception: specificity, recruitment and plasticity. *Brain Res Rev* **60,** 214-225.

Heppenstall P & Lewin G. (2006). A role for T-type Ca^{2+} channels in mechanosensation. *Cell Calcium* **40,** 165-174.

Hochman S, Garraway SM & Pockett S. (1997). Membrane properties of deep dorsal horn neurons from neonatal rat spinal cord in vitro. *Brain Res* **767,** 214-219.

Hongo T, Jankowska E & Lundberg A. (1968). post-synaptic excitation and inhibition from primary afferents in neurones of the spinocervical tract. *J Physiol* **199,** 569-592.

Huang L-YM. (1989). Calcium channels in isolated rat dorsal horn neurones, including labelled spinothalamic and trigeminothalamic cells. *J Physiol* **411,** 161-177.

Huc S, Monteil A, Bidaud I, Barbara G, Chemin J & Lory P. (2009). Regulation of T-type calcium channels: signalling pathways and functional implications. *Biochim Biophys Acta* **1793,** 947-952.

Huguenard JR. (1996). Low-threshold calcium currents in central nervous system neurons. *Annu Rev Physiol* **58,** 329-348.

Huguenard JR & Prince DA. (1992). A novel T-type current underlies prolonged Ca^{2+}-dependent burst firing in GABAergic neurons of rat thalamic reticular nucleus. *J Neurosci* **12,** 3804-3817.

Ikeda H, Heinke B, Ruscheweyh R & Sandkühler J. (2003). Synaptic plasticity in spinal lamina I projection neurons that mediate hyperalgesia. *Science* **299,** 1237-1240.

Ikeda H, Stark J, Fischer H, Wagner M, Drdla R, Jäger T & Sandkühler J. (2006). Synaptic amplifier of inflammatory pain in the spinal dorsal horn. *Science* **312,** 1659-1662.

Inagaki A, Ugawa S, Yamamura H, Murakami S & Shimada S. (2008). The $Ca_V3.1$ T-type Ca^{2+} channel contributes to voltage-dependent calcium currents in rat outer hair cells. *Brain Res* **1201,** 68-77.

Israel J-M, Poulain DA & Oliet SHR. (2008). Oxytocin-induced postinhibitory rebound firing facilitates bursting activity in oxytocin neurons. *J Neurosci* **28,** 385-394.

Jevtovic-Todorovic V & Todorovic S. (2006). The role of peripheral T-type calcium channels in pain transmission. *Cell Calcium* **40,** 197-203.

Jiang MC, Cleland CL & Gebhart GF. (1995). Intrinsic properties of deep dorsal horn neurons in the L6-S1 spinal cord of the intact rat. *J Neurophysiol* **74,** 1819-1827.

Johnson KO. (1974). Reconstruction of population response to a vibratory stimulus in quickly adapting mechanoreceptive afferent fiber population innervating glabrous skin of the monkey. *J Neurophysiol* **37,** 48-72.

Joksovic PM, Bayliss DA & Todorovic SM. (2005). Different kinetic properties of two T-type Ca^{2+} currents of rat reticular thalamic neurones and their modulation by enflurane. *J Physiol* **566,** 125-142.

Karrer EE, Lincoln JE, Hogenhout S, Bennett AB, Bostock RM, Martineau B, Lucas WJ, Gilchrist DG & Alexander D. (1995). In situ isolation of mRNA from individual plant cells: creation of cell-specific cDNA libraries. *Proc Natl Acad Sci U S A* **92,** 3814-3818.

Kawai F & Miyachi E. (2001). Enhancement by T-type Ca^{2+} currents of odor sensitivity in olfactory receptor cells. *J Neurosci* **21,** RC144 (141-145).

Kim DY, Choi HJ, Kim JS, Kim YS, Jeong DU, Shin HC, Kim MJ, Han H-C, Hong SK & Kim YI. (2005). Voltage-gated calcium channels play crucial roles in the glutamate-induced phase shifts of the rat suprachiasmatic circadian clock. *Eur J Neurosci* **21,** 1215-1222.

Klöckner U, Lee JH, Cribbs LL, Daud A, Hescheler J, Pereverzev A, Perez-Reyes E & Schneider T. (1999). Comparison of the Ca^{2+} currents induced by expression of three cloned α1 subunits, α1G, α1H and α1I, of low-voltage-activated T-type Ca^{2+} channels. *Eur J Neurosci* **11,** 4171-4178.

Knibestöl M. (1973). Stimulus-response functions of rapidly adapting mechanoreceptors in human glabrous skin area. *J Physiol* **232,** 427-452.

Kuo JJ, Lee RH, Zhang L & Heckman CJ. (2006). Essential role of the persistent sodium current in spike initiation during slowly rising inputs in mouse spinal neurones. *J Physiol* **574,** 819-834.

Latour I, Hamid J, Beedle AM, Zamponi GW & Macvicar BA. (2003). Expression of voltage-gated Ca^{2+} channel subtypes in cultured astrocytes. *Glia* **41,** 347-353.

Lee JH, Daud AN, Cribbs LL, Lacerda AE, Pereverzev A, Klöckner U, Schneider T & Perez-Reyes E. (1999a). Cloning and expression of a novel member of the low voltage-activated T-type calcium channel family. *J Neurosci* **19,** 1912-1921.

Lee JH, Gomora JC, Cribbs LL & Perez-Reyes E. (1999b). Nickel block of three cloned T-type calcium channels: low concentrations selectively block α1H. *Biophys J* **77,** 3034-3042.

Lee JH, Kim EG, Park BG, Kim KH, Cha SK, Kong ID, Lee JW & Jeong SW. (2002). Identification of T-type α1H Ca^{2+} channels ($Ca_V3.2$) in major pelvic ganglion neurons. *J Neurophysiol* **87,** 2844-2850.

Lee S, Han TH, Sonner PM, Stern JE, Ryu PD & Lee SY. (2008). Molecular characterization of T-type Ca^{2+} channels responsible for low threshold spikes in hypothalamic paraventricular nucleus neurons. *Neuroscience* **155,** 1195-1203.

Leresche N, Hering J & Lambert RC. (2004). Paradoxical potentiation of neuronal T-type Ca^{2+} current by ATP at resting membrane potential. *J Neurosci* **24,** 5592-5602.

Lin DM, Loveall B, Ewer J, Deitcher DL & Sucher NJ. (2007). Characterization of mRNA expression in single neurons. *Methods Mol Biol* **399,** 133-152.

Liss B & Roeper J. (2004). Correlating function and gene expression of individual basal ganglia neurons. *Trends Neurosci* **27,** 475-481.

Llinas R & Yarom Y. (1981a). Electrophysiology of mammalian inferior olivary neurones in vitro. Different types of voltage-dependent ionic conductances. *J Physiol* **315,** 549-567.

Llinas R & Yarom Y. (1981b). Properties and distribution of ionic conductances generating electroresponsiveness of mammalian inferior olivary neurones in vitro. *J Physiol* **315,** 569-584.

Lopez-Garcia JA & King AE. (1994). Membrane properties of physiologically classified rat dorsal horn neurons in vitro: correlation with cutaneous sensory afferent input. *Eur J Neurosci* **6,** 998-1007.

Lory P, Bidaud I & Chemin J. (2006). T-type calcium channels in differentiation and proliferation. *Cell Calcium* **40,** 135-146.

Lu Y & Perl ER. (2003). A specific inhibitory pathway between substantia gelatinosa neurons receiving direct C-fiber input. *J Neurosci* **23,** 8752-8758.

Lu Y & Perl ER. (2005). Modular organization of excitatory circuits between neurons of the spinal superficial dorsal horn (laminae I and II). *J Neurosci* **25,** 3900-3907.

Magee JC, Christofi G, Miyakawa H, Christie B, Lasser-Ross N & Johnston D. (1995). Subthreshold synaptic activation of voltage-gated Ca^{2+} channels mediates a localized Ca^{2+} influx into the dendrites of hippocampal pyramidal neurons. *J Neurophysiol* **74,** 1335-1342.

Magee JC & Johnston D. (1995). Synaptic activation of voltage-gated channels in the dendrites of hippocampal pyramidal neurons. *Science* **268,** 301-304.

Magistretti J & Alonso A. (1999). Biophysical properties and slow voltage-dependent inactivation of a sustained sodium current in entorhinal cortex layer-II principal neurons: a whole-cell and single-channel study. *J Gen Physiol* **114,** 491-509.

Magistretti J, Castelli L, Forti L & D'Angelo E. (2006). Kinetic and functional analysis of transient, persistent and resurgent sodium currents in rat cerebellar granule cells in situ: an electrophysiological and modelling study. *J Physiol* **573,** 83-106.

Mark RF & Steiner J. (1958). Cortical projection of impulses in myelinated cutaneous afferent nerve fibres of the cat. *J Physiol* **142,** 544-562.

Martin RL, Lee JH, Cribbs LL, Perez-Reyes E & Hanck DA. (2000). Mibefradil block of cloned T-type calcium channels. *J Pharmacol Exp Ther* **295,** 302-308.

Matthews EA & Dickenson AH. (2001). Effects of ethosuximide, a T-type Ca^{2+} channel blocker, on dorsal horn neuronal responses in rats. *Eur J Pharmacol* **415,** 141-149.

McDonough SI & Bean BP. (1998). Mibefradil inhibition of T-type calcium channels in cerebellar purkinje neurons. *Mol Pharmacol* **54,** 1080-1087.

McKay BE, McRory JE, Molineux ML, Hamid J, Snutch TP, Zamponi GW & Turner RW. (2006). Ca_V3 T-type calcium channel isoforms differentially distribute to somatic and dendritic compartments in rat central neurons. *Eur J Neurosci* **24,** 2581-2594.

McRory JE, Santi CM, Hamming KS, Mezeyova J, Sutton KG, Baillie DL, Stea A & Snutch TP. (2001). Molecular and functional characterization of a family of rat brain T-type calcium channels. *J Biol Chem* **276,** 3999-4011.

Melnick IV, Santos SF & Safronov BV. (2004a). Mechanism of spike frequency adaptation in substantia gelatinosa neurones of rat. *J Physiol* **559,** 383-395.

Melnick IV, Santos SF, Szokol K, Szucs P & Safronov BV. (2004b). Ionic basis of tonic firing in spinal substantia gelatinosa neurons of rat. *J Neurophysiol* **91,** 646-655.

Mittmann T & Alzheimer C. (1998). Muscarinic inhibition of persistent Na^{+} current in rat neocortical pyramidal neurons. *J Neurophysiol* **79,** 1579-1582.

Molander C, Xu Q & Grant G. (1984). The cytoarchitectonic organization of the spinal cord in the rat. I. The lower thoracic and lumbosacral cord. *J Comp Neurol* **230,** 133-141.

Molineux ML, McRory JE, McKay BE, Hamid J, Mehaffey WH, Rehak R, Snutch TP, Zamponi GW & Turner RW. (2006). Specific T-type calcium channel isoforms are associated with distinct burst phenotypes in deep cerebellar nuclear neurons. *Proc Natl Acad Sci U S A* **103,** 5555-5560.

Moolenaar WH & Spector I. (1978). Ionic currents in cultured mouse neuroblastoma cells under voltage-clamp conditions. *J Physiol* **278,** 265-286.

Morisset V & Nagy F. (1998). Nociceptive integration in the rat spinal cord: role of non-linear membrane properties of deep dorsal horn neurons. *Eur J Neurosci* **10,** 3642-3652.

Mouginot D, Bossu JL & Gähwiler BH. (1997). Low-threshold Ca^{2+} currents in dendritic recordings from Purkinje cells in rat cerebellar slice cultures. *J Neurosci* **17,** 160-170.

Murase K & Randic M. (1983). Electrophysiological properties of rat spinal dorsal horn neurones in vitro: calcium-dependent action potentials. *J Physiol* **334,** 141-153.

Niespodziany I, Derambure P & Poulain P. (1999). Properties of T-type calcium current in enkephalinergic neurones in guinea-pig hypothalamic slices. *Pflugers Arch* **437,** 871-880.

Nilius B, Hess P, Lansman JB & Tsien RW. (1985). A novel type of cardiac calcium channel in ventricular cells. *Nature* **316,** 443-446.

Nilius B, Talavera K & Verkhratsky A. (2006). T-type calcium channels: the never ending story. *Cell Calcium* **40,** 81-88.

Nowycky MC, Fox AP & Tsien RW. (1985). Three types of neuronal calcium channel with different calcium agonist sensitivity. *Nature* **316,** 440-443.

Parri HR & Crunelli V. (1998). Sodium current in rat and cat thalamocortical neurons: role of a non-inactivating component in tonic and burst firing. *J Neurosci* **18,** 854-867.

Perez-Reyes E. (2003). Molecular physiology of low-voltage-activated T-type calcium channels. *Physiol Rev* **83,** 117-161.

Perez-Reyes E. (2006). Molecular characterization of T-type calcium channels. *Cell Calcium* **40,** 89-96.

Perez-Reyes E, Cribbs LL, Daud A, Lacerda AE, Barclay J, Williamson MP, Fox M, Rees M & Lee JH. (1998). Molecular characterization of a neuronal low-voltage-activated T-type calcium channel. *Nature* **391,** 896-900.

Perez-Reyes E & Lory P. (2006). Molecular biology of T-type calcium channels. *CNS Neurol Disord Drug Targets* **5,** 605-609.

Phillips JK & Lipski J. (2000). Single-cell RT-PCR as a tool to study gene expression in central and peripheral autonomic neurones. *Auton Neurosci* **86,** 1-12.

Prescott SA & De Koninck Y. (2002). Four cell types with distinctive membrane properties and morphologies in lamina I of the spinal dorsal horn of the adult rat. *J Physiol* **539,** 817-836.

Prescott SA & De Koninck Y. (2005). Integration time in a subset of spinal lamina I neurons is lengthened by sodium and calcium currents acting synergistically to prolong subthreshold depolarization. *J Neurosci* **25,** 4743-4754.

Prescott SA & Sejnowski TJ. (2008). Spike-rate coding and spike-time coding are affected oppositely by different adaptation mechanisms. *J Neurosci* **28,** 13649-13661.

Rexed B. (1952). The cytoarchitectonic organization of the spinal cord in the cat. *J Comp Neurol* **96,** 414-495.

Reyes A. (2001). Influence of dendritic conductances on the input-output properties of neurons. *Annu Rev Neurosci* **24,** 653-675.

Rivera-Arconada I & Lopez-Garcia JA. (2005). Effects of M-current modulators on the excitability of immature rat spinal sensory and motor neurones. *Eur J Neurosci* **22,** 3091-3098.

Rozen S & Skaletsky HJ. (2000). Primer3 on the WWW for general users and for biologist programmers. In *Bioinformatics Methods and Protocols: Methods in Molecular Biology*, ed. Krawetz S & Misener S, pp. 365-386. Humana Press, Totowa, NJ.

Ruscheweyh R, Ikeda H, Heinke B & Sandkühler J. (2004). Distinctive membrane and discharge properties of rat spinal lamina I projection neurones in vitro. *J Physiol* **555,** 527-543.

Ruscheweyh R & Sandkühler J. (2002). Lamina-specific membrane and discharge properties of rat spinal dorsal horn neurones in vitro. *J Physiol* **541,** 231-244.

Ruscheweyh R & Sandkühler J. (2003). Epileptiform activity in rat spinal dorsal horn in vitro has common features with neuropathic pain. *Pain* **105,** 327-338.

Russo RE & Hounsgaard J. (1996a). Burst-generating neurones in the dorsal horn in an in vitro preparation of the turtle spinal cord. *J Physiol* **493 (Pt 1),** 55-66.

Russo RE & Hounsgaard J. (1996b). Plateau-generating neurones in the dorsal horn in an in vitro preparation of the turtle spinal cord. *J Physiol* **493 (Pt 1),** 39-54.

Russo RE & Hounsgaard J. (1999). Dynamics of intrinsic electrophysiological properties in spinal cord neurones. *Prog Biophys Mol Biol* **72,** 329-365.

Rustioni A & Kaufman AB. (1977). Identification of cells or origin of non-primary afferents to the dorsal column nuclei of the cat. *Exp Brain Res* **27,** 1-14.

Ryu PD & Randic M. (1990). Low- and high-voltage-activated calcium currents in rat spinal dorsal horn neurons. *J Neurophysiol* **63,** 273-285.

Safronov BV. (1999). Spatial distribution of Na^+ and K^+ channels in spinal dorsal horn neurones: role of the soma, axon and dendrites in spike generation. *Prog Neurobiol* **59,** 217-241.

Safronov BV, Wolff M & Vogel W. (1997). Functional distribution of three types of Na^+ channel on soma and processes of dorsal horn neurones of rat spinal cord. *J Physiol* **503,** 371-385.

Sahara Y, Xie YK & Bennett GJ. (1990). Intracellular records of the effects of primary afferent input in lumbar spinoreticular tract neurons in the cat. *J Neurophysiol* **64,** 1791-1800.

Sakata Y, Saegusa H, Zong S, Osanai M, Murakoshi T, Shimizu Y, Noda T, Aso T & Tanabe T. (2001). Analysis of Ca^{2+} currents in spermatocytes from mice lacking $Ca_V2.3$ (α_{1E}) Ca^{2+} channel. *Biochem Biophys Res Commun* **288,** 1032-1036.

Sandkühler J. (2009). Models and mechanisms of hyperalgesia and allodynia. *Physiol Rev* **89,** 707-758.

Sandkühler J & Eblen-Zajjur AA. (1994). Identification and characterization of rhythmic nociceptive and non-nociceptive spinal dorsal horn neurons in the rat. *Neuroscience* **61,** 991-1006.

Santos SFA, Rebelo S, Derkach VA & Safronov BV. (2007). Excitatory interneurons dominate sensory processing in the spinal substantia gelatinosa of rat. *J Physiol* **581,** 241-254.

Schneider S. (1992). Functional properties and axon terminations of interneurons in laminae III-V of the mammalian spinal dorsal horn in vitro. *J Neurophysiol* **68,** 1746-1759.

Schneider S, Sandiford D, Kavookjian A & Johnson B. (1995). Synaptic connectivity of local circuit neurons in laminae III and IV of hamster spinal cord. *J Comp Neurol* **355,** 380-391.

Schneider SP. (2003). Spike frequency adaptation and signaling properties of identified neurons in rodent deep spinal dorsal horn. *J Neurophysiol* **90,** 245-258.

Schneider SP. (2005). Mechanosensory afferent input and neuronal firing properties in rodent spinal laminae III-V: re-examination of relationships with analysis of responses to static and time-varying stimuli. *Brain Res* **1034,** 71-89.

Schneider SP. (2008). Local circuit connections between hamster laminae III and IV dorsal horn neurons. *J Neurophysiol* **99,** 1306-1318.

Shao Y, Alicknavitch M & Farach-Carson MC. (2005). Expression of voltage sensitive calcium channel (VSCC) L-type $Ca_V1.2$ (α_{1C}) and T-type $Ca_V3.2$ (α_{1H}) subunits during mouse bone development. *Dev Dyn* **234,** 54-62.

Shin H-S, Cheong E-J, Choi S, Lee J & Na HS. (2008). T-type Ca^{2+} channels as therapeutic targets in the nervous system. *Curr Opin Pharmacol* **8,** 33-41.

Shin J-B, Martinez-Salgado C, Heppenstall PA & Lewin GR. (2003). A T-type calcium channel required for normal function of a mammalian mechanoreceptor. *Nat Neurosci* **6,** 724-730.

SoRelle R. (1998). Withdrawal of Posicor from market. *Circulation* **98,** 831-832.

Sucher NJ & Deitcher DL. (1995). PCR and patch-clamp analysis of single neurons. *Neuron* **14,** 1095-1100.

Sun H & Wu SH. (2008). Physiological characteristics of postinhibitory rebound depolarization in neurons of the rat's dorsal cortex of the inferior colliculus studied in vitro. *Brain Res* **1226,** 70-81.

Talavera K & Nilius B. (2006). Biophysics and structure-function relationship of T-type Ca^{2+} channels. *Cell Calcium* **40,** 97-114.

Talley EM, Cribbs LL, Lee JH, Daud A, Perez-Reyes E & Bayliss DA. (1999). Differential distribution of three members of a gene family encoding low voltage-activated (T-type) calcium channels. *J Neurosci* **19,** 1895-1911.

Tarasenko AN, Kostyuk PG, Eremin AV & Isaev DS. (1997). Two types of low-voltage-activated Ca^{2+} channels in neurones of rat laterodorsal thalamic nucleus. *J Physiol* **499,** 77-86.

Thomson AM, West DC & Headley PM. (1989). Membrane characteristics and synaptic responsiveness of superficial dorsal horn neurons in a slice preparation of adult rat spinal cord. *Eur J Neurosci* **1,** 479-488.

Todorovic SM & Jevtovic-Todorovic V. (2006). The role of T-type calcium channels in peripheral and central pain processing. *CNS Neurol Disord Drug Targets* **5,** 639-653.

Treviño CL, Felix R, Castellano LE, Gutiérrez C, Rodríguez D, Pacheco J, López-González I, Gomora JC, Tsutsumi V, Hernández-Cruz A, Fiordelisio T, Scaling AL & Darszon A. (2004). Expression and differential cell distribution of low-threshold Ca^{2+} channels in mammalian male germ cells and sperm. *FEBS Lett* **563,** 87-92.

Uebachs M, Schaub C, Perez-Reyes E & Beck H. (2006). T-type Ca^{2+} channels encode prior neuronal activity as modulated recovery rates. *J Physiol* **571,** 519-536.

Urban NN, Henze DA & Barrionuevo G. (1998). Amplification of perforant-path EPSPs in CA3 pyramidal cells by LVA calcium and sodium channels. *J Neurophysiol* **80,** 1558-1561.

van Welie I, Remme MW, van Hooft JA & Wadman WJ. (2006). Different levels of I_h determine distinct temporal integration in bursting and regular-spiking neurons in rat subiculum. *J Physiol* **576,** 203-214.

Várnai P, Osipenko ON, Vizi ES & Spät A. (1995). Activation of calcium current in voltage-clamped rat glomerulosa cells by potassium ions. *J Physiol* **483,** 67-78.

Viana F, Van Den Bosch L, Missiaen L, Vandenberghe W, Droogmans G, Nilius B & Robberecht W. (1997). Mibefradil (Ro 40-5967) blocks multiple types of voltage-gated calcium channels in cultured rat spinal motoneurones. *Cell Calcium* **22,** 299-311.

Willis WD & Coggeshall RE. (2004). *Sensory mechanisms of the spinal cord.* Kluwer Academic/Plenum, New York.

Yasaka T, Kato G, Furue H, Rashid MH, Sonohata M, Tamae A, Murata Y, Masuko S & Yoshimura M. (2007). Cell-type-specific excitatory and inhibitory circuits involving primary afferents in the substantia gelatinosa of the rat spinal dorsal horn in vitro. *J Physiol* **581,** 603-618.

Ye J, Zhang J, Xiao C & Kong J. (2006). Patch-clamp studies in the CNS illustrate a simple new method for obtaining viable neurons in rat brain slices: glycerol replacement of NaCl protects CNS neurons. *J Neurosci Methods* **158,** 251-259.

Yoshimura M & Jessell TM. (1989). Membrane properties of rat substantia gelatinosa neurons in vitro. *J Neurophysiol* **62,** 109-118.

Yunker AM. (2003). Modulation and pharmacology of low voltage-activated ("T-type") calcium channels. *J Bioenerg Biomembr* **35,** 577-598.

Yunker AM & McEnery MW. (2003). Low-voltage-activated ("T-type") calcium channels in review. *J Bioenerg Biomembr* **35,** 533-575.

Yunker AMR, Sharp AH, Sundarraj S, Ranganathan V, Copeland TD & McEnery MW. (2003). Immunological characterization of T-type voltage-dependent calcium channel $Ca_V3.1$ (alpha1G) and $Ca_V3.3$ (alpha1I) isoforms reveal differences in their localization, expression, and neural development. *Neuroscience* **117,** 321-335.

Zhang D, Chen J, Saraf A, Cassar S, Han P, Rogers JC, Brioni JD, Sullivan JP & Gopalakrishnan M. (2006). Association of CatSper1 or -2 with $Ca_V3.3$ leads to suppression of T-type calcium channel activity. *J Biol Chem* **281,** 22332-22341.

Zhuravleva SO, Kostyuk PG & Shuba YM. (1999). Divalent cation selectivity of the subtypes of low voltage-activated Ca^{2+} channels in thalamic neurons. *Neuroreport* **10,** 651-657.

Zhuravleva SO, Kostyuk PG & Shuba YM. (2001). Subtypes of low voltage-activated Ca^{2+} channels in laterodorsal thalamic neurons: possible localization and physiological roles. *Pflugers Arch* **441,** 832-839.